Institut für Experimentelle Genetik

GSF – Forschungszentrum für Umwelt und Gesundheit

Identification of novel mouse Delta1 target genes:

Combination of transcriptomics and proteomics

Christine Hutterer

Vollständiger Abdruck der von der Fakultät Wissenschaftszentrum Weihenstephan für Ernährung, Landnutzung und Umwelt der Technischen Universität München zur Erlangung des akademischen Grades eines

Doktors der Naturwissenschaften

genehmigten Dissertation.

Vorsitzender: Univ.-Prof. Dr. A. Gierl

Prüfer der Dissertation: 1.   apl. Prof. Dr. J. Adamski

                                               2.   Univ.-Prof. Dr. W. Wurst

Die Dissertation wurde am 31.01.2005 bei der Technischen Universität München eingereicht und durch die Fakultät Wissenschaftszentrum Weihenstephan für Ernährung, Landnutzung und Umwelt am 13.05.2005 angenommen.

DANKSAGUNG

TABLE OF CONTENTS

Abstract

The Delta/Notch signal transduction pathway is an evolutionary conserved pathway involved in many diverse developmental processes. These include neurogenesis, somitogenesis, left-right development, pancreatic development and development of the sensory hair in the inner ear. Numerous genes have been identified in the last years that are part of the signal transduction pathway or can influence the pathway in a way. A model to explain the process of lateral inhibition, one of the main features of the pathway, has been established. However, it is not clear how the known genes involved in Delta/Notch signalling can account for such diverse processes.

In order to get new insights into the regulation of Delta/Notch signalling and to identify targets of *Dll1* the transcriptome and the proteome of E10.5 wildtype and *Dll1$^{-/-}$* embryos was analysed using DNA-chip technology and 2D-gelelectrophoresis combined with mass spectrometry. In the transcriptome analysis 22 up- and 30 downregulated transcripts were identified. In the proteome analysis 13 proteins were up- and 37 proteins were downregulated at E10.5.
Further methods to verify the data on transcriptomics side included whole mount *in situ* hybridisation and real-time PCR and semi-quantitative immunoblotting on the proteomics side.

The most promising candidate out of this analyses is the gene *Ifitm1* which shows expression in regions where Delta/Notch signalling is known to occur, namely the presomitic mesoderm and the latest formed somites. The expression was strongly reduced in *Dll1*, *Dll3* and *Jag1* mutants which indicates a direct connection between *Dll1* or Delta/Notch signalling respectively, and *Ifitm1*. Furthermore *Ifitm1* was only recently discovered as marker for primordial germ cells and has no assigned function so far. To assess the exact function of *Ifitm1* in the mouse a classical knockout targeting construct has been designed and prepared. The knockout animals will provide insights into the relevance of *Ifitm1* for somitogenesis and other developmental processes.

Further genes have been identified which show expression patterns indicative of Delta/Notch signalling and which also were altered in *Dll1* mutant mouse embryos, and some also in *Dll3* and *Jag1* embryos. These genes are *Csk, Ddx6, Nes, Sema5b and Smarcc1*.

On the protein level a number of interesting proteins have been identified. These include six subunits of the 26S proteasome, four translation initiation or elongation factors, proteins involved in cell signalling such as two 14-3-3 proteins and proteins involved in intracellular transport.

Taken the data from the transcriptome and proteome analyses together it seems to become clear that in the *Dll1* mutant many cellular processes might be altered. Regulation on the genomic level seems to be disturbed at the process of chromatin remodelling, regulation on post-transcriptional levels seems to be disturbed at the process of translation initiation and elongation as well as at the process of protein degradation through the proteasome.

Intracellular trafficking seems to be altered on the level of phosphorylation and dephosphorylation through protein phosphatase 2A (PP2A) and C-src tyrosine kinase (Csk), as well as through the 14-3-3 proteins. Further aspects of intracellular trafficking involve the cytoskeleton. Nestin and γ-tubulin, two components of the cytoskeleton were deregulated in the *Dll1* mutant. Furthermore intracellular membrane trafficking seems to be disrupted through the downregulation of the SNARE protein Nsf and its interaction partner Munc18-3. It also seemed to turn out that developmental processes are altered in the mutants. Four transcription factors have been identified which have not been brought into context with Delta/Notch signalling before. It is not clear yet if they might play roles on the side of the signalling (Delta expressing) or the receiving (Notch expressing) cell. Neural crest cell migration also seems to be altered since *Sema5b* a gene involved in axonal guidance was downregulated in the *Dll1* mutant embryos.

Using a combination of transcriptomics and the proteomics approaches it could be shown that RNA- and protein expression profiling are both versatile and powerful approaches which complement each other. Thus it was possible to gain new insights into regulatory processes which would not have been possible with one approach alone.

Zusammenfassung

Der Delta/Notch Signaltransduktionsweg ist eine an vielfältigen Entwicklungsprozessen beteiligte, evolutionär konservierte Signalkaskade. Bisher wurde die Wirkungsweise während der Neurogenese, Somitogenese, links-rechts Achsenbildung, Pakreasentwicklung und der Entwicklung der sensorischen Härchen im Innenohr beobachtet. In den letzten Jahren wurde eine Anzahle von Genen identifiziert, die direkt an der Signaltransduktion beteiligt sind, oder die den Wechselweg auf verschiedene Weise beeinflussen. Für den wichtigen Entwicklungsprozess der lateralen Inhibition, der von Delta/Notch Signaltransduktion gesteuert wird, wurde ein Modell etabliert. Es bleibt jedoch unklar, wie die begrenzte Anzahl an bisher identifizierten Genen eine solche Vielfalt an Entwicklungsprozessen steuern kann.

Um neue Einblicke in die Regulation der Delta/Notch Signaltransduktionskaskade zu gewinnen und um Zielgene von *Dll1* zu identifizieren wurde das Transkriptom, sowie das Proteom von 10.5 dpc Wildtyp und *Dll1* mutanten Mausembryonen untersucht. Dazu wurde die DNA-Chip Technologie und 2D-Gelelektrophorese kombiniert mit Massenspektrometrie durchgeführt. Durch die Transkriptomanalyse wurden in der *Dll1* Mutante 22 hoch- und 30 herunter regulierte Gene identifiziert. Die Proteomanalyse lieferte 13 hoch- und 37 herunter regulierte Proteine am Tag 10.5 der Embryonalentwicklung.
Zur Bestätigung und weiteren Analyse der identifizierten Kandidaten wurde Real-Time PCR und Ganzkörper *in situ* Hybridisierung auf Nukleinsäure-Ebene und semi-quantitatives Immunoblotting auf Protein-Ebene durchgeführt.

Der aussichtsreichste Kandidat der Analysen ist das Gen *Ifitm1*. Es ist in Regionen des Embryos exprimiert von denen man weiß, dass dort Delta/Notch Signalübertragung stattfindet, wie beispielsweise im präsomitischen Mesoderm und den jüngsten Somiten. In *Dll1*, *Dll3* und *Jag1* mutanten Mausembryonen war die Expression in diesen Regionen deutlich reduziert, was auf eine direkte Verbindung zwischen *Dll1*, bzw. Delta/Notch Signaltransduktion und *Ifitm1* hinweist. *Ifitm1* wurde erst kürzlich als Markergen für primordiale Keimzellen identifiziert, eine genaue Funktion ist bisher nicht bekannt. Um die Funktion von *Ifitm1* detailliert untersuchen zu können wurde ein klassisches Targeting Konstrukt entworfen und hergestellt. Mit Hilfe der Knock-out Tiere werden neue Einblicke in die Bedeutung von *Ifitm1* für die Somitogenese und andere Entwicklungsprozesse gewonnen werden.

Es wurden weitere Gene gefunden, die ein bezüglich Delta/Notch Signaltransduktion bemerkenswertes Expressionsmuster zeigen, und deren Expression in *Dll1* Mutanten, sowie auch in *Dll3* und *Jag1* Mutanten verändert war. Diese Gene sind *Csk, Ddx6, Nes, Sema5b* and *Smarcc1*.

Auch auf Protein-Ebene wurde eine Reihe interessanter Proteine identifiziert. Dazu gehören beispielsweise sechs Untereinheiten des 26S Proteasoms, vier „translation initiation" bzw. „elongation" Faktoren, Proteine der Signalisierungskaskade der Zellen, wie zwei 14-3-3 Proteine und Proteine, die in den intrazellulären Transport involviert sind.

Betrachtet man die Daten der Transkriptom- und Proteomanalyse gemeinsam so scheint klar zu werden, dass in der *Dll1* Mutante eine Anzahl an zellulären Prozessen beeinträchtigt sein könnte. Auf genomischer Ebene scheint die Regulation der Chromatin Modellierung verändert zu sein. Die post-transkriptionelle Regulation scheint auf der Ebene der Initiierung sowie der Elongation der Transkription ebenso gestört zu sein, wie auch bei dem Prozess der Protein Degradation am Proteasom. Intrazelluläre und regulatorische Transportmechanismen scheinen auf der Ebene der Phosphorylierung und Dephosphorylierung durch Protein Phosphatase 2A (PP2A) und C-src Tyrosin Kinase (Csk) und auch durch 14-3-3 Proteine verändert zu sein. Intrazellulärer Transport hängt weiterhin vom Cytoskelett ab. Zwei Komponenten des Cytoskeletts, Nestin und γ-Tubulin, sind reguliert in der *Dll1* Mutante. Durch verminderte Expression des SNARE Proteins Nsf, wie auch dessen Interaktionspartner Munc18-3, scheinen auch Transportmechanismen, die mit Hilfe der Zellmembran ablaufen, beeinträchtigt zu sein. Weiterhin scheinen auch Entwicklungsprozesse in der Mutante betroffen zu sein. Beispielsweise wurden vier Transkriptionsfaktoren identifiziert, die noch nie mit der Delta/Notch Signaltransduktion in Zusammenhang gebracht wurden. Im Moment bleibt offen, ob diese Transkriptionsfaktoren auf der Seite der Delta exprimierenden, signalgebenden Zelle, oder auf der Seite der Notch exprimierenden, signalempfangenden Zelle eine Rolle spielen. Eine mögliche Beeinträchtigung der Wanderung der Neuralleistenzellen könnte durch die verminderte Expression von *Sema5b* angezeigt werden. *Sema5b* ist in den Prozess der Wegleitung der Neuronen involviert.

Mit Hilfe einer Kombination aus Analysen des Transkriptoms und des Proteoms konnte gezeigt werden, dass RNA- und Protein-Expression Profiling zwei vielseitige und leistungsstarke Ansätze sind, die einander komplementieren. Es war auf diese Weise möglich neue Einblicke in regulatorische Mechanismen zu erhalten, die man mit einer Methode allein nicht hätte bekommen können.

1 Introduction

The development from a fertilized egg to a multicellular organism of characteristic size and shape is a regulated process of gene regulation on transcriptional, post-transcriptional, translational and post-translational levels. Unlike the situation in prokaryotes where the primary function of gene control is the adjustment of the enzymatic machinery of the cell to its immediate nutritional and physical environment, gene control in multicellular organisms is necessary for the regulation of a genetic programme that underlies embryonic development and tissue differentiation. The right gene has to be activated in the right cell at the right time during the development.

Transcriptional regulation or regulation of gene expression is a complex process and occurs at the first step in gene expression, the initiation of transcription. This event is for example dependent on the chromatin structure where the density of chromatin folding can inhibit transcription, or on transcription factors which are able to activate or repress transcription by interacting with the promoter of the gene. After transcription of a gene into the primary transcript by RNA polymerase a series of post-transcriptional modifications are initiated such as 5´capping and 3´polyadenylation. The functional mRNA then undergoes splicing events to remove introns. For the translation the mRNA is transported from the nucleus to the ribosomes in the cytoplasm where the RNA sequence gets translated into a peptide sequence via tRNA molecules. Following this step the peptide chain is transferred to the endoplasmatic reticulum where protein folding and post-translational modification occurs. These include covalent modifications such as removal of a signal peptide on one end of the protein, glycosylation or phosphorylation as well as establishment of disulfide bonds. A further level of regulation within all these steps comes from the cellular mechanisms to influence the stability of mRNA and proteins via programmed degradation processes such as ubiquitin-dependent degradation of proteins.

Within the last decade big effort has been put into the deciphering of genomes. The publication of the human sequence in February 2001 (Lander et al. 2001; Venter et al. 2001) and of the mouse sequence shortly after (Nadeau et al. 2001) has facilitated the possibilities to analyse gene function. Until now more than 150 genomes of bacteria, archae and eukaryotes have been completely sequenced (http://www.argosbiotech.de/700/omics/genomics/genometer2.htm). The sequence information is quite useful to identify novel genes according to their homology to other species. However, the sequence itself does generally not help to identify gene function of unknown genes. The genome research area of functional genomics is concerned with assignment of function to DNA sequences. A possible way to elucidate gene function is the establishment of a mutant model organism for the gene of interest to analyse the loss-of-function phenotype. Different approaches have been undertaken to establish mutants. On the one hand mouse genes have been targeted ("forward genetics") by removal of necessary elements (e.g. exons) of the gene ("knock-out") or by insertion of a reporter gene (e.g. lacZ) in the position of the gene ("knock-in"). On the other hand large scale mutagenesis projects

were initiated to target genes by random insertion of mutations ("reverse genetics") using mutagenic agents such as ENU (Ehling et al. 1985; Hrabe de Angelis and Balling 1998; Justice et al. 1999; Balling 2001; Beier and Herron 2004), radiation (Ehling et al. 1985; Anderson 1995) or gene trap approaches (Joyner et al. 1992; Wurst et al. 1995; Brown and Nolan 1998; Cecconi and Meyer 2000; Hansen et al. 2003).

The different methods to generate mutants are also reflected in the different ways to analyse mutants, genes or pathways. Using a "hypothesis-driven approach" already gained knowledge can inspire scientists to propose hypotheses which can then be tested by especially designed experiments. However the effort of this approach is dependent on the ideas which led to the formation of the hypothesis and also proper means (e.g. technical methods) to test it. Therefore within the last years methods have been developed which do not necessarily need a hypothesis to be successful. DNA-microarrays were established to analyse gene expression in a large set of genes simultaneously (transcriptome analysis) and 2D-gelectrophoresis combined with subsequent mass spectrometry techniques is now used for the analysis of proteomes and not just for displaying a status quo on gels. These types of analyses produce a large amount of data which can then be analysed in detail to identify novel connections no-one might have thought of before.

The Delta/Notch signal transduction pathway has been the object of intensive studies in many multicellular organisms since it has been shown to be involved in many distinct developmental processes. Nevertheless with the accessible knowledge the different facets of the signal transduction cascade cannot be explained adequately. Thus it is promising that the described techniques might help to gain new insights into the signalling cascade.

1.1 The Delta/Notch signal transduction pathway

The Delta/Notch signal transduction pathway is evolutionary conserved between many metazoan species. It was first identified in the fruit-fly *Drosophila melanogaster* (e.g.Cabrera 1990; Campos-Ortega and Knust 1990; Corbin et al. 1991; Heitzler and Simpson 1991; Muskavitch 1994) and has until now been shown to act in the spider *Cupiennius salei* (Stollewerk et al. 2003), the nematode *Caenorhabditis elegans* (e.g. Henderson et al. 1994; Kimble and Simpson 1997; Petcherski and Kimble 2000), the frog *Xenopus laevis* (e.g. Coffman et al. 1990) the zebrafish *Danio rerio* (e.g. Jiang et al. 1996), the chicken (e.g. Myat et al. 1996), the mouse *mus musculus* (e.g. Weinmaster et al. 1992; Lardelli and Lendahl 1993) and humans (Larsson et al. 1994). During the embryonic development of the mouse the Delta/Notch pathway is involved in diverse patterning processes: lateral specification during neurogenesis (Lewis 1998; Baker 2000; Lutolf et al. 2002) and pancreatic development (Apelqvist et al. 1999; Lammert et al. 2000), left/right organization (Krebs et al. 2003; Przemeck et al. 2003), and involvement in processes like the synchronization/organization of the segmentation clock (Conlon et al. 1995; Oka et al. 1995; Hrabe de Angelis et al. 1997; Dale and Pourquie 2000; Jiang et al. 2000; Schnell and Maini 2000; Koizumi et al. 2001; Bessho and Kageyama 2003; Pourquie 2003) and establishment and maintenance of somite boundaries during somitogenesis (Hrabe de Angelis et al. 1997) are some of them.

The Delta/Notch signal transduction can be explained extremely simplified such that specific ligands (chapter 1.1.1.2) on the cell surface of one cell bind to corresponding receptors (chapter 1.1.1.1) on the surface of a neighbouring cell. The activated receptors, with the help of effector genes (chapter 1.1.1.3), mediate the signal into the nucleus of the receiving cell where the expression of specific target genes (chapter 1.1.1.4) is activated (Figure 1).

1.1.1 Components of Delta/Notch signal transduction

The Delta/Notch signal transduction pathway is characterised by direct cell to cell interaction (Figure 1). In this context it is remarkable that so called "Regulated Intramembrane Proteolysis" (RIP) is an unusual mode of such signal transduction because of the following features. First, upon binding of the ligand the receptor molecule is proteolytically cleaved. The cleavage is irreversible. Thus each receptor molecule can only signal once, which means that the intensity and duration of signalling cannot be regulated by receptor desensitization. Second, the signalling is direct and not relayed by second messenger molecules. This leads to a limitation of possibilities for signal amplification. Third, the processing of the receptor releases extracellular by-products that may have the ability to further activate or downregulate signalling.
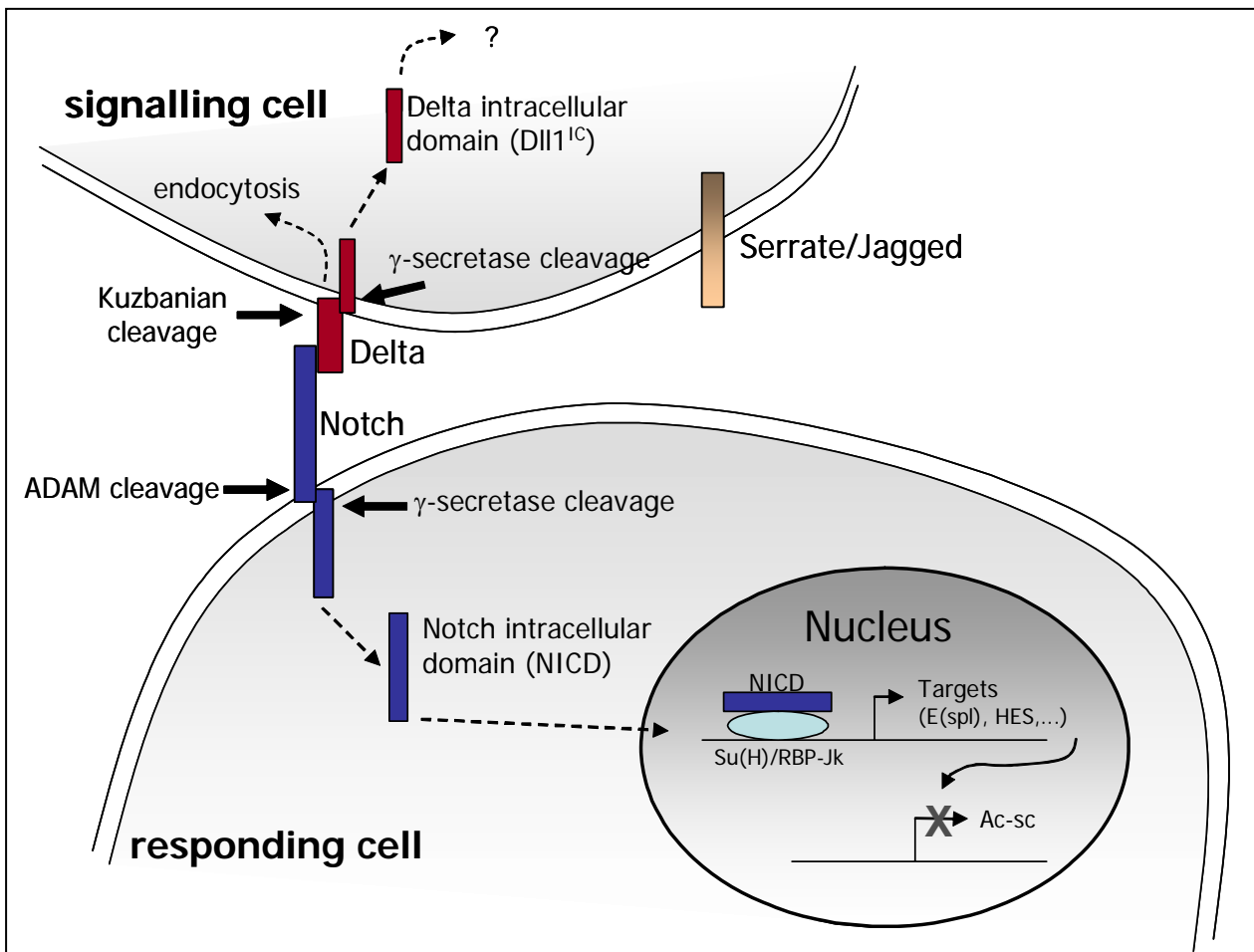
Figure 1: Schematic view of Delta/Notch signalling. Upon binding of the ligand Delta on the signalling cell to the receptor Notch on the responding cell the Notch receptor is cleaved by a ADAM protease on the extracellular side and a γ-secretase on the intracellular side which releases the intracellular domain of Notch (NICD). NICD translocates into the nucleus where it associates with the Su(H) and activates target genes. The ligand Delta also undergoes different cleavage processes by Kuzbanian and a γ-secretase which might lead to the release of an intracellular domain into the cell and an extracellular domain into the intercellular space.

1.1.1.1   Receptors

The family of Notch receptors encode single transmembrane proteins. They contain a large number of tandemly arranged extracellular EGF-repeats and a family-unique LNG (Lin12/Notch/Glp-1) region, named after the first identified receptor molecules LIN-12 and Glp-1 in *C. elegans* and Notch in *Drosophila* (Greenwald 1985; Wharton et al. 1985). On the intracellular side the Notch protein consists of a submembrane domain which is composed of a RAM domain, six ankyrin repeats, a TAD (transcriptional activator domain) and a PEST domain (proline-, glutamine-, serine-, threonine-rich region). Just prior to and following the ankyrin repeats two nuclear localization sequences are present (Baron et al. 2002).

A three-step proteolytic model has been suggested for the activation of the 300 kDa Notch protein (Baron et al. 2002). During secretory transport through the Golgi body occurs the first cleavage by a Furin protease at position S1 (Blaumueller et al. 1997; Logeat et al. 1998).

The resulting halves are held together non-covalently by a calcium-dependent interaction (Rand et al. 2000). At the plasma membrane the Notch protein undergoes a ligand-dependent cleavage on the extracellular side by a metalloprotease from the ADAM family such as TACE (TNF-α-converting enzyme) or Kuzbanian (Brou et al. 2000) at position S2. Thus the bulk of the extracellular domain is released into the extracellular space, leaving a Notch intracellular domain attached to the membrane. This is followed by a constitutive intramembrane cleavage by the presenilin-dependent γ-secretase activity at position S3 (De Strooper et al. 1999; Struhl and Greenwald 1999; Ye et al. 1999; Mumm et al. 2000; Struhl and Greenwald 2001). The resulting soluble Notch intracellular domain (NICD) can subsequently translocate into the nucleus where it binds to effector proteins of the CSL (Suppressor of Hairless (Su(H)), or CBF1 or RBP-Jκ in vertebrates) and MAML (mastermind-like) family (Baron 2003; Weng and Aster 2004) and activates transcription of downstream target genes (Jarriault et al. 1995; Kopan et al. 1996; Shawber et al. 1996b). The NICD contains the RAM domain, six ankyrin repeats and the TAD. Binding to CBF1 seems to be mediated by the RAM domain and the ankyrin repeats (Baron 2003). The binding to the effector protein as well as the TAD seem to be necessary to produce an open chromatin conformation by histone acetylase proteins (Kurooka and Honjo 2000).

In vertebrates four Notch genes have been identified (Notch1-4) (Coffman et al. 1990; Del Amo et al. 1992; Weinmaster et al. 1992). Apart from developmental defects observed in mice deficient of a receptor gene, in humans diseases due to the mutated receptors NOTCH1 and NOTCH3 have been identified. Defects in the NOTCH1 gene lead to acute lymphoblastic T-cell leukaemia (Capobianco et al. 1997; Joutel and Tournier-Lasserve 1998; Bresnick et al. 2000; Gridley 2004) and mutations in the NOTCH3 gene lead to CADASIL (cerebral autosomal dominant arteriopathy with subcortical infarcts and leukoencephalopathy). While the prevalence of CADASIL is unknown patients exhibit a variety of symptoms, including migraine with aura, mood disorders, recurrent subcortical ischemic strokes, progressive cognitive decline, dementia and premature death (Gridley 2003). The vascular lesions underlying CADASIL are a non-artherosclerotic, non-amyloid arteriopathy affecting primarily small cerebral arteries (Gridley 2003).

1.1.1.2 Ligands

As identified in *Drosophila* two distinct but related classes of ligands exist: Delta and Serrate. They are single transmembrane proteins which contain a number of EGF repeats on the extracellular side. One modified EGF repeat at the N-terminal region is called the DSL domain (Delta/Serrate/Lag-2). Delta and Serrate have been identified in *Drosophila* while Lag-2 was found in the nematode *Caenorhabditis elegans*. It is involved in receptor interactions. The number of EGF repeats present in DSL proteins can vary greatly. The intracellular domain of the ligands is short and shows little structural conservation. Evolutionary conserved homologues of the DSL proteins Delta and Serrate have been identified in many species (Bettenhausen et al. 1995; Chitnis et al. 1995; Henrique et al. 1995; Lindsell et al. 1995; Shawber et al. 1996a; Dunwoodie et al. 1997; Jen et al. 1997; Appel and Eisen 1998). In mouse three Delta proteins have been identified (*Dll1, Dll3, Dll4*) and two Serrate homologues called *Jagged 1* and *Jagged 2* (Bettenhausen et al. 1995; Shawber et al. 1996a; Dunwoodie et al. 1997; Oda et al. 1997; Shutter et al. 2000). It has

been believed for a long time that all events involved in signal transduction upon the binding of the ligand to the receptor happen on the side of the receptor expressing cell. Only recently it is becoming clear that Delta can be cleaved by the metalloprotease Kuzbanian on the extracellular side to release a soluble form, the Delta extracellular domain (DIED) (Six et al. 2003). The function of this soluble extracellular domain is not clear, though it is believed that secreted forms of Delta and Serrate act in a dominant-negative fashion in *Drosophila* and thus result in its inactivation (Mishra-Gorur et al. 2002). Furthermore it has been found that Delta is also cleaved by the γ-secretase presenilin on the intracellular side which leads to the release of the intracellular domain (Dll1^{IC}) and localises in part to the nucleus (Six et al. 2003). The role of the Notch intracellular domain has been convincingly established (Baron et al. 2002; Baron 2003; Schweisguth 2004), indicating that the intracellular domain of *Dll1* might as well play a specific role in the nucleus such as transcriptional regulation.

In accordance with the hypothesis that the Dll1^{IC} might be involved in a signalling process within the Delta expressing cell proteins have been identified that interact with the cytoplasmic domain of *Dll1* in mouse (Pfister et al. 2003a). Detailed analysis showed that the intracellular domain of Dll1 (Dll1^{IC}) contains a PDZ-binding motif and a nuclear localization signal, which are evolutionary conserved among Delta homologues from different vertebrate species (Pfister et al. 2003a). PDZ domains potentially regulate intracellular signalling via coordination of the assembly of multiprotein signalling complexes. Additionally, the identified interaction protein of Dll1^{IC} Activin receptor interacting protein 1 (Acvrinp1) also contains PDZ domains and physically interacts with Dll1^{IC} *in vivo* (Pfister et al. 2003a). These findings also led to the hypothesis that *Dll1* might mediate signal transduction.

Mutations in the ligand genes of the mouse include diverse defects ranging from skeletal disruptions (*Dll3*) to embryonic lethality (*Dll1, Jag2*). In humans mutations of the ligands DLL3 and JAG1 have been found and associated with distinct diseases. Spondylocostal dystosis (SD) is due to a missense mutation in the DLL3 protein (Bulman et al. 2000). The prevalence is undetermined. SD patients exhibit short trunk dwarfism due to multiple hemivertebrae accompanied by rib fusions and deletions. A similar phenotype is observed in mice carrying the pudgy mutation in the *Dll3* gene (Kusumi et al. 1998; Kusumi et al. 2001; Dunwoodie et al. 2002; Turnpenny et al. 2003; Kusumi et al. 2004). Mutations in the JAG1 gene have been reported to cause Alagille syndrome. The estimated prevalence is 1 in every 70.000 live births. This autosomal dominant disorder is characterised by developmental abnormalities of the liver, heart, eye, skeleton and several other organs (Krantz et al. 1997; Krantz 2002). Mice homozygous for a null mutation of the *Jag1* gene die in utero due to vascular defects in the embryo and the yolk sac (Kiernan et al. 2001).

1.1.1.3   Effector genes

The effector genes of Notch signal transduction are transcription factors of the CSL (CBF1/Supressor of Hairless/Lag-1) family and transcriptional co-activators of the mastermind-like (MAML, MAML1-3 in vertebrates) family. CSL proteins such as CBF1 in the mouse (also known as RBP-Jκ in other vertebrates) (Matsunami et al. 1989; Henkel et al. 1994), Suppressor of Hairless (Su(H)) in *Drosophila* (Ashburner 1982) or Lag-1 in *C. elegans* (Lambie and Kimble 1991) contain a conserved 400 amino acid DNA binding domain.

The effector genes come into action after the NICD translocated into the nucleus. There they form a ternary complex NICD-MAML-CSL which associates with the DNA via the CSL-binding domain and activates transcription of the target genes.

Because of the involvement of CSL proteins in the signal transduction this way is called CSL-dependent signalling. However CSL-independent ways of signalling also exist (1.1.2.3).

1.1.1.4   Target genes

The first genes that are activated are the basic helix-loop-helix (bHLH) genes of the *Enhancer of split* complex (*E(spl)*) (*Hes* genes in vertebrates). The transcriptional activation of *E(spl)/Hes* genes leads to the translation of the corresponding gene product which in turn represses the expression of the downstream *achaete-scute* (*ac-sc*) (*Mash* genes in vertebrates) complex. The *ac-sc* complex contains proneural genes that encode proteins involved in the segregation of neuronal and epidermal lineages and that appear to be necessary for Delta expression.

1.1.2 Levels of Notch regulation

Above, the core elements of the Delta/Notch signal transduction pathway were presented. However, many mechanisms have been identified which can influence and regulate the signal transduction in different ways.

1.1.2.1   Regulation of receptor-ligand interaction via glycosylation

Notch receptors are glycoproteins and can be modified by the addition of fucose to specific Serine and Threonine residues in their EGF-like repeats. The *O*-fucosylation of Notch is catalysed by the GDP-fucose protein *O*-fucosyltransferase1 (Ofut1). It could be shown that loss of Ofut1 mimics loss of Notch activity while overexpression of Ofut1 blocks Notch receptor signalling (Okajima and Irvine 2002). Ofut1 regulates receptor-ligand interaction by changing the affinity of Delta to Notch thus that a high level of *O*-fucosylation promotes Delta binding and therefore receptor activation while low level of *O*-fucosylation of the Notch protein reduces the affinity of Delta to Notch (Schweisguth 2004).

Notch is further glycosylated by Fringe (Drosophila) (Lunatic fringe in the mouse). Fringe is a β-1,3-*N*-acetyl-glucosaminyl (GlcNAc) transferase that physically interacts with Notch as it modifies O-linked fucose on the EGF-repeats. The GlcNAc modifications promote Delta-dependent signalling while inhibiting Serrate-dependent signalling, which represents a key step in defining a spatially restricted zone of Notch signalling at compartment boundaries (e.g. Drosophila wing dorsal-ventral boundary, and vertebrate embryonic somite boundaries) (Baron et al. 2002; Schweisguth 2004).

1.1.2.2   Regulated degradation of proteins

An important aspect of regulation of Delta/Notch signalling is ubiquitin-dependent protein degradation. The system is involved in the regulation of many basic cellular processes such as cell cycle and division, differentiation and development, the response to stress and

extracellular modulators, morphogenesis of neuronal networks, modulation of cell surface receptors, ion channels and the secretory pathway, DNA repair, regulation of the immune and inflammatory responses, biogenesis of organelles and apoptosis (Ciechanover 1998).

Degradation of a protein by the ubiquitin system involves two distinct and successive steps: (i) covalent attachment of multiple ubiquitin molecules to the target protein; and (ii) degradation of the tagged protein by the 26S proteasome (or, in certain cases, by the lysosome/vacuole). Conjugation of ubiquitin to the substrate proceeds via a three-step mechanism involving the ubiquitin activating enzyme E1, ubiquitin-carrier proteins or ubiquitin-conjugating enzymes (UBCs) (E2) which transfers ubiquitin form E1 to a member of the E3 ubiquitin-ligase family. The E3 enzyme catalyzes the covalent attachment of ubiquitin to the substrate. E3 ligases are regulating the specificity of that much used process in the cell (Ciechanover 1998).

Two main classes make up the E3 protein ligases. On the one hand Ring finger domain proteins which form non-covalently linked intermediates with ubiquitin and on the other hand HECT domain proteins which form covalently linked intermediates (Baron et al. 2002). Both classes have been linked to Notch pathway regulation.

Sel10 belongs to the cdc4-related F-box protein family of SCF ubiquitin ligases. The mammalian homologue of *Sel10* can stimulate ubiquitination of nuclear NICD and trigger its proteasome-dependent degradation (Baron et al. 2002).
Nrarp is a small protein with two ankyrin repeat domains. It binds to NICD in the presence of Su(H) and was shown to stimulate degradation of NICD in Xenopus (Baron et al. 2002).

Neuralized (neur) (Drosophila) and mind-bomb (mib) (zebrafish) are E3 ubiquitin ligases regulating the ubiquitination of Delta (Schweisguth 2004). They are localised at the cell membrane and promote endocytosis of Delta in the signal-sending cell which seems to stimulate Notch activation in the signal-receiving cell (Schweisguth 2004). Mutations in neur and mib result in Notch-like mutant phenotypes, also disrupting lateral inhibition during neurogenesis in Drosophila (Baron et al. 2002; Schweisguth 2004).
The positive regulator of *deltex* (*dx*) (Drosophila) contains two WWE domains in its N-terminal region. WWE domains are found in proteins linked to ubiquitination or ADP ribosylation. The C-terminal domain contains a ring finger domain which supports the idea that *dx* might be an E3 ubiquitin ligase. Mutations in Drosophila *dx* show phenotypes similar to Notch loss-of-function and constitutively active expression of NICD can rescue *dx* phenotypes (Baron et al. 2002).
The Drosophila protein Suppressor of deltex (Su(dx)) is a negative regulator of Notch signalling. The E3 ubiquitin ligase belongs to the family of HECT domain proteins and contains two to four WWE domains. The mouse homologue of Su(dx) Itch has been shown to be able to associate with Notch and ubiquitinate it (Baron et al. 2002).

Neur, mib, dx and Su(dx)/Itch are also known to promote endocytosis which might represent a further level of regulation during Delta/Notch signalling. It may positively regulate signal transduction since active receptors might be brought to specific intracellular compartments where they might associate with the signal transduction machinery (Baron et al. 2002; Schweisguth 2004).

The regulated secretion, internalization and degradation or recycling of receptors and ligands also offers much opportunity for the regulation of signalling on different levels. Drosophila mutants that affect trafficking processes have been uncovered as genetic modifiers of Notch activity. These include Ca^{2+} ATPase (involved in protein transport through the ER and Golgi), clathrin (involved in coated vesicle formation), Hsc70 (a chaperone protein), Nsf (involved in membrane fusion) and Rab6 (involved in Golgi to Golgi transport) (Baron et al. 2002).

1.1.2.3   Further regulatory mechanisms

Further processes seem to be involved in the regulation of proper Delta/Notch signalling and will be named in this chapter to emphasise the complexity of this signal transduction pathway.

Components of the Wnt pathway have been shown to be involved in Delta/Notch signalling (Aulehla et al. 2003; Galceran et al. 2004; Hofmann et al. 2004). Additionally proteins have been identified (such as Nur77, NF-κB p50 subunit, disabled and others) that can bind to NICD and thus mediate signalling independent of Su(H) (Baron et al. 2002).
The protein numb represents a further possibility to influence differentiation. It is asymmetrically distributed in a cell prior to mitoses to ensure that only one daughter cell inherits the numb protein which then downregulates Notch signalling in this cell (Baron et al. 2002; Schweisguth 2004).
Furthermore there is increasing evidence that signalling independent of CSL (CBF1) exists and that it prevents cells from expressing new patterns of genes in contrast to regulating the number of cells as in lateral inhibition (Martinez Arias et al. 2002). A general mode of action during Delta/Notch signalling is regulation by negative feedback loops which has been shown clearly for the Hes1 mRNA and protein (Hirata et al. 2002).

1.1.3 Functions of Delta/Notch signalling

Delta/Notch signalling regulates many important patterning processes, such as the formation of boundaries in both space and time. The most prominent processes will be explained below.

1.1.3.1   Lateral inhibition / Lateral induction

Delta/Notch signalling is best known for its involvement in lateral inhibition, a mechanism first identified during *Drosophila* neurogenesis (Artavanis-Tsakonas et al. 1995; Artavanis-Tsakonas et al. 1999). The model proposes that within a cluster of initially equipotent cells a prospective neuronal cell (neuroblast) inhibits the surrounding cells from adopting a neuronal fate by expressing increased amounts of Delta protein (Figure 2). The following activation of Notch in the neighbouring cells leads to a downregulation of Delta and their differentiation into epidermioblasts. Thus it results in differentiation of the primary cell fate as neuronal progenitor cells (neuroblasts) and a secondary fate as epidermal progenitor cells (epidermioblasts). Investigations of the homologues of Delta/Notch pathway components in Xenopus (Chitnis et al. 1995), chicken (Henrique et al. 1997) and zebrafish (Haddon et al. 1998a; Haddon et al. 1998b) suggest that a similar process also regulates neurogenesis in

vertebrates. Chitnis and co-workers. reported that injection of *in vitro*-transcribed *X-Delta-1* into one blastomere of a two-cell stage embryo causes a striking reduction or complete elimination of *N-tubulin* expressing cells at the injected site of embryos in the neural plate stage. *N-tubulin* is a neuron-specific type-II ß-tubulin gene, which is a very early differentiation marker for primary neurons. These and other results suggest that *X-Delta-1* expressing cells are prospective neurons and that this signal inhibits neighbouring cells to follow that fate either.
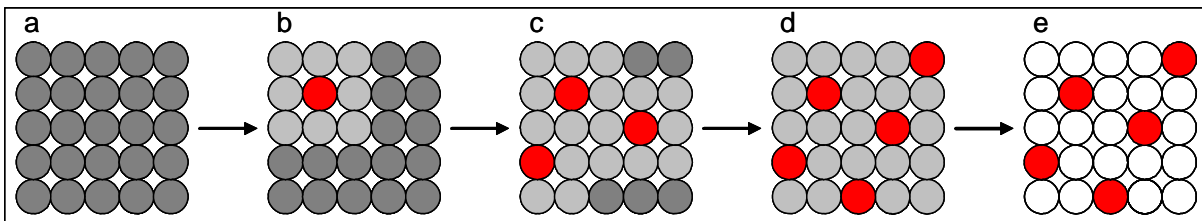
Figure 2: Schematic view of the process of lateral inhibition as observed during specification of the neuroectoderm in Drosophila. Cells in a cluster of equipotent cells express equal amounts of Delta and Notch (a). (b) Due to a stochastic change one cell in the cluster expresses more Delta (red cell) which leads to the downregulation of Delta in the surrounding cells (light grey). (c, d) The low levels of Delta protein in some cells (light grey) induce neighbouring cells to establish high Delta levels and thus downregulate the Delta expression in the surrounding cells. (e) Finally this cell-to-cell communication leads to a balance of cells that express only Delta (red) and cells that express only Notch (white).

Recent evidence for involvement in differentiation decisions during neurogenesis come from studies with neurospheres derived from neural stem cells of *Dll1*^{-/-} and wt mouse embryos (Grandbarbe et al. 2003). A neurosphere is the clonally progeny of a neural stem cell which is selected from embryonic brains through the action of EGF. It consists of a heterogeneous cell population, including the neural stem cells themselves and their progeny (Grandbarbe et al. 2003). The studies propose that Notch signalling acts in two steps, the first being the inhibition of the neural fate while promoting the glial cell fate. In a second step the differentiation into astrocytes is promoted by Notch while differentiation to neurons and oligodendrocytes is inhibited (Grandbarbe et al. 2003). The differentiation into astrocytes, however, seems to be dependent on the presence of the soluble ligand.

Apart from the nervous system the signalling pathway has been shown to define the selection between endocrine and exocrine cells during pancreas development in the mouse (Apelqvist et al. 1999). Studies of *Dll1* and *RBP-Jκ* deficient mouse embryos revealed, that impaired Notch signalling leads to an accelerated differentitation of pancreatic precursor cells into endocrine cells (Apelqvist et al. 1999). In the process of pancreas development obviously the endocrine cell fate represents the primary fate while development into exocrine cells represents the secondary fate.

1.1.3.2   Boundary formation

A fundamental patterning process during embryonic development of vertebrates is somitogenesis. The embryonic mesoderm is transiently composed of serially repeated epithelial segments called somites that emerge as bilaterally symmetrical pairs flanking the notochord and the neural tube along the anterior-posterior (AP) axis. In AP direction each somite finally matures and gives rise to the dermatome, the myotome and the sclerotome. Those differentiate further into the dermis, skeletal muscle and the axial skeleton.

The intervals between somites budding off from the anterior-most end of the presomitic mesoderm (PSM) differ from species to species (30 minutes in zebrafish, 90 minutes in chicken, 120 minutes in mouse and 8 hours in human) (Bessho and Kageyama 2003). This periodic event is controlled by the so called "segmentation clock" which runs in waves from the posterior end of the embryo to the anterior and thus defines the size of new somites. The process is characterised by waves of expression of oscillating genes, such as *Hes1, Hes7, Hey2,* and *Lfng* in the mouse (Forsberg et al. 1998b; Jouve et al. 2000; Leimeister et al. 2000; Bessho et al. 2001a; Bessho et al. 2001b; Dunwoodie et al. 2002) (Figure 3). Mutational studies have led to the hypothesis that Delta/Notch signalling is necessary for the segmentation clock (Aulehla and Johnson 1999; Dale and Pourquie 2000; Jiang et al. 2000; Schnell and Maini 2000; Bessho et al. 2003; Pourquie 2003).
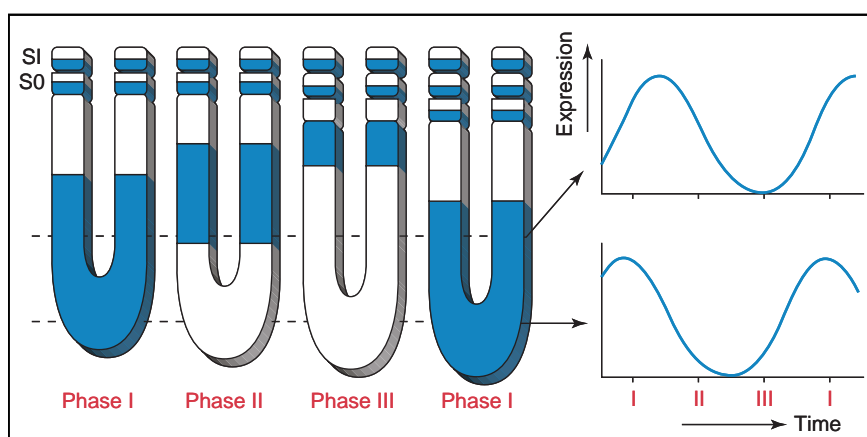
Figure 3: Oscillatory gene expression in the PSM. The expression of chairy1 mRNA (chick) sweeps across the PSM in a posterior-to-anterior direction repeatedly (blue shading), and each cycle is synchronous with the somite formation. This dynamic expression is not a result of cell movement. The cells at the indicated positions (dashed lines) periodically express chairy1 (graphs at right), and the phases are distinct depending on the anterior-posterior positions. (Adopted from Bessho and Kageyama 2003).

Dll1 null embryos exhibit a wavy neural tube and somites of irregular size and shape (Hrabe de Angelis et al. 1997). *Notch1* null embryos show significantly delayed and disorganised somitogenesis (Conlon et al. 1995). *RBP-Jκ* (*CBF1*) mutants exhibit an even more severe phenotype than *Notch1* mutants concerning somitogenesis (Oka et al. 1995) and mutants for further Delta/Notch pathway genes (*Dll3, Presenilin1, Hes1, Hes7*) (Kusumi et al. 1998; Ohtsuka et al. 1999; Koizumi et al. 2001; Hirata et al. 2004) also show somite phenotypes. These findings led to the conclusion that Delta/Notch signalling is essential for somitogenesis. Furthermore it is important for regional specificity of somitic compartments as the expression domains of these genes in the mouse suggest (Figure 4). *Dll1* for example is expressed throughout the PSM and is restricted to the posterior half of the prospective and

mature somites whereas *Dll3* is strongly expressed in the PSM and the prospective somite but not within epithelialised somites. These specific expression patterns are disturbed in Delta/Notch pathway mutants. In the *Dll1* mutant expression of the cyclic genes *Hes1* and *Lfng* is lost. Furthermore *Hes5* and *Jag1* is downregulated while *Dll3* is upregulated in the PSM and the primitive streak and *Notch1* is expressed normally within the PSM and the prospective somite (Barrantes et al. 1999). Additionally it has been shown that *Dll1* is responsible for the establishment and maintenance of somite boundaries in the mouse (Hrabe de Angelis et al. 1997). In the *Dll1* knockout the cranio-caudal polarity of the segments is lost (Hrabe de Angelis et al. 1997). The regional specificity of expression as well as disturbed cranio-caudal polarity in Delta/Notch pathway mutants shows that boundaries represent a key feature in this process.
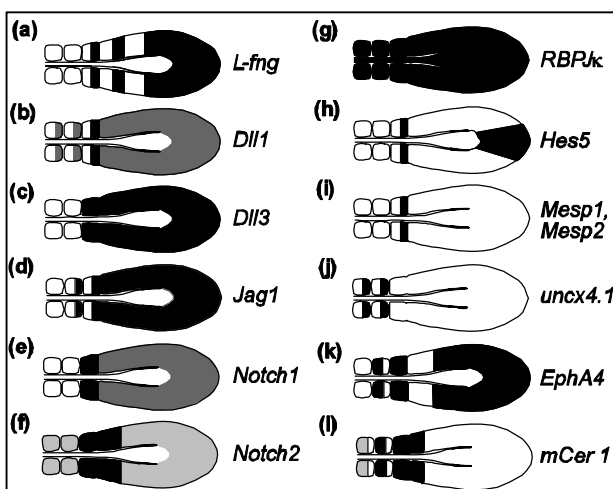
Figure 4: Schematic view of gene expression of Delta/Notch pathway genes in the PSM of the mouse. The illustration shows dorsal views with anterior to the left. The intensity of shading represents differences in gene expression levels for a gene but is not meant to describe differences in expression levels between genes. (Adopted from Barrantes et al. 1999)

However it was not known how the formation of the boundaries could be reached. Several models trying to explain the nature of the mechanisms underlying somitogenesis have been suggested, such as the "Clock and Wavefront" model (Cooke and Zeeman 1976), "Reaction-Diffusion" model (Meinhardt's model) (Meinhardt 1986), "Clock and Trail" model (Kerszberg and Wolpert 2000) and the "Einbahnstrasse" model (Duboule 1994) Recent results suggest that a gradient of the secreted growth factor Fgf8 could be implicated in converting the pulses of mRNA expression of cyclic genes into the periodic arrangement of segment boundaries (Dubrulle et al. 2001; Sawada et al. 2001; Pourquie 2003). *Fgf8* shows highest expression levels in the posteriormost part of the PSM while its expression progressively decreases in more anterior cells. The expression of *Fgf8* seems to maintain the cells in an immature state. Since the axis extends posteriorly during development the expression level slowly decreases in the most anterior cells until a threshold of Fgf8 signal is reached (determination front) which allows the cells lying anterior to it to switch on the their segmentation programme (Pourquie 2003). A similar mechanism was proposed for Wnt3a

(Aulehla et al. 2003). Wnt3a however acts upstream of Fgf8 in the PSM and thus could act together with or by way of the Fgf8 gradient (Pourquie 2003).

1.1.3.3   Left/right specification

A further important patterning process during vertebrate development is the establishment of the left-right (LR) axis. It is crucial for the correct morphogenesis of internal organs. The bending of the bilaterally organised heart tube to the right body side is the first visible sign of the body asymmetry in vertebrates (Beddington and Robertson 1999). The embryonic turning where the embryo twists around its rostro-caudal axis is another process (Faisst et al. 2002). Subsequently the asymmetric organization of visceral organs occurs. Three distinct steps are necessary for normal LR development. First, an initial asymmetry must become established in the embryo. Second, LR asymmetries must be consistently orientated with respect to the anterior-posterior and the dorsal-ventral axes. Third, global LR patterning information must become transmitted to organ primordia, which in turn must correctly interpret these positional cues and execute an appropriate morphogenetic response (Ramsdell and Yost 1998). If any of these processes fails disease conditions occur such as heterotaxia and situs inversus associated with cardiovascular defects.

Many genes in different organisms have been identified that show asymmetric expression or LR phenotypes when mutated. These include *iv, lefty1, pitx2, nodal* and others (Ramsdell and Yost 1998). Manipulation experiments revealed that the node (organiser in Xenopus, Henson's node in chicken) acts as an inducer of laterality (Danos and Yost 1995; Davidson et al. 1999). It is believed that in mammals directional rotation of cilia in the ventral node generates a laminar leftward flow of a morphogen which might be responsible for breaking the initial bilateral symmetry (Fujinaga 1997; Nonaka et al. 1998; Okada et al. 1999; Nonaka et al. 2002).

Although Delta/Notch signalling is involved in diverse patterning processes and cell fate decisions during development it has only recently been identified to be required for normal LR development (Krebs et al. 2003; Przemeck et al. 2003). It was observed that *Dll1* deficient embryos exhibit randomised heart looping and embryonic turning and randomised expression of LR-specific genes (Przemeck et al. 2003). Additionally it could be shown that the midline structures (notochord and floorplate) are altered concerning the number of cells building these structures, and also structural abnormalities of the node were observed (Przemeck et al. 2003). All these observations suggest that the Delta/Notch signalling pathway is essential for LR development and that it is involved in proper differentiation of node cells and node morphology (Przemeck et al. 2003).

1.2 Technologies for transcriptome and proteome analysis

1.2.1 DNA-microarray technology

DNA-microarray technology is a method to conduct large-scale analysis which allows simultaneous monitoring of the expression levels of thousands of genes. This method has been introduced in 1995 by M. Schena (Schena et al. 1995). There are many different applications such as RNA expression profiling, protein and antibody chips, tumor identification and characterization, drug target discovery and drug testing. The focus of this project is on RNA expression profiling with the identification of differentially expressed genes in wildtype and mutant mouse embryos.
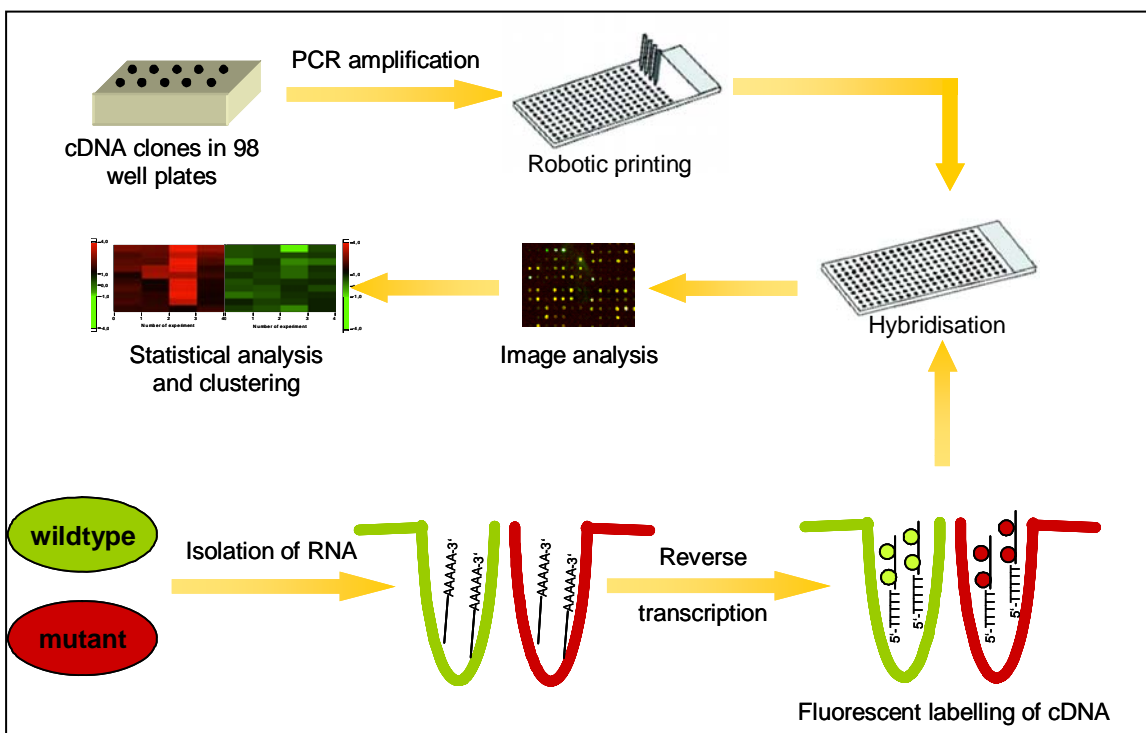
Figure 5: A scheme showing the microarray technology. cDNA clones which should be present on the microarray have to be amplified by PCR and subsequently printed in a solid surface such as a glass slide. RNA of the samples of interest has to be extracted, reversely transcribed and labelled, e.g. with the fluorescent dyes Cy3 and Cy5. In the following steps the labelled sample is hybridised to the microarray, unbound target is removed by washing and the array is scanned with a fluorescent scanner or phosphoimager. Using statistical procedures the raw data is analysed.

An overview over the procedure used in microarray technology is presented in Figure 5. DNA-microarrays (or DNA-chips) are nylon membranes or glass slides on which gene sequences in form of cDNAs or oligomers are immobilised as probes (designation according to *Nature Genetics* 21 (Suppl.), 1999). To obtain targets, which can then be hybridised to a

chip, RNA from cells or organs is reversely transcribed and labelled radioactively or with fluorescent dyes. According to the probe sequences, targets with the complementary sequence will bind to a certain spot. The amount of labelled cDNA bound to each probe can then be measured by autoradiography or the detection of the fluorescent intensity on each spot. Depending on the number of immobilised DNA samples it is possible to simultaneously measure expression levels of thousands of genes within a single experiment. Using the fluorescent labelling approach, two distinct samples, e.g. mutant and wildtype tissues, can be used on the same chip. With radioactive labelling, two hybridizations for two distinct samples have to be performed. Despite this disadvantage, the detection of radioactivity is more sensitive than of fluorescence. However, this technology represents a versatile method to identify gene functions or genetic interactions such as new target genes involved in developmental or metabolic pathways (Gullans 2000; Hughes et al. 2000; Miki et al. 2001).

Microarrays represent a powerful tool to conduct large-scale experiments as well as being a sensitive system. The quality of the results strongly depends on many features: the quality of the chip itself, the quality of RNA and labelling, the image processing and the computational analysis of the obtained raw data (Drobyshev et al. 2003a). The surface chemistry of the glass slide (poly-lysine, aldehyde-amine, gamma-amino-propyl-silane), the mechanism of immobilizing the DNA (covalent or non-covalent attachment) (Zammatteo et al. 2000), the kind of probe (cDNA, oligo) (Halgren et al. 2001; Kane et al., 2000), the selection of probe sequences (from 3´ UTR, coding region, etc.), the amount of immobilised probe and factors such as the spotting robot and the used pins (solid or split pins), influence the chip quality and have to be optimised to obtain good and reproducible results (Schuchhardt et al. 2000). The RNA used for expression profiling experiments has to be of best quality which can be reached by the selection of the RNA isolation protocol and subsequent quality control on denaturing agarose gels. The labelling procedure consists of reverse transcription of RNA and labelling with radioactive nucleotides or fluorescent dyes such as Cy3 and Cy5. The labelling efficiency of samples that will be compared should be equal. The next critical step is the image processing where bad and low intensity spots should be excluded from the analysis. The greatest challenge however might lie in the statistical analysis of the data to identify significant changes and biologically relevant information.

The main advantages of the method are that different kinds of biological questions can be investigated and that the expression of a large number of genes can be analysed simultaneously. Limitations lie in the relatively large amount of starting material needed to perform repetitions which are absolutely necessary to obtain significant data and the fact that only relative and no absolute expression levels can be measured. Furthermore it has to be kept in mind that biological noise can occur in heterogeneous samples such as embryos consisting of a large number of different cell types.

1.2.2 Tools for proteome analysis

Proteomics is defined as the analysis of the protein complement expressed by a genome (Pennington et al. 1997). It has been suggested as an approach to the quantitative description of the state of a biological system by the quantitative analysis of protein expression profiles (Wilkins et al. 1997). Proteome analysis is especially attractive because

of its potential to determine properties of biological systems that are not apparent by DNA or mRNA sequence alone, including the quantity of protein expression, the subcellular localization, the state of modification and the association with ligands and the rate of change with time of such properties (Gygi et al. 1999).

A common implementation of proteome analysis is the combination of two-dimensional gel electrophoresis (2D-ge) (isoelectric focusing-sodium dodecyl sulphate [SDS]-polyacrylamide gel electrophoresis) for the separation and quantitation of proteins with analytical methods for their identification, mainly mass spectrometric protein analysis techniques (Figure 6). As the 2D-ge displays the protein status of an organ/tissue/cell line at a specific time point it is just a descriptive technique. The combination of the descriptive 2D-ge with analytical mass spectrometric techniques has added the possibility of establishing the identity of the separated proteins. Furthermore, in combination with quantitative mRNA analysis it is now possible to correlate quantitative protein and mRNA expression data.
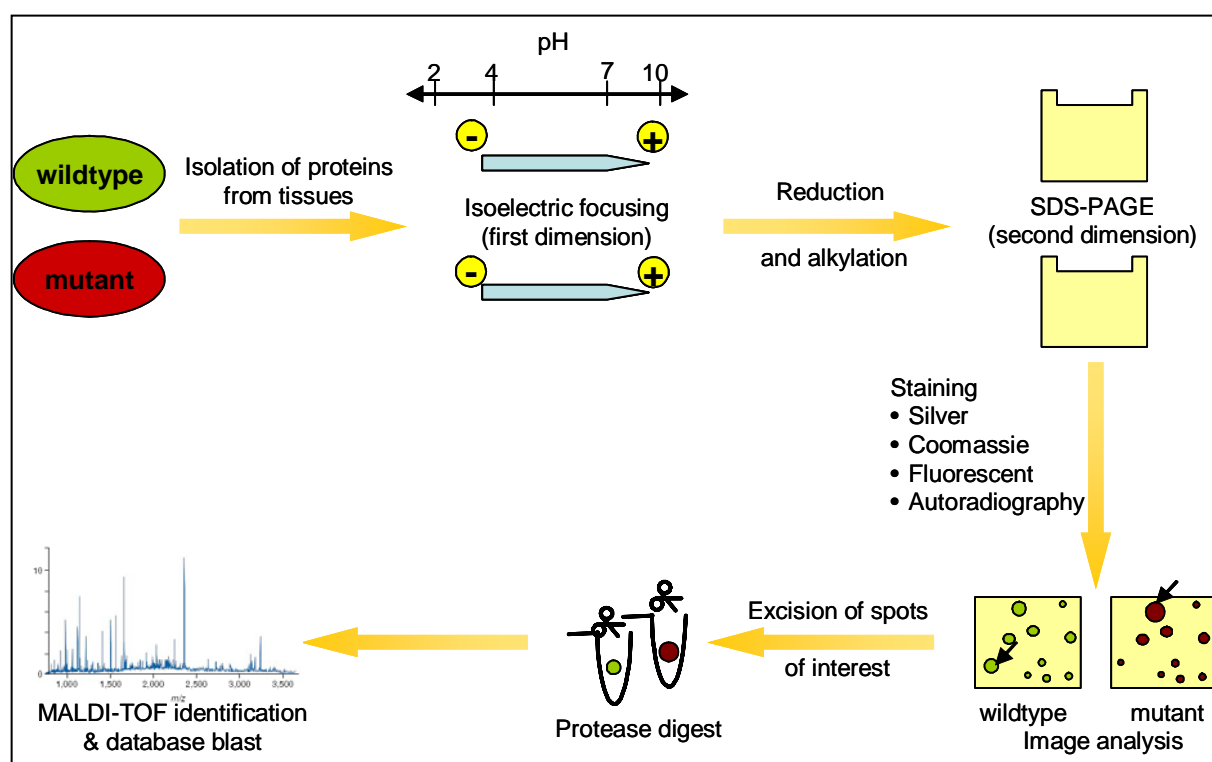
Figure 6: A scheme showing the 2D-gelelectrophesis based proteomics approach (modified from Pandey and Mann, 2000. Protein is isolated from test samples and loaded on immobilised pH gradient (IPG) stripes for isoelectric focussing as this represents the first dimension. After reduction and alkylation the second dimension sodium dodecyl sulphate (SDS)-polyacrylamide gel electrophoresis (PAGE) is performed to separate the proteins according to their molecular weight. Several methods which differ in sensitivity (silver, Coomassie, fluorescent staining, autoradiography) can be used to stain the gels and visualise the proteins. Following image analysis spots of interest are excised from the gels, digested by specific proteases and analysed by MALDI-TOF. The obtained spectra are subsequently blasted against protein databases to identify the protein.

2D-ge is used for the separation, visualization and quantitation of proteins on a single gel. However it is worth to note that the mouse genome contains roughly 20.000-25.000 genes (Consortium 2004). At a given time point during embryonic development maybe 5.000-10.000 genes might be expressed (estimation). The number of abundant proteins may be two to three-fold higher due to different cellular localizations, modifications and processing. Good two-dimensional gels can resolve approximately 1500-2000 proteins (A. Harder, personal communication). Thus it is obvious that only the most abundant proteins can be visualised on the gel if a crude protein mixture is used. A possible solution for this problem is to reduce complexity of a biological sample by fractionation.

A significant breakthrough in proteomics has been the mass spectrometric identification of gel-separated proteins. It relies on digestion of gel-separated proteins into peptides by a sequence-specific protease such as trypsin. The peptides are then analysed using a "peptide-mass mapping" approach which was initially suggested by Henzel et al. (Henzel et al. 1993). It results in a "peptide-mass fingerprint" of the studied protein. The mass spectrum is obtained by matrix-assisted laser desorption/ionization (MALDI), which results in a time-of-flight (TOF) distribution of the peptides in the mixture. The obtained mass spectra are used to search against protein sequence databases to identify the corresponding protein. As more and more genes will be completely annotated in the databases the success rate of MALDI with increase further.

The main advantages of this proteomics approach lie in the ability to identify post-translational modifications or different states of proteins due the changes in molecular weight. The relatively low level of resolution of 2D-gels is the major limitation. Furthermore, as for DNA-microarrays, analysis of heterogeneous samples represents a big problem.

1.2.3 Correlation between protein and mRNA abundance

It is becoming clear that neither of the both techniques by themselves is sufficient to describe a biological system quantitatively. This evidence comes from discoveries of posttranscriptional mechanisms controlling the translation rate (Harford and Morris 1997), the half-lives of specific proteins or mRNAs (Varshavsky 1996) and the intracellular location and molecular association of the protein products of expressed genes (Urlinger et al. 1997). The strict relationship between transcripts and the protein complement, which was postulated first by Archibald Garrod in 1909 and rediscovered in 1941 by George Beadle and Edward Tatum as "one gene one enzyme hypothesis", might not be completely correct at least in multicellular organisms. In mice or humans for example a number of roughly 20.000-25.000 genes (Consortium 2004) stand versus estimations of 100.000-400.000 proteins. This leads to the conclusion that proteomics and transcriptomics are complementary approaches which are both necessary to understand a biological system.

1.3 Aim of this work

The Delta/Notch signal transduction pathway is conserved between many species. During the embryonic development of the mouse the Delta/Notch pathway is involved in diverse patterning processes: lateral specification during neurogenesis and pancreatic development, left/right organization, and involvement in processes like the synchronization/organization of the segmentation clock and establishment and maintenance of somite boundaries during somitogenesis are some of them. Only a few of these developmental processes can be explained adequately by the classical Delta/Notch pathway model describing lateral inhibition.

In order to identify novel targets of *Delta1* on RNA, as well as protein level, I started to screen the transcriptome and proteome using DNA-chip technology and 2D-gelelectrophoresis combined with mass spectrometry of *Delta1* (*Dll1*)-deficient and *Dll1*-wildtype embryos at E10.5. The identified differentially expressed genes and proteins should be further analysed for their potential involvement in Delta/Notch signalling.

For the genes whole mount *in situ* hybridisations were carried out systematically as a scanning method to identify genes expressed in tissues where Delta/Notch signalling is functionally required, e.g. in the somitic and presomitic mesoderm and neural tissues.

Until now almost all expression studies concerning the Delta/Notch pathway have been performed on RNA level. Only very limited data on protein regulation during this developmentally important pathway is known. Therefore the protein candidates should first be verified with alternative methods and furthermore analysed according to their potential connection to Delta/Notch signalling.

The data sets from the RNA and protein expression analyses present distinct views on the same biological system. The data of both analyses should be compared to get new insights into regulatory processes of the pathway and cellular differences between wildtype and *Dll1* deficient embryos.

2 Material & Methods

2.1 Material

2.1.1 Antibodies

Primary Antibodies for Western Blot analysis:

- <u>Abcam</u>: anti-gamma Tubulin (ab11317) (1:1000), anti-GPR78 BiP (ab2902) (1 µg/ml), anti-hnRNP A1 (ab4791) (1:500), anti-hnRNP L (ab6106) (1:1500), anti-Hsp60 (ab8071) (1:300), anti-PPP2CA (ab1309) (1:1000), anti-USP14 (ab4554) (1 µg/ml), anti-67kD Laminin Receptor (ab711) (1:1000)

- <u>Santa Cruz Biotechnology</u>: AFP (C-19) (sc-8108) (1:300), ApoA-IV (M-19) (sc-19040) (1:300), Calregulin (N-19) (sc-6468) (1:500), EF-2 (V-18) (sc-13002) (1:300), eIF3 ζ (Y-20) (sc-16372) (1:300), Hemoglobin α (H-80) (sc-21005) (1:500), hnRNP A3 (C-17) (sc-16543) (1:300), MDGI (N-14) (sc-15974) (1:300), MTAP (C-20) (sc-17017) (1:300), Prealbumin (C-20) (sc-8104) (1:300), TH (C-20) (sc-7847) (1:300), Trx (FL-105) (sc-20146) (1:300), Unc18-3 (C-15) (sc-14567) (1:300), 14-3-3 ε (T-16) (sc-1020) (1:300), 14-3-3 ζ (C-16) (sc-1019) (1:300)

- <u>Sigma</u>: anti-β-Actin Clone AC-74 (A 5316)

- <u>Upstate</u>: Anti-Cu/Zn SOD (#07-403) (1:500), Anti-NSF (#07-364) (1:1000)

Secondary antibodies:

- Goat anti-Mouse, HRP conjugated: Biorad #1706516 (1:5000)

- Goat anti-Rabbit, HRP conjugated: Jackson Immuno Research #111-035-144 (1:10000)

- Rabbit anti-goat, HRP conjugated: Jackson Immuno Research #305035045 (1:5000)

- Anti-Digoxigenin-AP Fab fragments: Roche #1 093 274 (1:5000)

2.1.2 Buffers and Solutions

Buffer	pH	Composition
PBS	7.4	137 mM NaCl, 2.7 mM KCl, 10 mM Na_2HPO_4, 2 mM KH_2PO_4
TAE	8.0	40 M Tris-Ac, 1 mM EDTA
TE	8.0	100 mM Tris-HCl (pH 8.0), 10mM EDTA (pH 8.0)
Tail buffer		5 mM KCl, 1 mM Tris-HCl pH 8.3, 0.5% Gelatine, 0.45% NP40, 0.45% Tween20
Tris-HCl	7.x	121.1g Tris base in 800ml H_2O, x ml HCl (32%)
Tris-HCl	8.0	121.1g Tris base in 800 ml H_2O, 42 ml HCl (32%)
SSC (20x)	7.0	3.0 M NaCl, 0.3 M NaOAc
FA-gel buffer	7.0	200 mM MOPS, 50mM NaOAc, 10mM EDTA (pH 7.0)
Ripa		0.05% SDS, 75 mM NaCl, 5 ml NP40, 0.5 mM EDTA, 25 mM Tris-HCl pH 8, 0.5% Deoxycholate
PBT	7.4	PBS, 0.1% Tween20
Proteinase K buffer	7.0	10 mM Tris-HCl pH 7, 0.5 mM EDTA
Hybridisation buffer (wish)	6.0	50% deionised formamide, 5x SSC, 5 µl Heparin sol, 0.1% Tween20
Hybridisation buffer (chips)		50% deionised formamide, 6x SSC, 0.5% SDS, 5x Denhardt's solution
Prehybridisation buffer		6x SSC, 0.5% SDS, 1% BSA
SSC/FA/Tween20		50% deionised formamide, 2x SSC, 0.1% Tween20
TBST		137 mM NaCl, 2 mM Tris-HCl pH 6.7
RNase solution		5 mM NaCl, 0.1 mM Tris-HCl pH 7.5, 0.1% Tween20
Gel buffer (WB)		3 M Tris, 0.3% SDS
Cathode buffer		0.1 M Tris, 0.1 M Tricin, 0.1% SDS
Anode buffer (5x)		1 M Tris-Cl pH 8.9
Blotting buffer		48 mM Tris, 39 mM Glycin, 1.3 mM SDS, 20% Methanol
Laemmli sample buffer		50% glycerol, 0.16 M Tris-HCl pH 6.8, 5% 2-Mercaptoethanol, 2% SDS, 0.01% Bromphenol blue
Stripping buffer		100 mM 2-Mercaptoethanol, 2% SDS, 62.5 mM Tris-HCl pH 6.7

2.1.3 Chemicals and Reagents

All chemicals had pa grade and were purchased from Sigma except for:

Acrylamid/Bisacrylamid (30:1) (Roth)
Chloroform, Ethanol, 2-Propanol, Xylol (Merck);
dATP, dCTP, dGTP, dTTP (MBI Fermentas),
ECL Plus Western Blotting Detection Reagents (Amersham Biosciences)
Formamide, Phenol (Roth);
Glycogen (Roche)
Glycin (Amersham Biosciences)
Hematoxilin (Fluka);
TEMED (Biorad)
Tween (Fisher Scientific);

2.1.4 Clones

The 20k clone set containing gene specific sequences for DNA-chips were purchased from Lion Bioscience. All clones contain 300-800 bp inserts mostly derived from the 3´ untranslated region of a gene. Sequences are depleated of PolyA tails; they contain approximately 150 bp adaptor sequence instead. Coding region and repetitive elements have been avoided for clone selection. All inserts are sequence verified.

2.1.5 Competent cells

Chemically and electro-competent cells were purchased from Stratagene (XL10-Gold Ultracompetent Cells, XL1-Blue Competent Cells, SURE Competent Cells, ElectroTen-Blue Electroporation-Competent Cells) and Invitrogen (TOP10 Chemically and Electrocompetent cells).

2.1.6 DNA-Chips

Atlas GlassMouse1 (Clontech)

The Atlas GlassMouse 1 chip contains 1081 genes that are represented by ~80mers. For each gene three sequences from a region that does not show any homologies to other genes on the array and minimal homologies with related gene families were designed by sequence database analysis. The three oligomers per gene were tested for hybridization strength and specificity. The oligo that yielded the strongest signal and the lowest degree of crosshybridization to other genes on the array was then selected for spotting (CLONTECHniques, Jan 2001). The chip also contains a number of control spots. Each field (7x7 spots) contains a Cy 3-labelled oligo in position a1 or g1, which serves as an orientation marker and spotted buffer in the last position. In addition the chip contains a cluster of internal controls such as a cDNA Synthesis Control, a labelling reaction control (Coupling

Reaction Control Oligo), housekeeping genes and λ-phage sequences without homologies to known mouse sequences as negative controls.

20k cDNA mouse array

The clone set used for the 20k chip was purchased from Lion Bioscience. The cDNAs are 300-800 bp in length and mostly derived from 3´ UTRs (untranslated regions) depleated of coding regions and repetitive elements. Additionally polyA tails are eliminated and all clones are sequence verified. The complete clone set was amplified by PCR, and the integrity of the products was checked on agarose gels.

Additionally there were 205 cDNA clones spotted which were obtained from a RDA (representational difference analysis) screen. The RNA expression in the presomitic mesoderm and the first to second somite of *Dll1*-wt and *Dll1*$^{-/-}$ embryos was compared using a subtractive method. Identified cDNAs or ESTs were subcloned. The screen was performed during collaboration with the group of Dr. Jörg Hoheisel at the DKFZ in Heidelberg. The 20k chip contains 146 buffer spots as control.

2.1.7 Flurescent dyes

Cy3 and Cy5 fluorescent dyes were purchased from Amersham. The lyophilised dye was stored in the dark at 4°C and dissolved in 73 µl DMSO just prior to use. Spare dye solution was stored at -20°C.

2.1.8 Enzymes

- Restriction enzymes were purchased from MBI Fermentas except for BfrBI, EcoRI, FokI, NsiI, SalI, SmaI, SpeI (New England Biolabs) and SmaI, SpeI (Promega)

- Reverse Transcriptase SuperScript II was purchased from Invitrogen

- RNA Polymerases T3, T7 and Sp6 were purchased from Roche

- Taq enzymes were purchased from Biotherm. Pfu Ultra, EasyA and Herculase polymerases for large PCR products and including proof-reading activity were purchased from Stratagene

- Ligases were purchased from New England Biolabs (T4 DNA Ligase, Quick T4 DNA Ligase)

2.1.9 Laboratory equipment

- Blotter: Bio-Rad Trans-Blot SD, Semi-Dry Transfer Cell

- Centrifuges: eppendorf centrifuge 5415R, eppendorf centrifuge 5810R

- Film development: typon medical OPTIMAX

- Homogeniser: Heidolph DIAX 900

- Incubators: wtb binder, Hybaid Shake ´n` Stack

- Laser microdissection: P.A.L.M. Microbeam

- Microscopes: Leica MZ 95, Leica MZ APO, Zeiss Axioplan 2

- PCR Machines: MJ Research PTC-200, Stratagene Robocycler Gradient 96

- Photometer: eppendorf BioPhotometer

- SpeedVac: UNIEQUIP univapo 150ECH

- The Cloning Gun Bactozapper: Tritech Research

- Thermal Cyclers: eppendorf Thermomixer comfort

- Waterbath: B. Braun Thermomix BM

2.1.10   Mice

2.1.10.1   *Dll1*^{lacZ}

The *Delta-like 1* gene was knocked out by the replacement of amino acids 2-116 with the lacZ gene of *Escherichia coli* (Hrabe de Angelis et al. 1997). Heterozygous animals do not show any phenotype. Homozygous animals are not viable. They die around 11 dpc (days post conception) during embryonic development.

To obtain *Dll1*$^{lacZ/lacZ}$ mutants *Dll1*$^{lacZ/+}$ mice were mated. Noon of the day a vaginal plug was observed was taken as 0.5 dpc.

The homozygous embryos were identified by phenotypic inspection. Mutants show an undulated neural tube and irregular somites. At 10.5 dpc they consistently have inner bleeding in the head and neural tube and they are sometimes hydrocephalic (Hrabe de Angelis et al. 1997). Adult animals were genotyped by PCR.

2.1.10.2   *Dll3*^{pu}

The *pudgy* mutation in the *Dll3* gene arose during an X-ray mutagenesis screen at the Oak Ridge National Laboratory (Kusumi et al. 1998). *pu* mutants have a 4 bp deletion in the third exon which leads to a frame shift and early truncation of the expected *Dll3* product prior to the conserved DSL (*Delta-Serrate-Lag2*) domain.

Heterozygous animals are phenotypically normal. Homozygous animals are viable but show severe vertebral and rib deformities. *Dll3*$^{+/pu}$ and *Dll3*$^{pu/pu}$ are fertile and were mated to obtain heterozygotes and homozygotes. Noon of the day a vaginal plug was observed was taken as 0.5 dpc.

Adult animals and embryos were genotyped by PCR as described in (Kusumi et al. 1998).

2.1.10.3   *Jag1*^{htu}

The *Jag1*^{htu} mutant arose during an ENU mutagenesis screen at the GSF Research Centre. Heterozygous mice showed a head-tossing behaviour. Homozygotes are not viable and die

during embryonic development around day E11.5 because of defects in vascular remodelling (Kiernan et al. 2001).

Mapping and sequence analysis revealed a point mutation at position 1134 of the *Jag1* gene. This G→A transition leads to a missense mutation resulting in a nonconservative amino acid substitution of a glycine by an aspartic acid (Kiernan et al. 2001).

2.1.11   Molecular weight markers

- 100bp DNA Ladder, 1kb DNA Ladder, RNA Ladder was purchased from MBI Fermentas.
- Precision Plus Protein Standards was purchased from Biorad.

2.1.12   Ready-to-use-systems

- RNeasy, Mini prep, Gel extraction, QIAquick PCR purification and Nucleotide removal kits were purchased from Qiagen.
- Absolutely RNA Nanoprep Kit was purchased from Stratagene
- Wizard Plus Midiprep kit was purchased from Promega
- Rapid Ligation Kit was purchased from Roche
- MessageAmp^{TM} aRNA Kit was purchased from Ambion
- Platinum SYBR Green qPCR SuperMix UDG was purchased from Invitrogen

2.1.13   Software and databases

- GenePix Pro 3.0 (Axon Instruments)
- Genomatix Suite 3.3.0 (Genomatix)
- LabView (National Instruments)
- VectorNTI (Informax)
- Cluster software at http://rana.lbl.gov/EisenSoftware.htm
- Phosphorylation prediction NetPhos 2.0 at http://www.cbs.dtu.dk/services/NetPhos/
- Celera Genomics at http://myscience.appliedbiosystems.com/
- Ensembl at http://www.ensembl.org/
- Lion Database at http://www.rzpd.de
- MGI Database at http://www.informatics.jax.org/
- NCBI Unigene at http://www.ncbi.nlm.nih.gov/entrez/query.fcgi?db=unigene

2.2 Methods

2.2.1 Dissection of embryos

Embryos were obtained from timed pregnancies. The mother was sacrificed by carbon dioxide asphyxiation. Embryos including placentas were removed and placed into ice cold 1x PBS. Embryos were dissected in 1x PBS.

If the embryos were used for RNA or protein isolation they were put each into a separated tube. All liquid was removed and embryos were weighed and placed into liquid nitrogen immediately.

If the embryos were used for whole mount *in situ* hybridisation (wish) embryos were either pooled according to their phenotype (*Dll1*[lacZ]) or each embryo was placed into a separated tube. Yolk sac material was collected for PCR genotyping. The embryos were fixed in 4% PFA/PBS over night at 4°C. On the next day the embryos were dehydrated on ice through 25%, 50% and 75% MethOH/PBS for 10 min each and bleached in 14% H_2O_2/MetOH for 1 hr on ice. Embryos were washed two times with a large volume of 100% MetOH for 10 min on ice and stored at -20°C until further use.

2.2.2 Genomic typing

2.2.2.1   Isolation of DNA

For genotyping of adult mice tail clips were taken at three weeks of age. For the genotyping of embryos during dissection the amnion was removed carefully, washed in fresh PBS and placed in a separate tube.

The Proteinase K digestion was done in 300 µl (tail clips) and 30 µl (amnion) Tail buffer containing 20 µg/ml Proteinase K, respectively.

2.2.2.2   PCR

Dll1[lacZ]

25 µl reaction volume

2.5 µl	Qiagen 10x PCR buffer
5 µl	Qiagen solution Q
2 µl	10 µM Dll1 FP Primer
1 µl	10 µM Dll1 BP Primer
1 µl	10 µM LacZ3BP Primer
0.5 µl	10 mM dNTP-mix
11.7 µl	H_2O
1 µl	template DNA
0.3 µl	Qiagen Taq polymerase

Primer sequences:

Dll1 FP	5´ CAAGGGCGTCCAGCGGTAC 3´
Dll1 BP	5´ CCTTGCTAGGACGCAGAGGC 3´
LacZ3BP	5´ GCACCACAGATGAAACGCCG 3´

Conditions:

94°C	4 min
	35 cycles
94°C	30 sec
62°C	30 sec
72°C	40 sec
72°C	5 min

Dll3^{pu}

25 µl reaction volume

2.5 µl	10x PCR buffer
1 µl	25 mM MgCl$_2$
1 µl	100 mM Dll3pu1 primer
1 µl	100 mM Dll3pu2 primer
0.5 µl	25 mM dNTP-mix
14.5 µl	H$_2$O
4 µl	template DNA
0.5 µl	Taq polymerase

Primer sequences:

| Dll3pu1 | 5´ ACGAGCGTCCCGGTCTATAC 3´ |
| Dll3pu2 | 5´ AGGTGGAGGTTGGACTCACC 3´ |

Conditions:

94°C	5 min
	30 cycles
94°C	30 sec
61°C	30 sec
72°C	30 sec
72°C	10 min

Subsequently the PCR reaction is digested with HaeIII at 37°C for at least 2 hrs. The reaction was run on a 4-10% gradient acrylamide gel.

Bands for the wildtype allele are at 65 bp, and for the pudgy allele at 96 bp.

Jag1^{htu}

40 µl reaction volume

4 µl	10x PCR buffer with $(NH_4)_2SO_4$
4 µl	25 mM MgCl2
1.25 µl	10 µM Jag1f primer
1.25 µl	10 mM Jag1r primer
0.3 µl	25 mM dNTP-mix
26.7 µl	H_2O
2 µl	template DNA
0.5 µl	Taq polymerase

Primer sequences:

Jag1f	5´ GTCCACGGCACCTGCAATG 3´
Jag1r	5´ GTGATAATGGACTGAACCTC 3´

Conditions:

94°C	5 min
	40 cycles
94°C	45 sec
59°C	40 sec
72°C	35 sec
72°C	7 min

The PCR reaction is digested with FokI at 37°C for 1-2 hrs. The reaction is run on a 2% TAE agarose gel.

A band for the wildtype allele is at 240 bp and for the mutant allele at 190 bp and 50 bp.

2.2.3 Isolation of RNA

For the isolation of RNA from tissues RNeasy Mini or Midi kits from Qiagen were used according to the manufacturer's protocol.

RNA concentration was measured by spectrophotometry at 260 nm. Integrity of the RNA was checked on a denaturing formaldehyde agarose gel.

RNA samples were stored at -80°C until use.

2.2.4 Preparation of slides

Rehydration of slides

Slides are placed in a box containing a mixture of H_2O/Glycerin in a ratio of approximately 1:1, depending on humidity, for 1-3 days.

Blocking of slides

In a 50 ml falcon 0.1-0.2 g Sodium Borohydrid is placed. 30 ml 1x PBS and 10 ml 100% EtOH is added. Rehydrated slides are placed quickly into the blocking solution (water drops on the slides must not dry) and incubated for 5 min at RT. The slides are then boiled in dH$_2$O 3 times in a microwave, dipped in 100% EtOH and air-dried.

Prehybridisation of slides

The slides and coverslips were pre-hybridised in pre-hybridisation buffer for 1hr at 42°C. Subsequently, slides were washed three times with H2O and once with 70% EtOH and air-dried. The slide is ready to use.

2.2.5 Target labelling

The labelling used for the Atlas GlassMouse 1 chip and the 20k chip was indirect. During the reverse transcription reaction, aminoallyl modified dUTPs are incorporated into the cDNA. In a second step the fluorescent cyanine dye, Cy 3 or Cy 5 respectively, is chemically coupled to the modified dUTP. Thus a bias of the reverse transcriptase towards one kind of dye molecule is diminished.

For the Atlas GlassMouse 1 chip the labelling was performed according to the protocol of the manufacturer with a few changes to optimise labelling protocol. Glycogen (1 µg) was added and the precipitation duration was extended from 1 hr at −20°C to 2 hr at −70°C. These changes ensured that the efficiency of labelling was equal for Cy 3 and Cy 5.

Target labelling was performed according to a modified TIGR (The Institute for Genome Research) protocol (http://pga.tigr.org/sop/M004_1a.pdf).

Reverse Transcription and cDNA purification

To 20µg of total RNA 2 µl Oligo-dT primers are added and the final volume is brought to 18.5 µl with RNase-free water, followed by ten min incubation at 70°C.

A master mix is prepared:

5x First Strand Buffer	6 µl
0.1M DTT	3 µl
50x aminoallyl-dNTP mix	0.6 µl
SuperScript II RT	2 µl

The tubes are cooled on ice. 11.6 µl master mix is added and the samples are incubated at 42°C for three hrs to overnight. The RNA is hydrolyzed by adding 10 µl 1M NaOH and 10 µl 0.5 M EDTA and incubating for 15 minutes at 65°C. 10 µl 1M HCl is added to neutralise pH.

The cDNA is purified using a modified protocol for the QIAquick PCR purification kit.
The cDNA reaction is mixed with 5 volumes of buffer PB (Qiagen supplied) and transferred to a QIAquick column, followed by a 13.000 rpm centrifugation for 1 min. Flow-through is discarded. 750 µl Phosphate wash buffer (5 mM KPO$_4$ pH 8.5, 80% EtOH) is added and the column is centrifuged at 13.000 rpm for 1 min. Flow-through is discarded. Empty column is centrifuged an additional minute at full speed. The column is transferred to a new microfuge tube and 30 µl Phosphate elution buffer (4 mM KPO$_4$ pH 8.5) is added. Elution buffer is

incubated for 1 min on the column and eluted by centrifugation at 13.000 rpm for 1 min. The elution is repeated with further 30 µl of Phosphate elution buffer. The sample is dried in a speed vac.

Aminoallyl-coupling

The vacuum dried sample is resuspended in 4.5 µl 0.1 M sodium carbonate buffer (Na_2CO_3) pH 9.0. 4.5 µl of the appropriate NHS-ester Cy dye (dissolved in 73 µl DMSO) are added and the reaction is incubated for 1 hr at room temperature in the dark. Then, 35 µl 100 mM NaOAc pH 5.2 and 5 volumes of buffer PB are added. The sample is purified using the QIAquick PCR purification kit according to the manufacturer's protocol. For the elution two times 30 µl elution buffer are used.

At this step the Cy3 and Cy5 labelled samples are combined, 2 µl salmon sperm and 20 µl Poly-dA is added. The Cy3/Cy5 target mixture is dried in a speed vac and resuspended in 60 µl hybridisation buffer (50% deionised formamide, 6x SSC, 0.5% SDS, 5x Denhardt's solution).

2.2.6 Hybridisation and image processing

The slide was placed in a hybridisation chamber. The labelled sample was pipetted onto the slide. The coverslip was added and the hybridisation chamber was closed tightly. The hybridisation was performed for at least 16 hrs at 42°C in a water bath.

The hybridised slide was washed in a serious of washing solutions (3x SSC, 1.5x SSC, 1x SSC, 0.5x SSC, 0.1x SSC) by intensive shaking for 30 sec. Slides were transferred to a dry 50 ml falcon and centrifuged for 30 sec at 4000 rpm without lid for drying. Slides were scanned immediately with an Axon 4000A fluorescent scanner.

The scanned images were processed with the GenePix Pro 3 image analysis software. Grids were loaded into the GenePix software and aligned half-automatically.

2.2.7 Washing with increasing stringency for fractionation experiments and image analysis

The hybridisation for the fractionation experiments was performed as described above. After hybridisation slides with coverslips were immersed in 40 ml of 1x SSC pre-warmed at the hybridisation temperature and vigorously shaken to detach the coverslips. The slides were rinsed in 1x SSC and 0.5x SSC at room temperature and placed in a Petri dish with 0.25x SSC. Slides were trimmed to the length of 46 mm. A Gene Frame 19 x 60 mm microarray sealing spacer (Abgene) was attached to a clean coverslip (Erie Scientific), immersed in 0.25x SSC in a Petri dish with the hybridised slide and pasted to it such that the slots at the top and bottom, of the slide were not sealed (Figure 8a, p. 53 and Drobyshev, Machka et al. 2003).

This assembly was placed into the microarray scanner GenePix 4000A and the image was scanned at two wavelengths (532 and 635 nm). Aliquots of 700 µl of 0.25x SSC were pipetted onto one of the unsealed edges of the slide while the excess solution was removed

from the opposite unsealed side with filter paper. Then the slide was washed in the opposite direction with another 700 µl of the same solution. Further washes were done with increasing concentrations of formamide (in 3.5% steps) in the same 0.25x SSC buffer. The range of formamide concentrations was from 0 to 94.5%. After each washing the slide was incubated for 5 min and scanned again.

Scanned images of microarrays were analysed with the GenePix Pro 3 image analysis software. The mean pixel intensities for each single feature obtained after each washing step were plotted versus the stringency as fractionation curves (Figure 8, p. 53).

2.2.8 Data analysis

All unflagged spots detected by the GenePix image analysis software were used for the analysis.

Normalization procedure

For a chip that contains genes of many functional classes, as it is the case for the Atlas GlasMouse1 as well as the 20k chip, it is assumed that most genes do not change their expression level and only a few will be differentially expressed. Therefore all genes are used as the standard and not only selected housekeeping genes.

For each feature the local background is subtracted from the median feature intensity by the GenePix software. If the background is highly different in the two channels, the scatter plot will yield an arc-shape. To avoid this, the 5% quantile of intensity values of both channels is estimated and subtracted from all corresponding intensity values in addition to the local background values. In cases where the feature intensity is very low compared to the background these operations might result in a value that is smaller than 1 or negative. All values <1 are pushed to 1 in order not to get negative values in the next step. Taking the logarithm reduces the effects of a broad range of intensity values (approximately 100-

$$C = \frac{\left(x_i - \bar{x}\right) + \left(y_i - \bar{y}\right)}{\left|x\right| \times \left|y\right|}$$

C : the Pearson correlation coefficient

x, y : vectors of the dimension n

x_i, y_i : $i^{\wedge}$ th value of the measurement vector x or y respectively

$\bar{x}, \bar{y}$: mean values of the measurement

100.000). Thus numbers are within the same order of magnitude.

The next steps define spots within in the noise range, meaning that the expression intensity is due to unspecific binding. Therefore 20 steps are established from highly to low expressed features and the Pearson correlation coefficient is calculated:

The point where the coefficient drops off is defined as cut-off. All features below this cut-off are defined as "low expressed". Then the median of the differences (red minus green) of all not "low expressed" spots is calculated and subtracted from every value of the "stronger" channel in order to correct high variations between intensities. This can be done because of the assumption that most genes do not change their expression level. In the last step is an exponentiation to get back to the original order of magnitude.

2.2.9 Plasmid preparation

For plasmid Mini preparations 2 ml of overnight culture were used. The preparation was done according to the Qiagen Plasmid Mini Prep protocol.

For plasmid Midi preparations 50 ml of overnight culture were used. The preparation was done according to the Wizard Plus Midi protocol from Promega. For the elution of plasmid DNA from the column 2x 150 µl H$_2$O heated to 70°C was used.

2.2.10   Whole mount *in situ* hybridisation

2.2.10.1   Riboprobe synthesis

For the production of RNA sense and antisense riboprobes 10 µg of plasmid DNA was linearized using the corresponding restriction enzyme. The reaction volume was 100 µl. Completeness of the digest was checked on a DNA agarose gel. Linearised DNA was precipitated by adding 200 µl H$_2$0, 650 µl 100% EtOH and 95 µl 3M NaOAc. The tube was frozen for 30 min at -80°C and centrifuged for 20 min at 13.000 rpm. The pellet was washed with 70% EtOH, air-dried and dissolved in 50µl TE.

For the in vitro transcription 5 µl ($\approx$ 1 µg) linearized DNA was transcribed using 3 µl DIG RNA Labelling Mix (Roche), 3 µl 10x Transcription buffer (Roche), 16 µl H20, 1 µl RNase inhibitor (Roche) and 2 µl of the appropriate RNA polymerase (Roche) for 2 hrs at 37°C. 1 µl of the reaction was checked on a denaturing gel. If the transcription was satisfying 2 µl DNase I (Roche) was added for 15 min at 37°C. RNA was precipitated by adding 90 µl TE, 10 µl 4M LiCl and 300 µl 100% EtOH. The tubes were mixed, frozen for at least 30 min at -80°C and centrifuged for 20 min at 13.000 rpm. The pellet was washed with 70% EtOH, air-dried and suspended in 100 µl TE. Riboprobes were stored at -80°C until use.

For the hybridisation 10 µl riboprobe per 1 ml hybridisation buffer was used.

2.2.10.2   *In situ* hybridisation

Selected embryos were rehydrated through 75%, 50% and 25% MetOH/PBS on ice for 10 min each and washed twice for 10 min in PBT. Subsequently samples were incubated for 10 min in RIPA buffer and washed twice for 5 min with plenty of PBT without shaking. Embryos were refixed in 4% PFA/0.2% glutaraldehyde in PBT for 20 min and then washed twice for 5 min with PBT on ice. Embryos were incubated in hybe bfr/PBT (1:1) at RT for 10 min and prehybridised in hybe bfr containing tRNA at a concentration of 100 µg/ml at 68°C

for 3 hrs. The riboprobe was denatured at 80°C for 3 min and diluted 1:100 in hybe bfr containing tRNA. The hybridisation was performed at 68°C over night.

For the removing of the unbound probe the embryos were washed two times 30 min at 65°C with hybe bfr. Afterwards tubes were cooled to RT and washing proceeded with hybe bfr/RNase solution mixture (1:1) for 5 min at RT. Embryos were washed with RNase solution for 5 min and incubated for 1 hr in RNase solution containing RNase A at a concentration of 100 µg/ml at 37°C. The embryos were washed in RNase solution/ (SSC/FA/Tween20) (1:1) for 5 min at RT. The following stringent washing steps included 2x 5 min, 3x 10 min and 5x 30 min with SSC/FA/Tween20 at 65°C. Embryos were cooled to RT and washed 2x 10 min in TBST and 2x 10 min in MABT. The samples were incubated for 1 hr at RT in 5% DIG blocking solution and then incubated over night in 1% DIG blocking solution containing Anti-Digoxigenin-AP Fab fragments antibody at a dilution of 1:5000 at 4°C.

For removing unbound antibody embryos were washed 3x 5 min and 8x 1 hr in TBST at RT.

For the staining reaction BM purple AP substrate solution from Roche was used. Embryos were washed 3x 10 min in 1x Detection buffer (Roche). Per tube staining solution was prepared by using 1 ml BM purple, 2mM Levamisole/TBST and 0.1% Tween20. The solution was centrifuged for 5 min at 13.000 rpm and the supernatant was applied to the embryos. Development was performed at 4°C in a dark box. When the staining was sufficiently strong the reaction was stopped by washing the embryos 3x 10 min in 1x Detection buffer followed by over night fixation in 4% PFA/PBS.

2.2.11   Reverse Transcription-PCR (RT-PCR) and Real-time PCR

2.2.11.1   Primers

For RT- and real-time PCR

Gene	Product size	5´ Primer	3´ Primer
1110017I16Rik (MG-8-86g2) RT-PCR1	315	TGGGGACTTCCAAGATACCTCAC	TCTCTCTGTTCCTCCACGAAGTTC
1110017I16Rik (MG-8-86g2) RT-PCR2	320	CAGTGGCGCCAGTGGCATTA	GCTCTGATTCTGTTTCTGGTGGCT
1110021J02Rik (MG-4-3k8) RT-PCR1	186	CTGGTCCAGCGCGGAAAAGA	TCCTTCTCCAGAGACCTCCTGTCC
1110021J02Rik (MG-4-3k8) RT-PCR2	220	GAGGACAGGAGGTCTCTGGAGAA	CTACTAAGCAGAAGGAAGCACTACCAC
18SrRNA	119	ATTCGAACGTCTGCCCTATC	ATGTGGTAGCCGTTTCTCAG
Alas1	206	CTGTCCGAGTCACATCATCC	TGACCAGCAGCTTCTCCAC
Atm RT-PCR1	324	GCAGCCCTTAACATTTTCCTC	GACAGCAATATTACGAGATCCTGA
Atp5h 5´/3´	375	GGTCGGTGAAGTATCCCAAG	GCTGCTTCTCATACTCCTGGA
Atp5h RT-PCR1	339	GCCAAGCCTGGCTTGGTGGAT	TTATTTCATGTCGGCCGGGGCTC
B2M	172	TCGCTTCAGTCGTCAGCATGG	GGGTGGAACTGTGTTACGTAGC
Bnip3 5´/3´	619	TGTCGCCTGGCCTCAGAACT	GCCAATGGCCAGCAGATGA
Bnip3 qPCR	217	CAGTTGGGTTCGGGCTCCTT	GGTGGGCTGTCACAGTGAGAAC
Chst12 RT-PCR1"	334	AGAACGTGAGAGGCTACGACTG	GTGTTGTGCACGTGTTCCCG
Chst12 RT-PCR1	318	GGCGATTTCGGCTGCAGAAT	TCCTCCACCAATCCCTGGGT
Csk RT-PCR1	314	CGTCATGACGCAACTTCGGC	GAGTGCTGGAGGCTTCCTTAGTG
Csk RT-PCR2	617	CCTGGCCATCCGGTACAGAA	CCCCAGCATCACATCTCCAA
Ddx6 RT-PCR1	341	TCCAGTCAGAACGGCCAGCT	GGAATGCTCTCCTCCTGGATAGG
Dio2 RT-PCR1	349	TTTTTCCCTGTCCCTCACCC	TGTAGGCATCTAGGAGGAAGCTG
Dio2 RT-PCR2	328	TGAATTCCCAAAATGCAACA	TTCCCCATTATCCCTTTTCC
Eno1 RT-PCR1	328	TTCTCAGGATCCACGCCAGA	AGGATGGCATTTGCACCAAA

Eno1 RT-PCR2	310	TACATCACGCCCGACCAGCT	ATCGGTGGGACACCATGACG
Eraf RT-PCR1	261	GAAGACACACAAACCCCGAGG	CATGGCCCTGTCTTGCTCCT
Eraf RT-PCR2	210	AGCAAGACAGGGCCATGACA	AGCAACATCTTGGGAGAACGG
Fes RT-PCR1	216	TGAGGCTGGCAAGGTGTCCA	CGCTTCTGCTCCTTCAGCCA
Fes RT-PCR2	275	TGCTGTGTGCCCTTTGAACC	TCACTGCCACCACCTACACTGTC
Fgf6 RT-PCR1	317	TAAATGGTTTGATCTCACCCTGC	CAATGCAGGCACCTGAAGCA
Fgf6 RT-PCR2	345	CACAACGGTGAGTTCTGCGG	CCAGTTCAGCAACTCAGACCTGAT
Gamt RT-PCR1	215	GGCCTATGACGCGTCTGACA	GGAAGACCCCATCATTGCACT
Gamt RT-PCR2	221	ACCTACCCTGCCTGACGGTCACT	GCACCTGCGTCTCCTCAAACAT
Gapdh	150	CAACAGCAACTCCCACTCTT	TACTCCTTGGAGGCCATGTA
Glu1 RT-PCR1	301	GCCACCGCTCTGAACACCTT	GTCTTTGCGGAAGGGGTCTC
Glu1 RT-PCR2	327	TGGCATTTCTTGGTCCTCCG	GTGGTGGCAAGCAGTGGCAT
Hmx2	311	TCTGCATTCCTCACGCCAGA	CCCATCCTCAAGATGAAGGGAATA
Hprt	224	GTTGGATACAGGCCAGACTTTGT	CACAGGACTAGAACACCTGC
Ifim1 RT-PCR2	276	GAAACACATAGCAAGCCTGGGA	GGGGCAAATGGTCAGGACTAAGT
Ifitm1 RT-PCR1	376	CAAGAGGTGGTTGTACTGGGGT	TATGCCTACTCCGTGAAGTCTAGG
Mark3 RT-PCR1	326	AGCTTCCTGTGCAGATGAACAGC	CCTTCATTCTTCCATGTGCAACC
Mt1 5´/3´	382	ACTTCAACGTCCTGAGTA	AGACTCAAACAGGCTTTT
Mt1 qPCR	173	CACCACGACTTCAACGTCCTG	GCAGCAGCTCTTCTTGCAGGA
Mt2 5´/3´	336	CCATCACGCTCCTAGAACTCT	TGGAGAACGAGTCAGGGTTGTA
Mt2 qPCR	189	TCTCGTCGATCTTCAACCGC	TCTTTGCAGATGCAGCCCTG
Nes RT-PCR1	346	AAAGTGAGCCAGGTCTCCCTCG	CCTCTTTCACCACAGAGCTCAGTG
Nes RT-PCR2	312	TCTGTGGATGAGAACCAAGAGGT	CTCTGCCTTATCCTCAGTTTCCAC
Nr1h2 RT-PCR1	207	AGGCTGCTTCGTGACCCACT	TGCGCTCAGGCTCATCCTCT
Nr1h2 RT-PCR2	244	GCAGGCTTGCAGGTGGAATT	TCATGAGCATGCGTGGGAAG
Nup155 RT-PCR1	303	TGATGGTGGCCTCTACGTCG	AAACGCCCATCATGCAGTTG
Nup155 RT-PCR2	385	TCTGCTGCTGGAAACATTGCT	GGGTTGTCATCTGAGTTTCCATCA
Pbgd	255	GCCTACCATACTACCTCCTG	GCACTGAATTCCTGCAGCTC
Pdgf-α RT-PCR1	421	CCCACATCGGCCAACTTCCT	CACACTGAACAAACGGACACTGT
Pdgf-α RT-PCR2	308	CTGGCTTTGCACTCGCTGCT	CCCGGATGCTGTGGATCTGA
Pdgfr-α qPCR	310	TACCCGACGCCCAGGATATC	TTTCTGGAAGAGGGGTGCCT
Pdgfr-α RT-PCR1	300	TCTGAACTCACAGTGGCGGC	CATTACAGGTTGGGACCGGC
Ptma 5´/3´	622	GGAGAAGAAGGAAGTTGTGGAG	GGTTTGGTCACCCGTTATCA
Rcvrn RT-PCR1	221	CATCACGCGGCAGGAGTTCGAA	TGGTCCCATTGCCGTCTACGTC

Rcvrn RT-PCR2	200	ACAGTGATGGGCACCGTTTG	GGATGGGGAGGACACTGAAGAC
S100a10 RT-PCR1	224	TCGTGGTGTGCCCAGCTCTT	CACAGCCAGAGGATCCTTTTGA
S100a10 RT-PCR2	208	GTAAACATGAAGCAGAAGGGGA	CAGAAGCTTCTCTGCCATTGGATT
Sema5b RT-PCR1	884	CGCTTCGCACTGCCCAGT	GCATGCCCCCTGGCTATGAT
Sema5b RT-PCR2	304	ACTCGGGTTCTTGCCTGTGC	CCCCAGGAAGCCCAGAAGAT
Smarcc1 5´/3´	621	GGCCAGCAAGTTTTGGGA	TGGACCCAAGTGTCATAGCTG
Smarcc1 RT-PCR1	306	CCAAGGACATGGAAGACCCC	CACCGCGTTCAATGACATGA
Tlx1 RT-PCR1	231	CTTGCCTACAGTGCCCTCTGTG	TCCGCCGAAGCCAAGTACTT
Trfc	145	AGAGTTTGCTGACACCATCA	GTGTTCATCTCGCCAGACTT
Wnt10b RT-PCR1	219	GCCGTTCACGAGTGTCAGCA	ACTACCCTTCCATCCGCAGC
Wnt10b RT-PCR2	235	CTCCCGGAAGCTCAGAGCAT	GGAAGAGGAGTGGCCAAAAGAT

For in situ probe production

Gene	Product size	5´ Primer	3´ Primer
Mt2	351	CCATCACGCTCCTAGAACTCT	GGAGAACGAGTCAGGGTTGTA
Mt1	382	ACTTCAACGTCCTGAGTA	AGACTCAAACAGGCTTTT
Bnip3 5´/3´	619	TGTCGCCTGGCCTCAGAACT	GCCAATGGCCAGCAGATGA
Hmx2	311	TCTGCATTCCTCACGCCAGA	CCCATCCTCAAGATGAAGGGA ATA
Ptma	622	GGAGAAGAAGGAAGTTGTGG AG	GGTTTGGTCACCCGTTATCA
Nes	771	TGTCCCTCATTCCCTGCTCC	CCTCCCAGTGGGTATTGGCT
Smarcc1 5'/3´	621	GGCCAGCAAGTTTTGGGA	TGGACCCAAGTGTCATAGCTG

2.2.11.2   RT-PCR

For the RT-PCR a standard protocol was used.

<u>Reverse Transcription:</u>

Master Mix:

4 µl	5x First-Strand buffer (Invitrogen)
2 µl	10x DTT (Invitrogen)
1 µl	RNase Inhibitor (40 U/µl) (Roche)
1 µl	10 mM dNTP-mix
1 µl	Superscript II (Invitrogen)

1 µg total RNA is transferred into a 0.2 ml PCR tube and the volume is adjusted to 10 µl. 1 µl of 0.1 mM random hexamers (Roche) is added and the sample is heated to 70°C for 5 min, followed by immediate cooling on ice. 9 µl of the Master Mix is added to the sample and incubation proceeds at 42°C for at least 1 hr. Then the sample is incubated at 70°C for 15 min to inactivate Superscript II reverse transcriptase.

Samples were purified using Qiagen Nucleotide Removal kits and the cDNA concentration adjusted to 10 ng/µl.

<u>PCR:</u>

50 µl reaction volume

5 µl	10x PCR buffer with (NH4)2SO2
3 µl	50 mM MgCl2
1.5 µl	10 µM Fwd Primer
1.5 µl	10 µM Rev Primer
0.5 µl	25 mM dNTP-mix
37 µl	H20
1 µl	cDNA template
0.5 µl	Taq polymerase

Conditions:

95°C	5 min
	30 cycles
95°C	30 sec
X°C	45 sec
72°C	45 sec
72°C	5 min

X°C: Annealing temperature was selected according to the primer sequences (2.2.11.1).

2.2.11.3   Real-time-PCR

The Real-time PCR was done using the cDNA as described above. The Platinum SYBR Green qPCR SuperMix UDG (Invitrogen) was used for the Real-time PCR reaction.

50 µl reaction volume

25 µl	Platinum SYBR Green qPCR SuperMix-UDG
1 µl	ROX Reference Dye
1 µl	10 µM Fwd Primer
1 µl	10 µM Rev Primer
21 µl	H_2O
1 µl	cDNA template

The reaction was performed in an ABI Prism 7700 Sequence Detection System from Applied Biosystems.

Conditions:

50°C	2 min
95°C	2 min
	45 cycles
95°C	15 sec
55°C	30 sec
72°C	30 sec

2.2.12 PCR amplification of homologous arms

The PCR reactions were performed according to the protocol delivered with the used polymerase. In the cases of the left and right arm Stratagene's EasyA Polyerase was used.

Primers

Right arm:	fwd	5´ ATAGGGTACCTCTGGGGCCTCCCAGGCTTGCTATG 3´
	rev	5´ TCCCAAAGCAGACCCTCTTCTGTCAGCCAG 3´
Left arm:	fwd	5´ GCGGACTAGTTAAGTTTCCAATGACCTCAAATGGT 3´
	rev	5´ CAGTATGCATCTCTCGGCTTTTGAAGCTGCAGAGTG 3´

2.2.13 TopoTA Cloning

PCR products ranging from 200 bp to 5 kb were cloned using the TopoTA cloning protocol. The cloning reaction was performed according to the manufacturer's protocol. Cloned fragments were analysed by restriction digests and gel electrophoresis as well as subsequent sequencing to ensure correct orientation and sequence.

2.2.14 Restriction digest

Restriction digests for subsequent cloning were done in a total volume of 100 µl containing 5-15 µg plasmid DNA and 1-5 µl of the corresponding enzyme/s.

2.2.15 Fragment purification/Gel extraction

For the isolation of DNA fragments from agarose gels the QIAquick gel extraction kit from Qiagen was used according to the manufacturer's protocol. For the elution from columns Elution buffer or water heated to 60°C was used. The column was incubated for 5 min at RT before the final centrifugation step.

Concentration of isolated fragments was measured with spectrophotometry at 260 nm. Additionally fragments were checked on agarose gels.

2.2.16   Ligation

The amount of vector and insert used for ligations was adjusted depending on the sizes of vector and insert fragments and on the characteristic of the ends of the fragments (sticky or blunt). The pmol of 5´(or 3´) ends was calculated and the amount of insert adjusted such that the 5´ends of the insert were between 1x – 5x in excess.

The ligation reaction was performed in a total volume of 10-20 µl at 5-20°C for 2-20 hrs.

If the Quick T4 DNA ligase (NEB) or the Rapid Ligation Kit (Roche) was used the reactions were done according to the manufacturers protocol.

2.2.17   Transformation of DNA

2.2.17.1   CaCl$_2$-competent cells

For the transformation of CaCl$_2$-competent cells between 1-10 µl of the ligation reaction was used.

The competent cells were thawed on ice. Cells purchased from Stratagene were aliquotted in 75 µl and placed into prechilled 15 ml falcons. 4 µl of β-mercaptoethanol (provided with the cells) were added and the mixture was incubated on ice for further 10 min. Then DNA was added to the cells, mixed gently by swirling the tubes gently and incubated for 30min on ice. During this time SOC medium was warmed to 42°C. The cells were heat-pulsed for exactly 30 sec and incubated on ice for 2 min. 450 µl of pre-warmed SOC medium was added to each transformed tube and incubated at 37°C for 1 hr shaking at 200-225 rpm.

Of each transformation 50 and 200 µl were plated on LB agar plates containing 100 µg/ml ampicillin or 50 µg/ml kanamycin, respectively, and incubated at 37°C over night.

2.2.17.2   Electrocompetent cells

For the transformation of electrocompetent cells between 0.1-2 µl of the ligation reaction was used.

The TOP10 electrocompetent cells were thawed on ice. Cuvettes (Pipectrodes^{TM}) were thawed on ice for approximately 5 min. The DNA was added to the electrocompetent cells and mixed by gentle swirling. Then the cuvette was placed into the Bactozapper Cloning Gun and the cells were sucked carefully into the cuvette. The electric pulse is induced by pulling the trigger. The cells are pipetted into 0.5 ml of ice-cold 15% glycerol solution. Cells can be plated immediately on LB agar plates. Between 10-50 µl were plated.

2.2.18   RNA amplification

The T7 based RNA amplification was done with the MessageAmp^{TM} aRNA Kit from Ambion. Between 10 ng and 5 µg of total RNA was used as starting material.

First-Strand cDNA Synthesis

The total RNA was placed into a sterile PCR tube and 1 µl of T7 Oligo(dT) Primer was added. Nuclease-free water was added to 10 µl final volume. The sample was incubated for 10 min at 70°C and then at 42°C. A Master Mix containing 2 µl 10x First Strand Buffer, 1 µl Ribonuclease Inhibitor and 4 µl dNTP Mix per reaction was mixed and incubated at 42°C for 2 min to adjust the temperature. Then 7 µl of the Master Mix were pipetted to the RNA sample, mixed thoroughly by pipetting up and down. 1 µl Reverse Transcriptase was added to each sample and the complete reaction was incubated for 2 hrs at 42°C. The tubes were placed on ice immediately.

Second-Strand cDNA Synthesis

At room temperature the following reagents were added to each sample. 63 µl Nuclease-free H_2O, 10 µl 10x Second Strand Buffer, 4 µl dNTP Mix, 2 µl DNA Polymerase, 1 µl RNase H. The sample was mixed and placed at 16°C for 2 hrs.

cDNA Purification

Before beginning Nuclease-free H_2O was heated to 50°C.

1 Filter Cartridge per sample was equilibrated by adding 100 µl cDNA Binding Buffer and incubation for 5 min. 250 µl of cDNA Binding Buffer was added to each sample and mixed by gentle vortexing. The cDNA sample/cDNA Binding Buffer mixture was pipetted onto the equilibrated Filter Cartridge and centrifuged for 1 min at 10.000 x g. The flow-through was discarded. 650 µl of cDNA Wash Buffer was added to each Filter Cartridge and centrifuged for 1 min. The flow-through was discarded and the tubes were centrifuged for an additional minute at full speed. The Filter Cartridge was transferred to a fresh microfuge tube and 50 µl of preheated H_2O were pipetted onto the filter. The filter was incubated for 2 min at room temperature and centrifuged for 1 min. The elution step was repeated. Then the sample was concentrated in a vacuum centrifuge until the volume was reduced to 8 µl or less. It is important not to dry the sample completely.

In Vitro Transcription to Synthesize aRNA

For the in vitro transcription the following reagents were pipetted together:

8 µl	double-stranded cDNA
1.5 µl	5-(3-aminoallyl)-UTP (50 mM)
2 µl	T7 ATP (75 mM)
2 µl	T7 CTP (75 mM)
2µl	T7 GTP (75 mM)
1 µl	T7 UTP (75 mM)
2 µl	T7 10x Reaction Buffer
2 µl	T7 Enzyme Mix

The reaction was incubated for 6-24 hrs at 37°C. Then 2 µl DNase I was added to each sample and incubated for 30 min at 37°C.

aRNA Purification

Nuclease-free H$_2$O was heated to 50°C.

1 Filter Cartridge per sample was equilibrated by adding 100 µl aRNA Binding Buffer and incubation for 5 min. 78 µl aRNA Elution Solution was added to each sample. 350 µl of aRNA Binding Buffer was added to each aRNA sample and mixed thoroughly. Then 250 µl of 100% EtOH was added and mixed. Each sample was immediately pipetted onto a Filter Cartridge and centrifuged for 1 min at 10.000x g. The flow through was discarded and 650 µl aRNA Wash Buffer was added to each Filter Cartridge. The tube was centrifuged for an additional minute to remove residual ethanol. For the elution the filter was transferred to a fresh microfuge tube and 50 µl of preheated RNase free H$_2$0 was pipetted onto the filter and incubated for 2 min at room temperature. The sample was then centrifuged for 1 min and the elution step was repeated. Labelled aRNA was concentrated using a vacuum centrifuge and the concentration determined by spectrophotometry.

The samples were immediately used for DNA-chip hybridisation.

2.2.19   Isolation of protein

For 2D-gel electrophoresis

For each gradient, pH 4-7 and 6-11, different preparation protocols were applied. For the acidic gradient, approximately 60mg embryo tissue was dissolved in 200µl lysis buffer containing 7M urea, 2M thiourea, 2% DTT, 4% CHAPS, 0,8% Pharmalyte 3-10. The suspension was vortexed 10 times for 2s, then sonicated for 10 cycles with an agitation time of 1s (60W). After sonication, the sample was kept shaking for 30min at 25°C, followed by spinning for 5min at 14000rpm. The supernatant was collected and a protein determination (modified Bradford) was performed. 350µg protein was loaded onto each 4-7 IPG strip.

For the pH gradient 6-11, 500µl of the lysis buffer extract (acid preparation) was diluted with 1500µl cold (4°C) TCA / acetone 20 (v/v) / 50% (v/v). After sonication for 15min (30W) in a cold water bath (4°C), the suspension was diluted with 1,2 ml TCA/acetone 20% (v/v) / 50% (v/v). The solution was vortexed for 2min and then kept for 16h at 4°C. After precipitation, the sample was spun down for 30min at 14000rpm (4°C). Then the pellet was washed in 200µl acetone, sonicated in a cold (4°C) water bath for 20min and then centrifuged for 30min at 14000rpm (4°C). Washing was repeated twice. The washed protein pellet was resuspended in 200µl lysis buffer (7M urea, 2M thiourea, 2% DTT, 4% CHAPS 0,8% Pharmalyte 3-10) and sonicated 10 times for 1s (60W) on ice. Sample was kept shaking at RT for 45min and spun down for 5min at 14000rpm. The supernatant was collected and the Bradford protein determination was done. 350µg protein was loaded onto 6-11 IPG strips.

For 1D-gel electrophoresis

For the isolation of proteins to perform 1D-SDS-PAGE the protocol as described above for the pH 4-7 was used. Protein concentration was determined using the Bradford method.

2.2.20   2D-Gel electrophoresis and peptide-mass-fingerprint

The 1st dimension, the isoelectric focussing, was carried out with 18cm IPG (immobilised pH gradient) strips from Amersham Bioscience. For each sample the pH - gradients 4-7 and 6-11 were performed. Five gels of each sample were done under identical running. For the acid gradient 24kVh and for the basic gradient 38kVh were performed. After focussing to the steady state, the strips were loaded with SDS and equilibrated in DTT and Iodacetamide according to Görg et al.

The second dimension was performed as a SDS – PAGE. T12% and C2,8% SDS gels were casted and run vertically in a Höfer ISO - Dalt chamber with 10 gels in parallel. The SDS PAGE was stopped, when the bromophenol blue front had disappeared from the gels; in general between 1800Vh and 2000Vh were applied. In the second dimension the Laemmli buffer system was used.

After SDS electrophoresis the gels were removed from glass plates and stained with Sypro Ruby^{TM} according to the manufacturers protocol. The Sypro Ruby^{TM} stained gels were scanned with an Fuji fluorescence scanner to obtain 16bit tif images. The spot detection, matching and quantification was carried out with the Definiens 2D image software ProteomWeaver. Master gels were created out of five replicas from one tissue in each gradient.

In addition, Coomassie stained micropreparative gels were run with a 500µg protein load per gel for the identification of low abundant spots.

The identification of the selected protein spots was performed by a peptide mass fingerprint (PMF)- MALDI - TOF analysis.

For the peptide mass fingerprint, the spots were picked from the SDS gel, washed 3 times with 10mM NH_4HCO_3, 30% ACN and incubated overnight in 5µl trypsin buffer at 37°C. The trypsin buffer contained 25ng/µl trypsin (Roche) dissolved in 10mM NH_4HCO_3, pH 8. After digestion the tube was kept in a sonication bath for 20min at 25°C. The supernatant was removed and concentrated in a SpeedVac. For desalting the concentrated solution was processed through a C18 reversed phase ZipTip column (Millipore). The elution buffer contained 0,1% TFA and 80% acetonitrile. The eluted peptides were put on a target and cocristalised with an equal amount of dihydroxybenzoeic acid. MALDI - TOF analysis (Applied Biosystems Voyager STR) was performed in reflector mode in the peptide range from 700 to 4000 Daltons. The obtained spectra were matched with the NCBI database using the ProFound software (Genomic solutions) to identify the corresponding protein.

2.2.21   1D-SDS-PAGE and Western Blotting

For the 1D-SDS-PAGE 10% Tricingels were used.

Preparation of 2 resolving Tricingels (10%):

3.3 ml	Acrylamid/Bisacrylamid (30:1)
3 ml	Gel buffer (3 M Tris, 0.3% SDS)
1 ml	H_2O
2.5 ml	Glycerol 50%
20 µl	TEMED
50 µl	10% Ammoniumpersulfate (APS)

Use approximately 3.5 ml resolving gel, pipette 1 ml H_2O on it until the gel has polymerized.

Preparation of 2 stacking Tricingels (4%):

0.67 ml	Acrylamid/Bisacrylamid (30:1)
0.67 ml	Gel buffer
3.67 ml	H_2O
7 µl	TEMED
40 µl	10% APS

Remove the water from the resolving gel, add 1.3 ml of stacking gel and insert a comb.

Samples were mixed with 1 volume of Laemmli sample buffer, heated to 98°C for 10 min, placed on ice and loaded on the gels. Proteins were resolved for 1.5 hrs and the gels immediately transferred into blotting buffer for 5 min. For semi-dry blotting two filter papers soaked with blotting buffer were placed on the anode. The PVDF membrane was put into 100% MetOH, followed by blotting buffer and placed on the filter paper. Then the gel was placed onto the PVDF membrane and covered with two filter papers soaked with blotting buffer. Air bubbles were squeezed out using a 5 ml-pipette. Gels were blotted for 30 min at 20 V.

The blots were removed from the gels and incubated shaking for 30 min in 5% milk powder in PBS to block unspecific binding sites for antibodies. The blots were washed in PBS and incubated for 2 hrs at room temperature or over night at 4°C in primary antibody solution diluted in 0.5% milk powder in PBS. After incubation with the first antibody the blots were washed 3x for 5 min with PBS and subsequently incubated for 1 hr at room temperature with the secondary antibody at the corresponding dilution. The blots were washed 3x for 5 min with PBS.

For the immunodetection the ECL Plus Western Blotting Detection Kit (Amersham) was used. Detection solutions A and B were mixed in a ratio of 40:1, for each blot 700-1000 µl solution was used. Excess washing solution was removed from the blots by putting the edges of the blot on a filter paper. The blot was placed protein side up into a dish and the Detection solution was pipetted onto it and incubated for 5 min at room temperature. Then

excess liquid was removed as described above and the blot was placed in a clear plastic bag without bubbles between the blot and the plastic cover. The wrapped blot was placed in an x-ray film cassette. In the dark room a sheet of autoradiography film was placed on top of the membrane for 15 sec to 10 min, depending on the intensity of the expected signal. After development of the first film it was estimated if a second film needs to be exposed and for how long this would be necessary.

2.2.22   Stripping of Western Blots

In order to reuse the Western blots they were stripped, removing the primary and secondary antibodies. Thus they were submerged in stripping buffer shaking for 30 min at 50°C. Then the membrane was washed 3x for 10 min in PBT at room temperature with large volumes of solution. Then the membrane was blocked for 30 min in 5% milk powder in PBS and incubated with the primary antibody as described above.

3 Results – Transcriptome analysis

3.1 Microarray analysis

3.1.1 DNA-chip design

In order to establish the technical procedure of microarray experiments in our laboratory the commercially available DNA-chip Atlas GlassMouse 1 from Clontech was used to investigate the expression pattern of E10.5 *Dll1*-wt and *Dll1*$^{-/-}$ embryos in the beginning.

The Atlas GlassMouse 1 chip contains 1081 genes that are represented by ~80mers. For every gene three gene specific sequences producing strong signals and low levels of cross-hybridisation can be found on the array.

In the meantime a cDNA-chip containing 20734 cDNAs (20k chip) was developed and produced in our laboratory (see Material & Methods).

3.1.2 Labelling procedure

For the labelling, total RNA extracted from whole embryos was used. Phenotypically identical embryos from the same litter were pooled before RNA isolation. Approximately 30-60 µg total RNA can be expected from one E10.5 embryo. 20 µg total RNA is used for one labelling reaction allowing repetitions only in a limited number of experiments. However, repetition of hybridizations is very important to use the data for statistical analysis (Lee et al. 2000). By using RNA pools the chance to detect randomly high expressed genes is reduced. Rather a mean of expression levels is produced and only those that are really differentially expressed will be detected on the chip. Third, pooling extremely reduces the amount of hybridizations that need to be done to identify differential expression.

The labelling performed for the Atlas GlassMouse 1 as well as the 20k chip was indirect.

3.1.3 Slide analysis

After the hybridization and washing as described in Material & Methods, the slides were dried and scanned with the GenePix 4000A scanner. The scanner contains a dual-laser scanning system, one for the excitation wavelength for the fluorophore Cy 3 and the other for the fluorophore Cy 5. The emission wavelength is 532nm for Cy 3 and 635nm for Cy 5. It is possible to adjust the Photo Multiplier Tube (PMT) Voltage for each channel separately. This allows compensation for the fact that Cy 5 often exhibits a weaker signal than Cy 3 and to some extends for unequal labelling. The software used was GenePix Pro 3.0.

3.1.4 Image analysis

Each individual spot of DNA is called a *feature*, and is assigned a *feature-indicator*. *Flags* characterise a feature, e.g. good, bad, absent, not found.

The ratio image displays the ratio of Cy 5/Cy 3 intensity. The imaging software GenePix Pro 3.0 displays the images from the two wavelengths and a ratio image. The two channels are displayed by pseudo colour images with green representing Cy 3 and red representing Cy 5. In an overlay or ratio image features with stronger Cy 3 signal appear green and features with stronger Cy 5 signal appear red, while features that have the same intensity in the Cy 3 and Cy 5 channel appear yellow. White colour of spots displays saturation.

For the image analysis a grid is overlaid to the image and the feature-indicators are aligned and flagged automatically. However the programme sometimes does not recognise all features correctly or applies incorrect flags. The size of the feature indicator, the position and the flag was manually adjusted in these cases.

The software automatically calculates and subtracts local background effects before analysis calculations. By using local background values, unequal washing of the slide or irregular features and contaminations can be compensated.

3.1.5 Statistical analysis

The statistical analysis of the raw data obtained by the image analysis software was done using LabVIEW based analysis tools (Drobyshev submitted).

The raw data files of all chips to be analysed were loaded into the software.

Normalisation procedure

To compensate for experimental variations due to cDNA synthesis, cDNA labelling or labelling efficiency raw data were then normalised according to the procedure described by Beissbarth and co-workers (Beissbarth et al. 2000). The normalization algorithm was implemented into the LabVIEW analysis tool. For detailed description of the normalization procedure see Material & Methods (chapter 2.2.8, p. 34).

LabVIEW analysis tool

The LabVIEW analysis software allows the comparison and simultaneous analysis of many DNA-chip experiments. Figure 7 shows an example of an analysis with the LabVIEW software. Figure 7a displays the window as it is displayed during a typical analysis procedure. First, the data is loaded into the software (Figure 7b). Dye swap or colour flip experiments are marked by checking the "cf" box. During the upload process the normalization as described in the previous chapter is performed. Following the upload the experiments are sorted according to their absolute log-ratios in descending order (Figure 7c). In the left part the upregulated and in the right part the downregulated genes are listed. The level of regulation is displayed graphically in red for the upregulated and in green for the downregulated genes. Each column represents one chip experiment. Using the box above slides can be excluded from the analysis, for example if they do not correlate well. Further it

is possible to set a threshold of expression intensity to be able to remove genes expressed in the background level from the analysis (Figure 7c, below the sorted genes).

If one gene is selected from the list the slide ID and the corresponding log-ratios and intensity values are displayed in the centre part of the upper half. By clicking on these values the corresponding scatter plot is shown to the right and the selected gene is marked by a red circle. To the left of the list the correlation plot is shown. The log-ratios of one experiment are plotted against the log-ratios of another experiment.
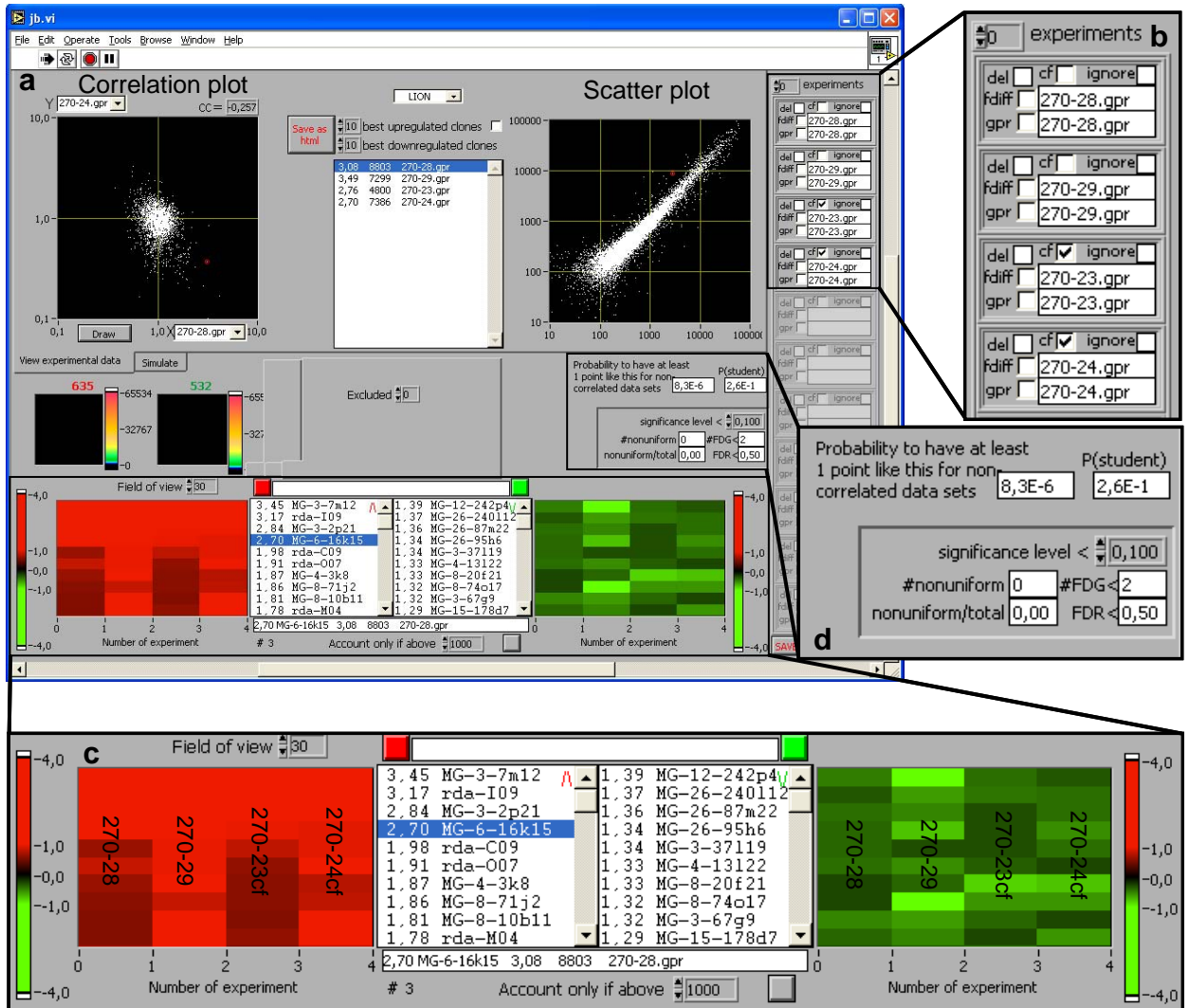
Figure 7 (a) LabVIEW software as displayed for the analysis. The window contains different sections. In the upper part the correlation plot (left plot), the scatter plot (right plot) and the log-rations, intensity values and corresponding slide ID (middle part) are displayed. (b) Section for the upload of the experiments. (c) Experiments are sorted according to their absolute log-ratios in descending order. (d) Section where statistical values for the selected gene are displayed. Additionally the middle section contains different features, e.g. to exclude data sets from the analysis, and to sort the genes according to different statistical criteria.

In order to identify significantly regulated genes statistically relevant values are also displayed (Figure 7d). The values are shown for each gene individually as you select it from

the list (Figure 7c). The first value is the "probability to have at least one gene like this for non-correlated data sets". This value indicates a likelihood for the observed results for a gene to occur randomly. Next to it is the calculation of the Student-T-test. In the box below the significance level representing the null hypothesis can be selected. The "number of non-uniform genes" describes how many genes in the list above the selected gene are not regulated in the same direction in all experiments. Depending on the significance level an estimation of "number of false discovered genes" (FDG) is performed. This means that within a set of selected genes two (in the example in Figure 7d) might show this result randomly and are not differentially expressed. The ratio of non-uniform patterns versus total number of patterns gives a reference on the number of genes that might not be reproducibly expressed in all experiments. The "false discovery rate" (FDR) is the ratio of the number of false discovered genes versus the total number of selected genes.

The selected genes can be saved in an html-file which contains the images of the spot, the ratio, the expression intensity and the gene name.

The LabVIEW analysis tool was developed in our laboratory.

3.1.6 Assessing the reliability of expression profiling data

RNA expression profiling has been proven to be a powerful tool for the analysis of molecular interactions and expressional changes in various biological systems, for example analysis of mutants (Hughes et al. 2000), developmental stages (White et al. 1999) or inflammatory diseases (Heller et al. 1997; Lee et al. 2000; Tseng et al. 2001). However, a major concern is the reliability of expression profiling data.

A highly specific characteristic of double stranded DNA is its melting temperature. It depends on the DNA sequence and is maximal for full-length perfect matches. Thus it is possible to assess the specificity of hybridisation via the analysis of melting curves over increasing hybridisation or washing stringencies (Drobyshev et al. 2003b). If different fractions of target are hybridised to a probe, these will be washed off the array at different stringencies due to different extends of double strand formation.

Post-hybridisation signal intensities of every feature *in situ* after gradual increases in washing stringencies using 0.25x SSC containing formamide between 0-94.5% were analysed (Figure 8a) (Drobyshev et al. 2003b). The mean pixel intensities for each single feature obtained after each washing step were plotted versus the stringency as fractionation curves (Figure 8b). The obtained curves are representative for specific or cross hybridisation.

The comparison of fractionation curves and transition stringencies, which mark the mid point of the transition of a fractionation curve, obtained from different mouse organs used for this analysis revealed that genes exist that have reduced transition stringencies in certain organs (Drobyshev et al. 2003b). This indicates that the specificity of a hybridisation is not only dependent on experimental procedures but also on the tissue hybridised to the array. Detailed analysis of different organs hybridised against each other led to the conclusion that at least 0.2-1.7% of the probes produce signals that result from non-specific hybridisation (Drobyshev et al. 2003b).
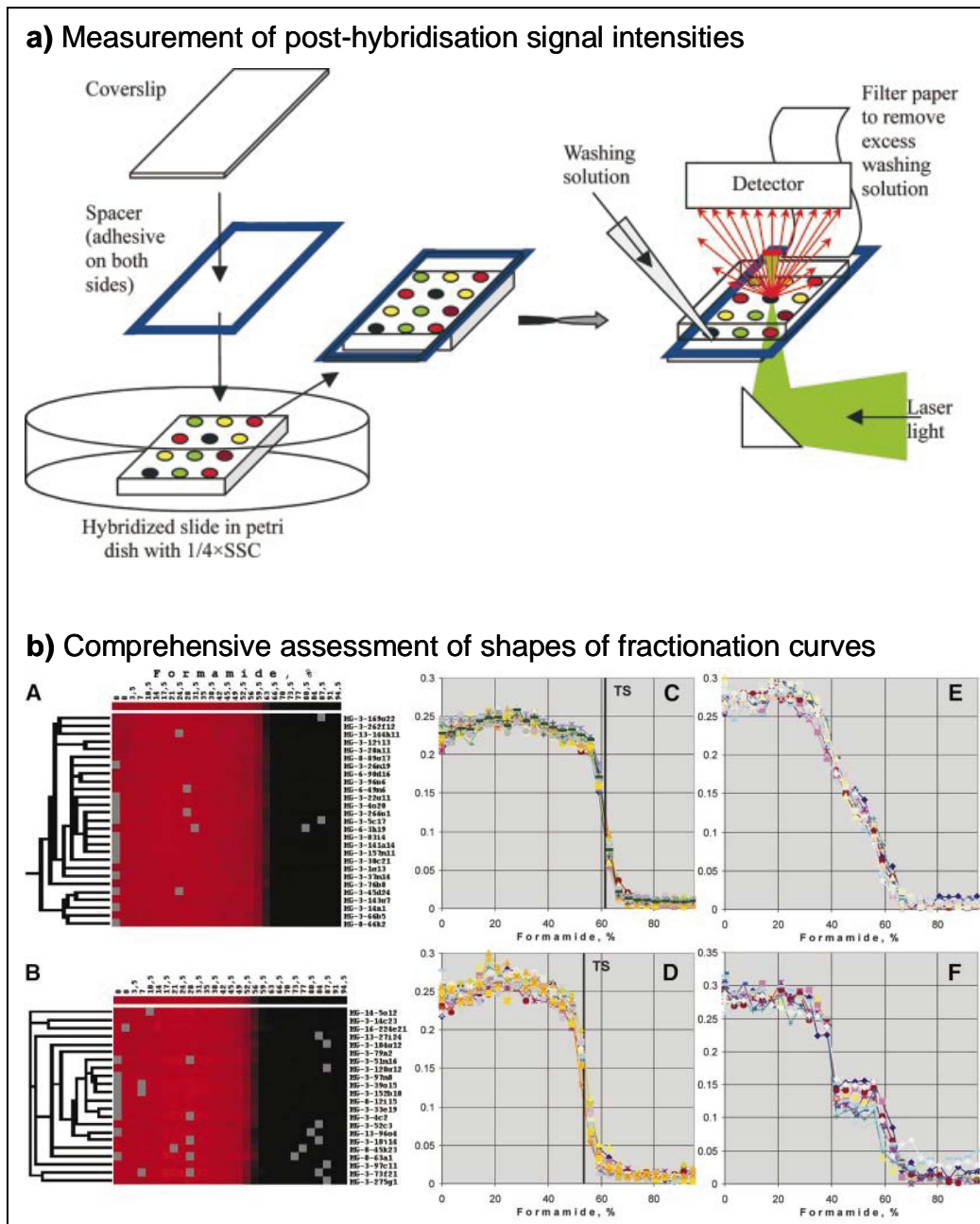
Figure 8: Experimental setup and results from fractionation experiments. a) Experimental setup for the measurement of post-hybridisation signal intensities. For detailed description see Material and Methods (2.2.7, p. 33). b) (A) Part of the hierarchical tree with genes having sharp transitions from the hybridised to non-hybridised state near 62% formamide that cluster together. (B) As (A) but with genes that have a sharp transition near 55% formamide. (C) Normalised signal intensities (y-axis) over increasing formamide concentrations (x-axis) of the same 27 genes as in (A). The vertical line indicates the transition stringency (TS), the mid-point of the transition from hybridised to dehybridised signal intensities. (D) Fractionation curves (x-axis, normalised signal intensities; y-axis, formamide concentration) of the same 21 genes as in (B). Vertical line indicates the transition stringency (TS) in this cluster of fractionation curves. (E) Cluster of 14 fractionation curves having broad transition

regions. (F) Cluster of 10 fractionation curves having a two-step transition from the hybridised to non-hybridised state. Adopted from Drobyshev et al. 2003b.

3.1.7 Biological Resources

For the RNA expression profiling analysis *Dll1* wildtype (wt) and *Dll1$^{-/-}$* embryos (Hrabe de Angelis et al. 1997) at embryonic day 10.5 have been used. These mice were kept on an isogenic 129SvJ background.

The embryos were phenotyped during the preparation process. Embryos which were phenotypically normal (*Dll1$^{+/+}$*, *Dll1$^{+/-}$*) were grouped together. The second group consisted of embryos which were phenotypically mutant. *Dll1$^{-/-}$* embryos exhibit clear defects at E10.5. The neural tube is undulated, somites are irregular in size and shape, somites in the tail region are missing, embryonic turning and heart looping is randomised, many are hydrocephalic and exhibit inner bleeding in the head and the neural tube (Hrabe de Angelis et al. 1997; Przemeck et al. 2003).

Of each of the two groups embryos were pooled and RNA isolated subsequently.

3.1.8 Statistical analysis of DNA-chips of wt versus *Dll1$^{-/-}$* embryos

Atlas GlassMouse 1 Array

Nine chip hybridisations were performed and analysed together. The threshold of signal intensity was set to 50 units and the "probability to have one gene like this for non-correlated datasets" was selected to be <10%. The number of spots identified to be above 50 scanner units in all nine experiments was 457.

At a significance level of 0.1 the number of non-uniform upregulated genes was 1 and the number of FDG < 2. The number of non-uniform downregulated genes was 0 and the number of FDG <1. The ratio of non-uniform/total patterns was 0 and the FDG < 0.12.

Using these criteria six upregulated and ten downregulated genes could be selected.

20k chip

Four chip hybridisations were performed and analysed for the 20k chip. The threshold of signal intensity was set to 1000 units and the "probability to have one gene like this for non-correlated datasets" was selected to be <10%.The number of spots found in all four experiments to be above 1000 scanner units was 1808.

At a significance level of 0.1 the number of non-uniform upregulated genes was 0 and the number of FDG <2. The number of non-uniform downregulated genes was 4 and the number of FDG <7. The ratio of non-uniform/total patterns was 0 for the upregulated genes and 0.05 for the downregulated genes. The FDR was <0.06 for the upregulated and <0.09 for the downregulated genes.

Using these criteria 26 upregulated and 21 downregulated genes could be selected. Ten of the upregulated and one of the downregulated candidates were rda clones. Sequencing of

these clones revealed that the spotted sequences mostly represented vector sequence. Thus, these genes were false positives and excluded from further analysis. In total 22 upregulated and 30 downregulated genes were chosen for further analyses.

In Table 1 the selected candidates from both chip analysis are presented. The genes are sorted according to their minimal factor of regulation.

Detailed information on the identified candidate genes will be given in chapter 3.3.

Upregulated genes (Clontech and 20k chip)	Gene Symbol	Acc. No.	Ratio	Function
Metallothionein 1	Mt1	NM_013602	3.5-13.1	ion binding
Metallothionein 2	Mt2	NM_008630	3.0-9.5	ion binding
BCL2 adenovirus E1B 19 kDa-interacting protein 1 NIP3	Bnip3	NM_009760	2.7-3.6	cell cycle
Fibroblast Growth Factor 6	Fgf6	AK086530	2.5-4.2	cell cycle
RIKEN cDNA 1110021J02 gene	MG-4-3k8	AK003900	1.9-3.5	no function
Nucleoporin 155	Nup155	NM_133227	1.9-2.4	transport
Hemoglobin beta adult minor chain	Hbb-b2	NM_016956	1.8-3.6	transport
MAP microtubule affinity-regulating kinase 3	Mark3	NM_021516	1.8-3.5	cell metabolism
Hemoglobin Y beta-like embryonic chain	Hbb-y	NM_008221	1.7-3.1	transport
Erythroid associated factor	Eraf	NM_133245	1.7-2.3	transport
mf36d02.r1 Soares mouse embryo NbME13.5 14.5 Mus musculus cDNA	MG-4-146d10	AK005069	1.7-2.9	cell metabolism
RIKEN cDNA 1110017I16 gene	MG-8-86g2	NM_026754	1.7-2.8	no function
Alpha-enolase	Eno1	NM_023119	1.7-5.3	ion binding
Guanidinoacetate methyltransferase	Gamt	NM_010255	1.6-3.0	cell metabolism
ii27f08.x1 Melton Amplified Mouse E16 5 Pancreas 3 M16S1 A M	MG-4-3k1		1.6-3.2	no function
Zinc finger protein Rlf (Rearranged L-myc fusion gene protein) (Zn-15 related protein)	MG-8-54o6		1.6-3.0	no function
Hemoglobin beta chain. (MG-68-143l7)	HBB	AB020013	1.5-3.4	transport
Ataxia telangiesectasia gene mutated in human beings	Atm	NM_007499	1.3-7.1	cell cycle
c-src tyrosine kinase	csk	NM_007783	1.3-3.7	cell signalling
S100a10, S100 calcium binding protein A10 (Calpactin I light chain)	S100a10	NM_009112	1.3-2.8	ion binding
Wingless related MMTV integration site 10b	Wnt10b	NM_011718	1.2-3.6	cell signalling
Recoverin	Rcvrn	NM_009038	1.2-3.5	ion binding
Downregulated genes (Clontech and 20k chip)	**Gene symbol**	**Acc. No.**	**Ratio**	**Function**
Glutamate-ammonia ligase glutamine synthase	Glu1	NM_008131	2.0-4.4	cell metabolism
RIKEN cDNA 2210411K11 gene	MG-8-96d13	AK008900	1.8-2.9	no function
Integral membrane transporter protein.	MG-8-118g23		1.8-3.4	no function
RIKEN cDNA 0610009D10 gene	MG-8-118d15	NM_027862	1.8-3.0	transport
hypothetical protein E230025N21	MG-8-17n2		1.7-3.3	no function
UI-M-CG0p-bdf-d-05-0-UI.r1 NIH_BMAP_Ret4_S2 Mus musculus cDNA	MG-26-73n1		1.6-1.9	no function
no functional assignment	MG-8-12b14		1.6-4.3	no function
Ran binding protein 5 (rda-A09)			1.6-3.2	not in MGI db
Deiodinase iodothyronine type II	Dio2	NM_010050	1.5-2.3	cell metabolism
Nestin	Nes	NM_016701	1.5-1.7	neurogenesis
SWI SNF related matrix associated actin dependent regulator of chromatin subfamily c member 1	Smarcc1	NM_009211	1.4-2.5	cell cycle
mai17e04.y1 McCarrey Eddy type A spermatogonia Mus musculus	MG-3-21l10		1.4-1.7	no function
EST594220 Rat gene index, normalized rat, norvegicus Rattus	MG-8-1k1		1.4-2.6	no function
DEAD aspartate-glutamate-alanine-aspartate box polypeptide 6	Ddx6	D50494	1.4-3.0	cell cycle
Semaphorin 5B (Semaphorin G)	Sema5b	NM_013661	1.4-2.1	neurogenesis
Feline sarcoma oncogene	Fes	NM_010194	1.3-5.5	cell cycle
Distal-less homeobox 7			1.3-2.4	not in MGI db
Chondroitin 4-sulfotransferase 2	Chst12	NM_021528	1.3-1.9	cell metabolism
UI-M-CG0p-bqe-g-10-0-UI.r1 NIH_BMAP_Ret4_S2 Mus musculus cDNA	MG-26-87m22		1.3-1.7	no function
lectin mannose-binding 2-like	MG-4-13l22		1.3-1.8	no function
Chloride channel 1	Clcn1	AK002779	1.3-2.2	no function
Weakly similar to cyclin-dependent kinase 6 (Fragment)	MG-3-67g9		1.3-1.9	no function
H6 homeo box 2	Hmx2	AK053014	1.2-3.3	cell signalling
LIM homeo box protein 3	Lhx3	NM_010711	1.1-1.8	cell signalling
T-cell leukemia homeobox 1	Tlx1	NM_021901	1.1-2.7	cell signalling
Ubiquitously-expressed nuclear receptor 2	Nr1h2	NM_009473	1.1-1.4	cell signalling
Prothymosin alpha	Ptma	NM_008972	1.1-2.4	no function
Platelet derived growth factor receptor alpha	Pdgfra	NM_011058	1.0-5.0	cell metabolism
Platelet derived growth factor alpha	Pdgfa	NM_008808	0.7-1.8	cell cycle
Interferon induced transmembrane protein 1	Ifitm1	NM_026820	0.7-1.5	no function

Table 1: Differentially expressed genes identified using the Atlas GlassMouse 1 (Clontech) and the 20k chip. The upper part shows the upregulated genes and the lower part the downregulated genes. Genes are sorted according to their factor of regulation (fourth column). The gene name, gene symbol, accession number and GO classification are also shown.

3.2 Functional assessment of regulated genes

As shown in the previous section 52 genes have been identified to be differentially expressed in *Dll1*^{-/-} embryos at E10.5. The now following part describes the classification of the candidate genes into functional classes. Based on the Gene Ontology (GO) classifications of the MGI database (Harris et al. 2004) the selected genes were grouped according to their functional annotation (Table 1, last column).

The upregulated genes can be grouped in six functional classes. Genes involved in cell cycle processes make up 14% as well as cell metabolism genes, cell signalling/signal transduction genes and genes without functional annotation. The category "no functional assignment" includes yet unknown genes as well as known genes without functional annotation so far. Genes involved in transport or ion binding processes make up 22% each. The distribution of functional classes within the downregulated genes is different. Although cell cycle, cell metabolism and cell signalling/signal transduction genes also account each for 14% of the candidates, 7% are neurogenesis genes which are not present within the set of upregulated genes. Involved in transport functions are 3% of the downregulated genes compared to 22% of the upregulated genes. No genes with functions in ion binding could be identified in the downregulated genes. The number of genes without functional annotation is much bigger in the downregulated genes (49% to 14%).
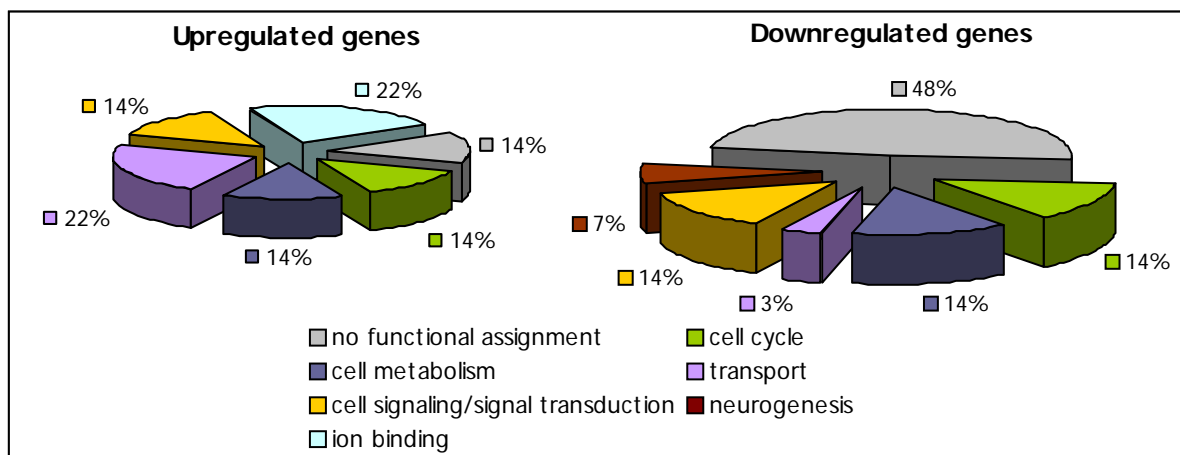
Figure 9: Regulated genes and functional annotation. The identified candidate genes are grouped according to their functional annotation based on the Gene Ontology classification. Genes holding functions in cell cycle, cell metabolism, cell signalling and signal transduction, transport, ion binding and neurogenesis, as well as genes without functional annotation are presented.

To check for potential interaction expression patterns were analysed using whole mount *in situ* hybridisation.

3.3 Whole mount *in situ* hybridisation screen

So far none of the identified differentially expressed genes has been brought into direct context to Delta/Notch signalling. Additionally, many of the genes do not have assigned functions. Thus the publicly available information is limited and for many genes also no information on the expression pattern exists.

Delta/Notch signalling is known to be involved in many different processes during embryonic development (see introduction). In all these tissues the involvement can be surveyed with specific marker genes using *in situ* hybridisation.

To identify potential connections between the candidate genes and Delta/Notch signalling the identified candidate genes were systematically screened using whole mount *in situ* hybridisation (wish). In a first step all probes were used on *Dll1*-wt embryos. If the obtained pattern was indicative of Delta/Notch signalling the probe was also used on *Dll1*$^{-/-}$ embryos.

3.3.1 Selection of probes

In order to be able to compare the results received from the DNA-chip analysis with the results of the wish analysis it is reasonable to use exactly the same sequences for the wish as were spotted on the array. However, this was not possible for the candidates obtained from the Atlas GlassMouse1 Array. Thus different kinds of riboprobes were used for the wish.

For the candidate genes obtained from the 20k chip the same sequences as spotted on the array were used. This means that the probes are also mostly 3´ UTRs, 300-800 bp, depleated of coding regions, repetitive elements and polyA tails. The clones contain a tag of roughly 150 bp at the 3´end of the gene specific sequence. The cDNAs from Lion Bioscience for the production of DNA-chip targets are directionally subcloned into pBluescript (Figure 10). Thus for antisense probes plasmids were digested with SacI and in vitro transcribed with T3 RNA polymerase, for sense probes plasmids were digested with Acc65I and in vitro transcribed with T7 RNA polymerase.

In some cases the obtained probes exhibited multiple bands after *in vitro* transcription. Additionally, nine probes produced no expression pattern and 11 probes high background signals. In cases where increasing the stringency of the hybridisation and washing steps did not improve the results and to survey if these patterns are due to the probe sequence new riboprobes were cloned using other parts of the genes as probe sequence.

The regions for alternative riboprobes were selected using different criteria. The selected parts of the coding region varied for the different genes between a few hundred to two thousand basepairs, avoiding gene family specific homologies and repetitive regions. Primers were selected using VectorNTI software (Informax). Reverse transcription (RT) PCR was performed on a pool of murine samples including whole embryos at E10.5, E11.5, E12.5, adult liver, brain and kidney to ensure that the particular gene is expressed in at least one of these tissues. The PCR products were subcloned using TopoTA cloning kits and the insert was sequence verified.
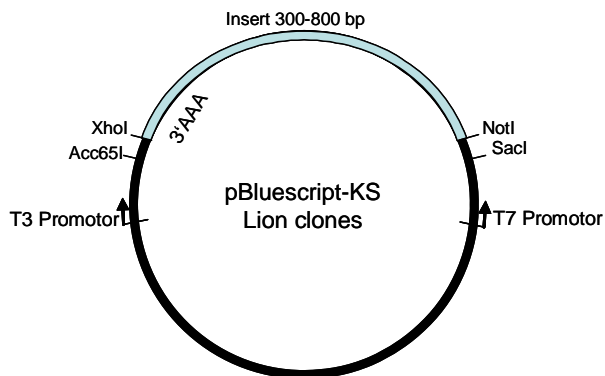
Figure 10: Representative scheme of Lion clones. 300-800 bp fragments representing 3´UTRs of the genes were directionally cloned into a pBluescript-KS vector at XhoI and NotI restriction sites. The 3´ poly A tail would be located next to the XhoI site. For antisense riboprobes vectors were linearised with SacI and in vitro transcribed with T3 RNA polymerase.

The Atlas GlassMouse 1 array contains oligomers (~80mers) as targets. An oligomer of ~80 bases in length would be too short to use it as riboprobe. Nevertheless, Clontech does not provide sequence information of the spotted oligomers. Therefore it was not possible to select riboprobes from the same region of the gene that was spotted on the array. As consequence, for some of the genes published probes have been used. For others probes have been selected using publicly available sequence information, amplified by RT-PCR and were subsequently subcloned as previously described for genes from the 20k set.

3.3.2 Whole mount *in situ* hybridisation

In order to identify novel expression patterns of the candidate genes and also to get hints on the involvement in Delta/Notch signalling all candidate genes were screened systematically, first on *Dll1*-wt embryos.

3.3.2.1   Expression patterns indicative of Delta/Notch signalling

Riboprobes derived from Lion clones, RT-PCR amplified parts of genes and published sequences have been used for wish.

Genes that showed expression in regions of the embryo where Delta/Notch signalling is normally involved e.g. the presomitic and paraxial mesoderm or neural tissues were chosen to hybridise *Dll1*$^{-/-}$ embryos additionally.

Figure 11 shows the wish results of *Dll1*-wt and *Dll1*$^{-/-}$ E10.5 embryos. Genes are sorted according to their function.

Cell cycle

Cell metabolism

| E10.5 wt | E10.5 Dll1⁻/⁻ |
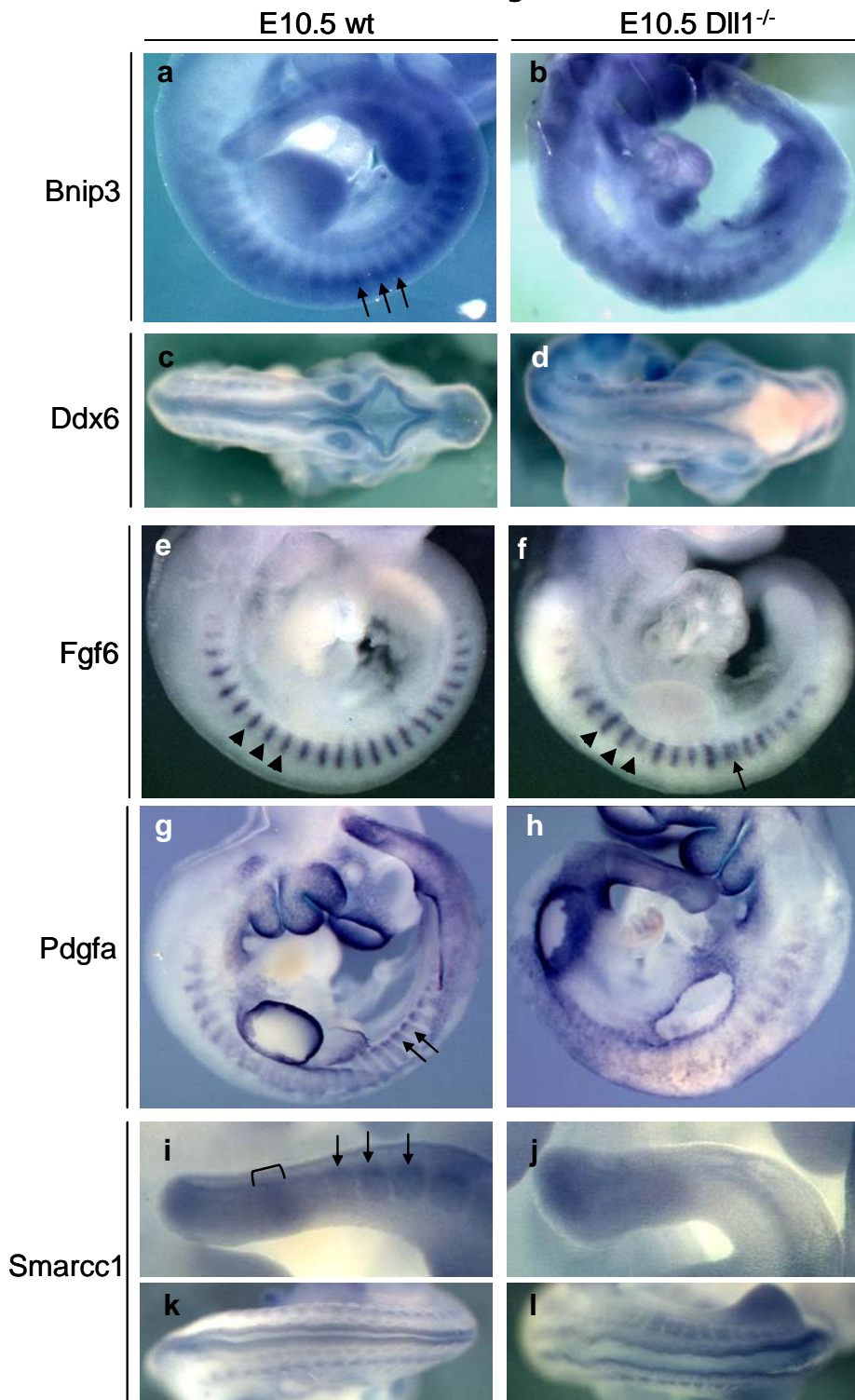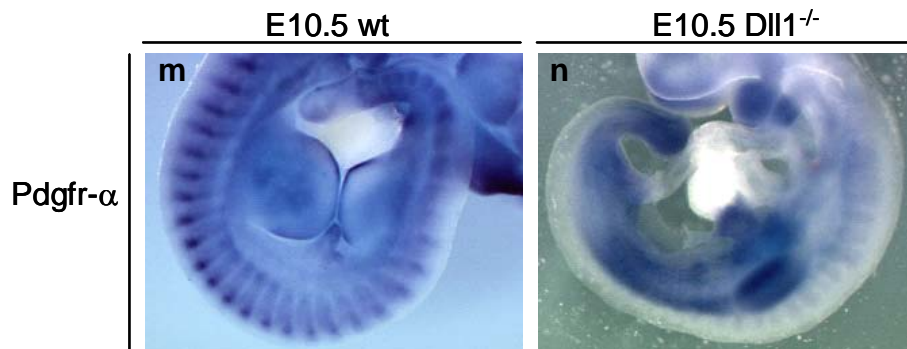
Cell signaling / Signal transduction

| E10.5 wt | E10.5 Dll1⁻/⁻ |

Ion binding

| E10.5 wt | E10.5 Dll1⁻/⁻ |

Neurogenesis

Unknown function
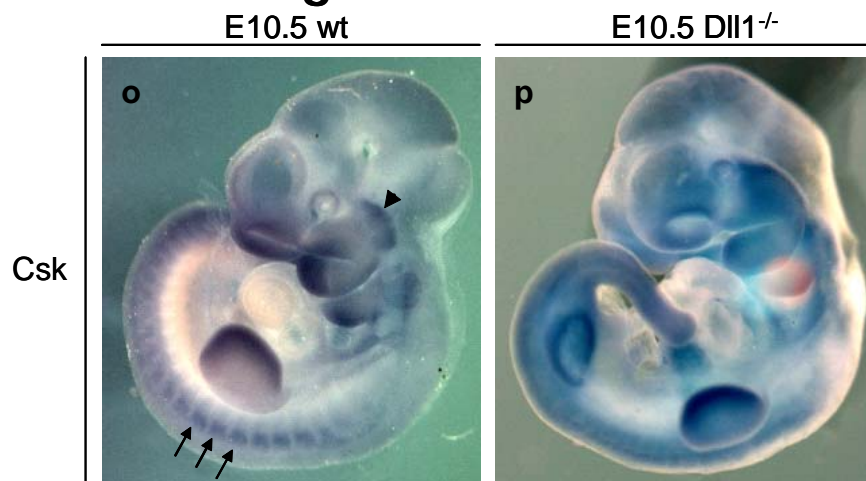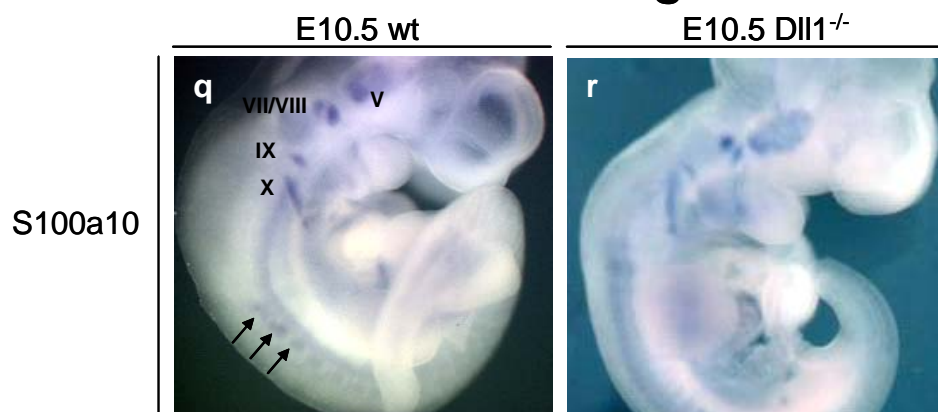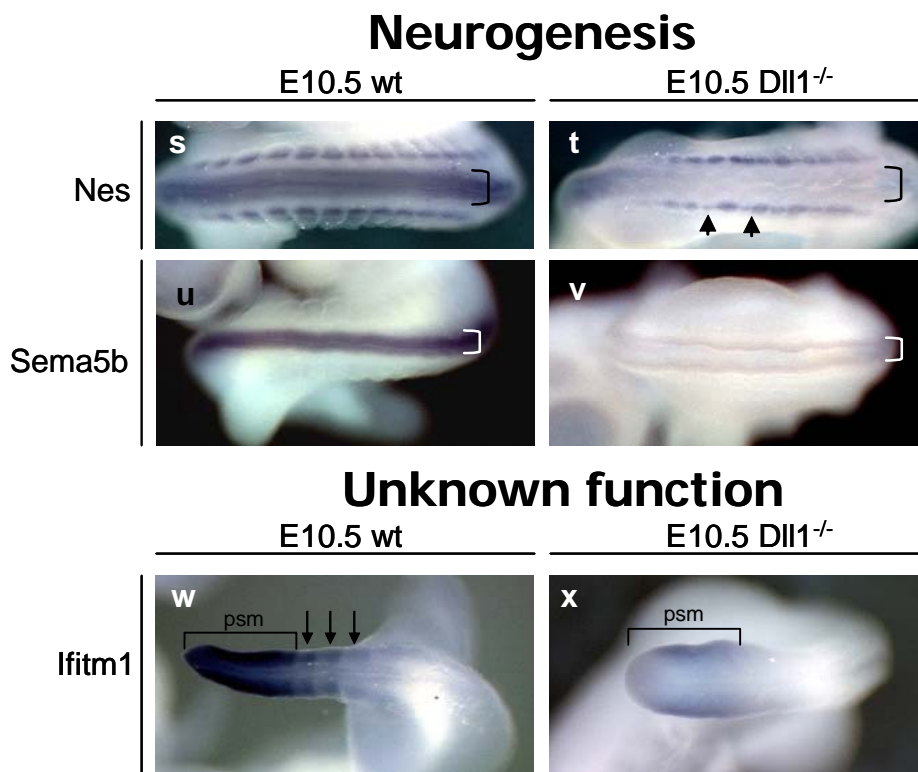
Figure 11: Wish analysis of potential Dll1 targets. The expression pattern in wt and Dll1$^{-/-}$ embryos is presented. Genes are sorted according to their function. (a) Expression of Bnip3 was observed in a segmented fashion along the anterior-posterior axis in the wt. In the Dll1$^{-/-}$ (b) the segmented expression was reduced. (c) Ddx6 expression was observed in the neural tube and in a segmented way along the anterior-posterior axis, maybe in the dorsal root ganglia or somitic compartments. (d) In the mutant the expression in the neural tube is reduced. Fgf6 is expressed in the myotome of somites (e). In the Dll1 mutants the regularity of the expression was disrupted and segments were fused (f, arrow). In the wt Pdgfa is expressed in the dermomyotome, branchial arches and the surface ectoderm (g). In the mutant expression in the dermomyotomal compartments is strongly reduced while expression in the other domains is maintained (h). (i, k) Smarcc1 was expressed in a stripe in the psm and the somites. It was also expressed in the neuroepithelium of the neural tube. (j, l) In the Dll1$^{-/-}$ the expression in the psm and the somites is lost; expression in the neuroepithelium is maintained. Pdgfr-α is expressed in the dermomyotome and branchial arches in the wt (m) while in the Dll1 mutants expression in the dermomyotome was lost (n). (o, p) Csk was found in a segmented fashion in the dorsal root ganglia and the trigeminal ganglion in the wt. In the Dll1$^{-/-}$ expression in the dorsal root ganglia was lost. S100a10 was found to be expressed in the neural crest derivatives (arrows) and in the cranial ganglia V, VII/VIII, IX and X (q). In the mutants only expression in the neural crest derivatives seemed to be altered (r). (s, t) The strong expression of nestin in the neuroepithelium along the anterior-posterior axis was lost in the Dll1$^{-/-}$. Expression in neural crest cells is still present in the mutant although irregular and weaker. (u) Sema5b is expressed in the neuroepithelium of the neural tube. In the mutant expression was still present but strongly reduced (v). (w) In the wt Ifitm1 was found to be expressed in the psm and the last formed somites while in the Dll1 mutant (x) expression in the psm was strongly reduced, the expression domain was smaller and expression in the somites was lost.

psm: presomitic mesoderm; V: trigeminal ganglion, VII/VIII: facial/auditory ganglia;

Bnip3 (BCL2 adenovirus E1B 19kDa-interacting protein 1 NIP3)

Bnip3 belongs to the family of Bcl-2 related proteins. They are supposed to function as sensors to distinctive cellular stresses which lead the cell to apoptosis (Itoh et al. 2003). The mRNA encodes for a membrane bound protein located in the mitochondrial membrane (Guo et al. 2001).

No expression data of embryonic stages exists. Using wish expression was detected in the wt in a segmented fashion along the anterior-posterior axis (arrows in Figure 11a) and also evenly in the whole embryo. In the *Dll1^{-/-}* embryo the segmented expression was reduced although the overall expression level seemed to be similar.

Ddx6 (DEAD aspartate-glutamate-alanine-aspartate box polypeptide 6)

Ddx6 is a gene coding for a RNA helicase from the DEAD-box family which is found in almost all organisms and which have important roles in RNA metabolism. In wt (Figure 11c) embryos expression was observed in the neural tube and in ganglia or somatic compartments along the anterior-posterior axis. In the mutants expression in the neural tube was reduced but the segmented expression was maintained (Figure 11d).

Fgf6 (Fibroblast growth factor 6)

Fgf6 belongs to the fibroblast growth factor (FGF) family of tyrosine kinases. *Fgf6*, in particular, is expressed in the myotomal compartment of the somites around E9.5-E11.5 (deLapeyriere et al. 1993). Starting at E13.5 *Fgf6* expression occurred only in the developing skeletal muscles. Accordingly it was demonstrated that *Fgf6* loss-of-function leads to reduced regeneration of muscle tissue in adult mice, suggesting that *Fgf6* functions during embryonic development as well as in the adult mouse (Floss et al. 1997).

Using wish the expression pattern described by (deLapeyriere et al. 1993) could be confirmed (Figure 11e). In contrast to the regularly segmented expression pattern of the wildtype (Figure 11f arrowheads), the size of the segments in *Dll1^{-/-}* embryos differed and fusions between segments occurred (Figure 11f arrow).

Pdgfa (Platelet derived growth factor alpha)

Platelet derived growth factors (Pdgfs) have been shown to regulate cell growth and survival as well as various aspects of cell morphology and movement, such as scattering, chemotaxis or deposition of extracellular matrix (Soriano 1997).

As described in the literature (Orr-Urtreger and Lonai 1992) *Pdgfa* is expressed in the 1st branchial arch, surface ectoderm, myotome, floor plate, optic cup, optic stalk, otocyst and pharynx. In general, the ligand Pdgfa is expressed in the epithelium or endothelium while the receptor Pdgfr-α is expressed in the surrounding mesenchyme. Figure 11g shows that the known expression pattern was reproduced. In the mutant embryo the expression in the dermomyotome is strongly reduced Figure 11h).

Smarcc1 (SWI SNF related matrix associated actin dependant regulator of chromatin subfamily c member 1)

Smarcc1 (also known as *Srg3*) is a core component of the SWI/SNF complexes which are known to be involved in chromatin binding (Kim et al. 2001). Published information about the expression at E10.5 is not available. As shown in Figure 11i in the wt expression was observed in the somites in the tail (arrows) and the presomitic mesoderm (psm). Especially a roughly one somite broad stripe was observed in the psm of wt embryos (bracket). Figure 11k shows the same embryo from another perspective. Expression was observed in the neuroepithelium of the neural tube and in a segmented fashion along the anterior-posterior axis. This might either be expression in one of the somitic compartments (dermomyotome or sclerotome) or in dorsal root ganglia. Further histological analysis has to clarify this. Figure 11j and I shows the expression in the *Dll1$^{-/-}$* mutant. The segmentation of the tail and the expression in the somites is lost. Expression in the neuroepithelium of the neural tube is maintained but the clear segmentation is disrupted (Figure 11l).

Pdgfr-α (Platelet derived growth factor receptor alpha)

Pdgfr-α is required for normal development of mesoderm and cephalic neural crest derivatives (Zhang et al. 1998).

Pdgfr-α is known to be expressed, except for the eye, in the mesenchyme of the developing otocyst, branchial arch, AER, dermis, head mesenchyme, dermatome and sclerotome (Orr-Urtreger and Lonai 1992; Harris et al. 2004). In the wt the described expression pattern was confirmed (Figure 11m) whereas in the *Dll1* mutant embryo expression in the dermomyotome and sclerotome is reduced (Figure 11n). Other expression domains are maintained.

Csk (C-src tyrosine kinase)

Csk is a gene coding for a non-receptor protein tyrosine kinase involved in intracellular trafficking processes (Avrov and Kazlauskas 2003). *In situ* expression data is not available so far. Wish at E10.5 revealed expression in the branchial arches, trigeminal ganglion, limb buds and dorsal root ganglia (Figure 11o). In the *Dll1$^{-/-}$* embryos expression in all domains is maintained while expression in the dorsal root ganglia is reduced and segmentation is lost (Figure 11p).

S100a10 (S100 calcium binding protein A10; Calpactin I light chain)

S100a10 belongs to a multigenic family of Ca^{2+}-binding proteins of the EF-hand type known as S100 proteins (Donato 1999).

At E10.5 expression was observed in neural crest derivatives (arrows) and cranial ganglia number V, VII, IX and X.

Nes (Nestin)

Nestin encodes an intermediate filament protein and thus a component of the cytoskeleton. Intermediate filament genes are also expressed at specific stages and in specific cell types during development of the central nervous system (CNS). *Nestin* is expressed at E10.5 in multipotent neuroepithelial cells in the rostral and caudal part of the neural tube, migrating

neural crest cells, cells in the dorsal root ganglia and cells in the myotome of somites (Dahlstrand et al. 1995; Lutolf et al. 2002).

Figure 11s and t show a dorsal view of the neural tube between the hindlimb buds (to the left) and the forelimb buds. In the wt expression in the neural tube (bracket) and neural crest cells is clearly visible. The expression in the neural tube is missing in *Dll1*^{-/-} embryos (bracket) while the expression in the neural crest cells is still present. Segmentation is not as regular as in the wt (arrows) and segments are smaller.

Sema5b (Sema domain, seven thrombospondin repeats (type 1 and type 1-like), transmembrane domain (TM) and short cytoplasmic domain, (semaphorin) 5B)

The protein family of semaphorins is involved in axonal guidance. All members contain a conserved domain of 500 amino acids and 16 conserved cysteins, the so called semaphorin domain. *Sema5b* is likely to encode an integral membrane protein containing seven thrombospondin repeats but no Ig motif. Expression of *Sema5b* was analysed by Adams et al. 1996. It was found to be expressed in the neuroepithelium along the entire anterior-posterior axis. In the caudal part of the neural tube the signal is weak. In the wt the described expression was confirmed (Figure 11u) while in the *Dll1* mutant (Figure 11v) the expression in the neuroepithelium was strongly reduced.

Ifitm1 (Interferon induced transmembrane protein 1)

Ifitm1 was identified as a marker for primordial germ cells (Tanaka and Matsui 2002; Lange et al. 2003). Expression of embryos at E10.5 has not been studied by these authors. Figure 11w and Figure 11x show expression from wt and *Dll1* mutant embryos. In the wt strong expression was found in the psm (bracket) and the last few somites (arrows). In the mutant (Figure 11x) expression in the psm is reduced and the expression domain is smaller (bracket) than in the wt. Expression in the somites is missing completely.

3.3.2.2   Ubiquitous and no expression pattern

In some cases the tested genes (*Nup155, Glu1*) were expressed ubiquitously or continuously strong in the surface ectoderm of the embryos (Figure 12 a, b).

Nup 155 (Nucleoporin 155)

Nup155 is a major component of the nuclear pore complex. The human *NUP155* has been found to be ubiquitously expressed in many tissues including heart, brain, placenta, lung, liver, skeletal muscle, kidney and pancreas (Zhang et al. 2002).

Wish on E10.5 embryos revealed ubiquitous expression in the whole embryo (Figure 12a).
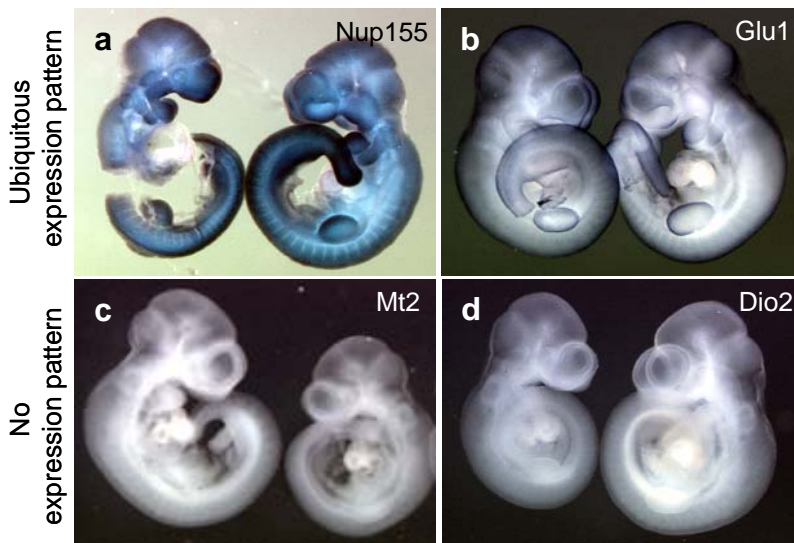
Figure 12: Wish of 10.5 dpc mouse embryos. (a, b) Nup155 and Glu1 as examples of genes with ubiquitous expression patterns. (c, d) Wish of Mt2 and Dio2 as examples of genes with no detectable expression.

Glu1 (Glutamtate-ammonia ligase glutamine synthase)

Glial cells perform diverse functions, one of them being a nutritive function. Glial cells in the mammalian brain (essentially astrocytes) transform the glucose they take from the blood and supply substrates of energy metabolism and amino acids to neurons (Tsacopoulos 2002). *Glu1* is a cytosolic multicomponent iron-sulfur flavoprotein belonging to the class of N-terminal nucleophile amidotransferases (van den Heuvel et al. 2004). It catalyzes the fixation of NH_4^+ and thus transforms cytosolic glutamate to glutamine in an ATP-dependent reaction (Tsacopoulos 2002).

Using *in situ* hybridisation ubiquitous expression pattern was observed (Figure 12b).

Other genes such as *Mt2* or *Dio2* (Figure 12 c, d) did not show any visible expression pattern.

Mt2 (Metallothionin 2)

Metallothioneins have fundamental roles in various processes such as homeostasis of essential metals (zinc and copper), heavy metal detoxication and in the acute-phase response to stress (Michalska and Choo 1993; Masters et al. 1994; Kimura et al. 2000b). They are constitutively expressed at low levels in many different cell types and tissues but their transcription can be induced by metal ions, glucocorticoids and lipopolysaccharides (Michalska and Choo 1993; Kimura et al. 2000a). Expression analysis revealed high expression levels in the parietal and visceral endoderm of post-implantation mouse embryos and in fetal mouse liver, indicating functions during embryonic development.

Wish on E10.5 embryos revealed no expression pattern (Figure 12c).

        Dio2 (Deiodinase iodothyronine type II)

The *Dio2* gene encodes the type 2 deiodinase which is involved in the basal energy homeostasis in brown adipose tissue (Christoffolete et al. 2004).

In E10.5 embryos no expression of *Dio2* was observed.

3.4 Real-time PCR verification

Using wish a number of genes with expression patterns that might be connected to Delta/Notch signalling have been identified from the DNA-chip candidates. However, results obtained from wish cannot be quantified. To verify the results from the DNA-chip experiments real-time PCR was used for a random selection of up- and downregulated genes. Real-time PCR was also performed if the wish expression pattern indicated potential involvement in the Delta/Notch pathway.

Real-time PCR is a very sensitive method to analyse the relative or absolute quantity of RNA via measuring a fluorescent signal of labelled nucleotides incorporated during a PCR reaction. The cycle number in which exponential signal amplification is observed for the first time is the basis for the calculation of relative quantities and for the comparison of a test and a reference sample. PCR reactions containing defined amounts of template DNA are used as standard curve for absolute quantification. In experiments serving to confirm an observed factor of regulation, relative quantification is sufficient.

As starting material the same RNA as used for the DNA-chips was used for reverse transcription. Subsequently, cDNA was purified, the concentration determined by spectrophotometry and the concentration of wt and *Dll1* knockout samples was adjusted. To ensure consistent results of the PCR two primer pairs for most of the tested genes were used. Different primer pairs were selected from different regions of the gene if possible. The primer design feature of VectorNTI software (Informax) was used to design gene specific primers producing products of 150-350 bp in length. Expected products were blasted against mouse cDNAs to avoid homology dependant amplification. Each reaction was repeated at least twice. Dissociation curves which are produced following the real-time run indicate amplification of only one specific PCR product.

All real-time PCR results in comparison to DNA-chip results are shown in Table 2. On the left side genes that were upregulated on the DNA-chip are presented while on the right side the downregulated candidates are shown. Tested genes are named in the first column. The last two columns show the tendency of regulation using real-time PCR in relation to the housekeeping gene Hprt. If the dissociation curve indicated an unsuccessful PCR no result was obtained. Those cases are marked as "no result" in the table. Cases where only one pair of primers was used are also marked.

Genes upregulated on DNA-chip	Real-time PCR Primer 1	Real-time PCR Primer2	Genes down-regulated on DNA-chip	Real-time PCR Primer 1	Real-time PCR Primer 2
Atm	up	no primer	Atp5h	down	equal
Bnip3	up	up	Chst12	down	down
Csk	up	down	Ddx6	down	no primer
Eno1	up	up	Dio2	no result	down
Eraf	up	equal	Fes	down	down
Fgf6	up	up	Glu1	down	down
Gamt	down	down	Hmx2	equal	no primer
Mark3	up	no primer	Ifitm1	down	equal
MG-4-3k8	down	down	Nes	down	down
MG-8-86g2	no result	equal	Nr1h2	up	down
Mt1	up	up	Pdgf-a	down	down
Mt2	up	up	Pdgfr-a	no result	down
Nup155	equal	equal	Ptma	down	no primer
Rcvrn	equal	no result	Sema5b	down	down
S100a10	equal	equal	Smarcc1	down	no result
Wnt10b	down	down	Tlx1	down	no primer

Table 2: Real-time PCR analysis of selected DNA-chip candidates. In general two primer pairs have been used (Real-time PCR Primer 1 and 2). The results are shown in column 3 and 4 of the up- and downregulated candidates respectively.

In five cases Primer 1 and Primer 2 produced opposing results (*Csk, Eraf, Atp5h, Ifitm1, Nr1h2*). In eight cases the used primers produced inversive results compared to DNA-chip findings (*Gamt*, MG-4-3k8, MG-8-86g2, *Nup155, Rcvrn, S100a10, Wnt10b, Hmx2*). Genes that were found by real-time PCR to be equally strong expressed in the wt and the mutant are also quoted as opposite expression compared to the DNA-chip results.

However, in case of 19 genes the up- or down-regulation found in the DNA-chip experiments could be verified by real-time PCR. Including all genes which showed differential expression in wish (*Bnip3, Fgf6, Ddx6, Nes, Pdgf-a, Pdgfr-α, Sema5b*) except for two genes (Csk, Ifitm1), which did not show clear results.

3.5 Connections to Delta/Notch signalling

As shown in chapter 3.3.2.1 several of the genes identified using DNA-chips show not only interesting but also differential expression patterns. Changes in expression pattern might indicate direct or indirect involvement in Delta/Notch signalling as downstream targets, enhancers or other regulating elements of this pathway might be influenced. To check further indicators of involvement of the identified genes wish was performed on further Delta/Notch mutants. Mice carrying a mutation in *Dll3* and *Jag1*, respectively, which lead to loss-of-function of the genes were used (Kusumi et al. 1998; Kiernan et al. 2001). To be able to compare the results to the previous study the analysis was performed at E10.5.

Figure 13 shows the expression of the genes *Csk, Ddx6, Ifitm1, Nes, Sema5b* and *Smarcc1* in wt embryos and in several Delta/Notch pathway mutants at 10.5 dpc.

Csk (C-src tyrosine kinase) (Figure 13a-d)

In the wt Csk is expressed in the branchial arches, trigeminal ganglion, limb buds and dorsal root ganglia (for detailed information see 3.3.2.1). The segmented expression of *Csk* in the dorsal root ganglia is disrupted in the *Dll1* mutant. In the *Dll3$^{+/pu}$* and *Dll3$^{pu/pu}$* embryos the segmented expression seems to be present although weaker and not as clearly visible as in the wt. The expression in the trigeminal ganglion and the branchial arches is maintained in all mutants.

Ddx6 (DEAD aspartate-glutamate-alanine-aspartate box polypeptide 6) (Figure 13e-h)

In the wt *Ddx6* is expressed in the neural tube and in ganglia or somitic compartments along the AP axis (for detailed information see 3.3.2.1). In the *Dll1* mutants the expression in the neural tube is reduced while the segmented expression along the AP axis is maintained. In the *Dll3$^{+/pu}$* and *Dll3$^{pu/pu}$* embryos the segmented expression as well as the expression in the neural tube is strongly reduced.

Ifitm1 (Interferon induced transmembrane protein 1) (Figure 13i-m)

Ifitm1 is of special interest because of its expression pattern. In the wt expression was observed in the psm and the latest formed somites (for detailed information see 3.3.2.1). In the *Dll1$^{-/-}$* as well as the *Dll3$^{pu/pu}$* and the *Jag$^{htu/htu}$* mutant embryos the expression in the tail tip is missing, the expression level and domain is reduced in the psm and the expression in the somites is completely missing. In *Dll3$^{+/pu}$* heterozygous embryos the expression domains and levels seem to be similar to the wt condition.

Nes (Nestin) (Figure 13n-q)

At E10.5 *Nestin* is expressed in the wt in multipotent neuroepithelial cells in the rostral and caudal part of the neural tube, migrating neural crest cells, cells in the dorsal root ganglia and cells in the myotome of somites (for detailed information see 3.3.2.1). In the *Dll1* mutant the expression in the neural tube is missing while expression in the neural crest cells is still visible. However, expression in these segments is weaker and not as regular as in the wt. In *Dll3$^{+/pu}$* embryos the expression is comparable to wt expression. In *Jag1$^{htu/htu}$* embryos expression seems to he weaker than in the wt but all expression domains are maintained.

Sema5b (Sema domain, seven thrombospondin repeats (type 1 and type 1-like), transmembrane domain (TM) and short cytoplasmic domain, (semaphorin) 5B) (Figure 13r-u)

S*ema5b* is expressed at E10.5 in the wt in the neuroepithelium along the entire AP axis (for detailed information see 3.3.2.1). In the *Dll1$^{-/-}$*, *Dll3$^{+/pu}$* and *Dll3$^{pu/pu}$* embryos the expression is weaker than in the wt but is still present along the complete AP axis.
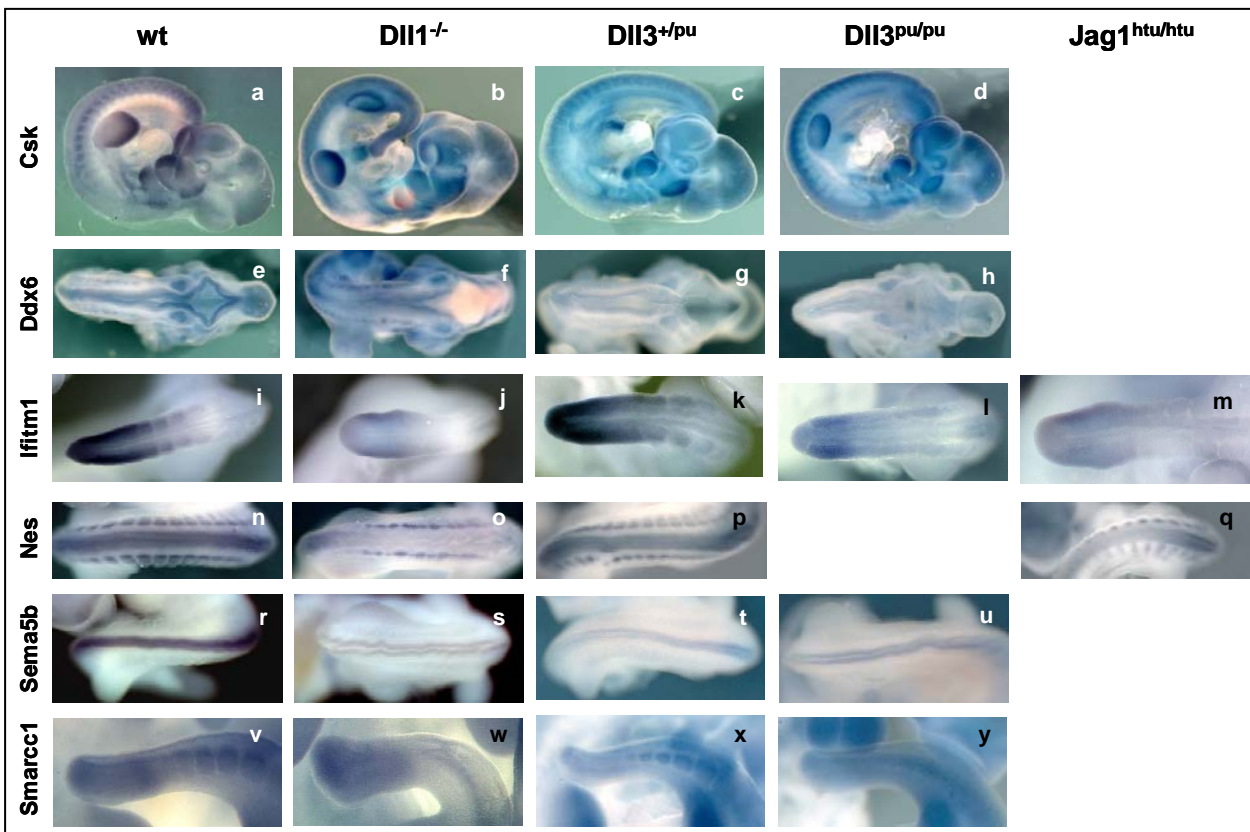
Figure 13: Potential targets of Delta/Notch signalling. Wish analysis in embryos mutant for Dll1, Dll3 or Jag1 was performed. Expression of Csk (a-d), Ddx6 (e-h), Ifitm1 (i-m), Nes (n-q), Sema5b (r-u) and Smarcc1 (v-y) was analysed on E10.5 embryos. (b-d) Segmented expression of Csk in the dorsal root ganglia as in the wt (a) is disturbed in Delta/Notch pathway mutants. (e-h) Expression of Ddx6 was altered in the Dll1 and Dll3 mutants as compared to the wt. (i-m) Expression of Ifitm1 in the psm and the somites is strongly reduced in Dll1^{-/-}, Dll3^{pu/pu} and Jag1^{htu/htu} mutant embryos while in the Dll3^{+/pu} heterozygous embryo the expression is similar to the wt condition. (n-q) Expression of Nestin in Dll1 mutants, Dll3^{+/pu} heterozygotes and Jag1^{htu/htu} mutants. The normal expression in the neuroepithelium is lost in the Dll1^{-/-} but maintained in the other analysed embryos. Expression in the neural crest cells is present in Dll1^{-/-}, Dll3^{+/pu} and Jag1^{htu/htu} but segmentation is irregular in the Dll1 mutant. (r-u) Sema5b is expressed in the neuroepithelium along the AP axis. The expression level is reduced in the analysed Delta/Notch pathway mutants. (v-y) The wt expression of Smarcc1 in a stripe in the psm and in the somites is almost maintained in the Dll3^{+/pu} embryo. In the Dll1^{-/-} and the Dll3^{pu/pu} the expression in the psm and in the somites is completely lost.

Smarcc1 (SWI SNF related matrix associated actin dependent regulator of chromatin subfamily c member 1) (Figure 13v-y)

Expression of *Smarcc1* in the wt was observed in the somites in the tail and the psm. In the psm a roughly one somite broad stripe could be observed. *Smarcc1* is also expressed in the neuroepithelium of the neural tube and in a segmented fashion along the AP axis (for detailed information see 3.3.2.1). In *Dll1* mutant embryos the segmentation of the tail and the

expression in the somites is lost. In the neuroepithelium of the neural tube expression is maintained but the clear segmentation is disrupted (see also Figure 11l). In the *Dll3*$^{+/pu}$ embryos expression as in the wt was observed except for the missing stripe of expression in the psm. The expression in *Dll3*$^{pu/pu}$ embryos is very similar to *Dll1*$^{-/-}$ embryos. Expression in the psm and the somites is lost.

3.6 Laser microdissection and RNA amplification

The DNA-microarray technology is a sensitive method for the analysis of gene expression in biological systems. However, with rising complexity of the analysed sample the possibility to obtain results which might be due to secondary effects increases strongly. Therefore it might be useful to reduce the complexity of a biological system in order to get more specific results. At E10.5 many developmental processes take place within an embryo. Thus it is a highly complex system. In this context laser microdissection is a promising method to dissect only discrete parts of an embryo to perform DNA-microarray analysis with them. However, the amount of RNA which can be obtained from microdissected tissues is very low and RNA needs to be amplified to get enough starting material for DNA-chip analysis. In order to assess the possibility to use laser microdissection and RNA amplification several primary experiments have been performed (Figure 14).

Different amounts of tissue ranging from $1*10^3$ µm^2 to $4*10^6$ µm^2 were excised from 5 µm thick adult mouse liver cryosections (Figure 14a). The tissue sizes were translated in number of cells. The cell size was measured from E10.5 embryo sections. From each tissue size three samples were excised in order to test three different RNA isolation protocols. The RNA was isolated using Qiagen RNeasy Mini, Phenol-Chloroform extraction (with additional DNase digest) and Stratagene Nanoprep RNA kit respectively.
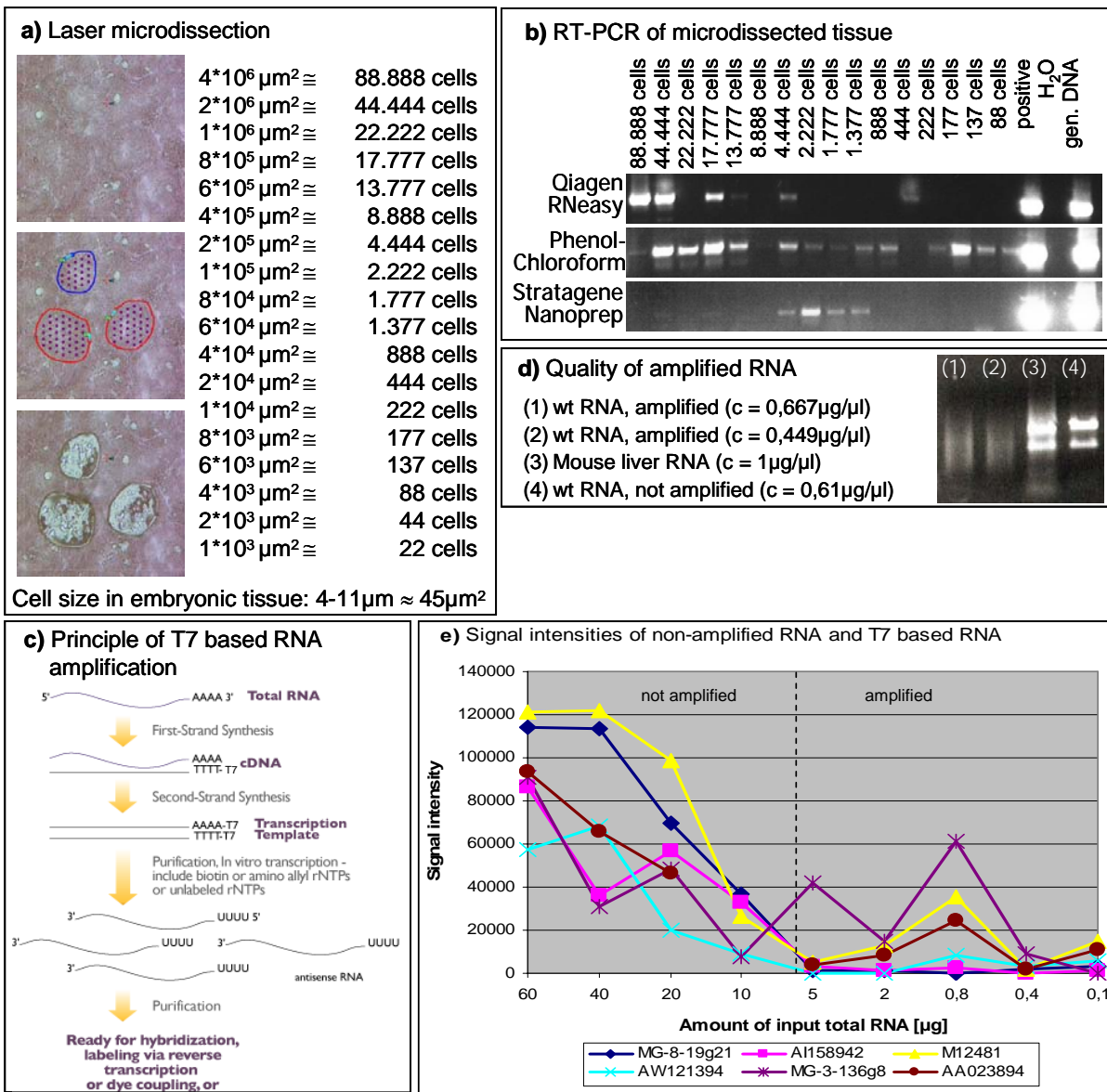
Figure 14: Assessment of quality and reproducibility of laser microdissection and RNA amplification. a) Laser microdissection of mouse tissue. Cell sizes in embryonic tissues were determined empirically and were approximately 45 µm². The area of microdissected tissue and the corresponding number of cells is presented. b) Three different RNA isolation protocols were tested (QIAGEN RNeasy Mini Kit, Phenol-Chloroform extraction with DNase digest, Stratagene Nanoprep RNA Kit). The isolated RNA was applied to RT-PCR for Gapdh. c) Principle of T7 based RNA amplification resulting in antisense RNA. d) Assessment of RNA quality after RNA amplification. Two independent reactions of the same starting RNA were amplified (lane (1) and (2)). Lane (3) shows a mouse liver standard RNA of 1 µg/µl. Lane (4) shows the RNA used for amplification. e) Signal intensities of six randomly selected clones from non-amplified RNA (60 µg-10 µg) and T7 based amplified RNA (5 µg-0.1 µg).

In order to analyse if intact and amplifiable RNA can be obtained from laser microdissected samples the isolated RNA was subjected to RT-PCR using three different housekeeping genes (Gapdh, Hprt, Actin-β) (Figure 14b). The results for Hprt and Actin-β are not shown. The Qiagen RNeasy Mini kit showed positive results up to 4.444 cells. The Stratagene Nanoprep RNA Kit columns were probably overloaded when samples between 88.888 and 8.888 cells were used since it is designed for 1000-10.000 cells according to the manufacturer. Positive RT-PCR results were obtained for the range between 44.444 and 1.377 cells. The best results were obtained using the Phenol-Chloroform extraction protocol where positive results could reproducibly be obtained using the 88 cells-sample. This analysis leads to the result that intact RNA can be isolated from microdissected samples but that the RNA isolation procedure is a critical step.

Nevertheless even the 88.888 cells-sample does not contain enough RNA for the use with DNA-chips. Thus it is necessary to linearly amplify the RNA. A common method for this is the so called T7-based RNA amplification. The principle of this procedure is as follows (Figure 14c). Total RNA containing polyadenylated mRNA is reversely transcribed into cDNA using an Oligo-dT Primer containing the sequence of the T7 promotor at its 5´ end for the first strand synthesis. For the second strand synthesis a Poly-dA primer which also contains the sequence of the T7 promotor is added. This results in double strand cDNA molecules containing the T7 promotor sequence. In a next step these cDNAs serve as template for *in vitro* transcription using the T7 RNA polymerase. Aminoallyl labelled rNTPs are included in the reaction to be able to label the resulting antisense RNAs for DNA-chip use afterwards. This protocol should lead to an up to 1000 fold amplification of mRNA and maintenance of the relative ratios of the single RNA species.

The quality of amplified RNA was analysed by denaturing gel electrophoresis (Figure 14d). Two reactions including the same wt RNA sample were amplified and subjected to gel electrophoresis (lane 1 and 2). The wt starting RNA (lane 4) and a mouse standard RNA (lane 3) was also applied. The amplified RNA molecules had a size of 0.3-4 kb. The factor of amplification was in all amplification reactions between 300-400 fold.

In order to analyse the reproducibility of RNA amplification on the one hand and the optimal amount for the subsequent DNA-chip hybridisation different amounts of starting RNA were used (Figure 14e). 60, 40, 30, 20 and 10 µg of total RNA were reversely transcribed, labelled and hybridised without amplification of RNA. 5, 4, 2, 1, 0.8, 0.4, 0.2, 0.1, 0.05 and 0.01 µg of total RNA were subjected to T7 based RNA amplification, labelled and hybridised. The signal intensities of six randomly selected spots in relation to the amount of starting RNA are shown in Figure 14e.
In a normal DNA-chip experiment 20 µg of total RNA is used. It can be seen that the signal intensity at 20 µg starting material is overall stronger that in any of the amplified samples. Furthermore it can be observed that within the amplified samples the signal intensities are not reliable and sometimes differ greatly between the selected genes and also between the different starting amounts. However it seems that the best signal intensities of amplified samples were obtained using 0.8 µg of total RNA as starting material. Nevertheless it became obvious during the analysis that the method is very sensitive and susceptible to

variations. The technical difficulties can occur at many steps of the protocol which most times result in loss of large amounts or the total template.

3.7 Summary – Transcriptome analysis

- RNA expression analysis of wt and *Dll1*^{-/-} embryos was performed using two different DNA-microarrays.

- 22 upregulated and 30 downregulated genes were identified to be reproducibly differentially expressed.

- 16 upregulated and 16 downregulated genes have been analysed by Real-Time PCR. 60% of the DNA-chip results were confirmed.

- All identified candidate genes were screened for expression patterns indicative of Delta/Notch signalling using whole mount *in situ* hybridisation.

- Genes exhibiting promising expression patterns were: *Bnip3, Ddx6, Fgf6, Pdgfa, Smarcc1, Pdgfr-α, Csk, S100a10, Nes, Sema5b, Ifitm1*.

- The likelihood for involvement in Delta/Notch signalling has been analysed by whole mount *in situ* hybridisation of *Dll3* and *Jag1* mouse mutants.

- As a future perspective for the use of DNA-microarray technology with specific cell types or compartments of mouse embryos the possibility to use laser microdissection and linear RNA amplification was assessed. Phenol-Chloroform extraction proved to be the best RNA isolation protocol, and 800 ng of total RNA seemed to be the best amount of starting material for linear RNA amplification.

4 Results - Proteome analysis

The analysis of the *Dll1* mutant has mostly been restricted to RNA expression patterns so far. It is not known if and how the changed level of expression observed, e.g., in wish studies influences the transcription and thus the expression of proteins. To address this question 2D-gelelectrophoresis combined with MALDI-TOF technology was performed.

4.1 2D-Gelelectrophoresis

4.1.1 Biological material

As for the RNA expression profiling analysis *Dll1* wildtype (wt) and *Dll1$^{-/-}$* embryos at embryonic day 10.5 have been used (Hrabe de Angelis et al. 1997). Additionally E11.5 wildtype and mutant embryos have been analysed. The mice were kept on an isogenic 129SvJ background.

Phenotyping has been done as described in chapter 3.1.7.

4.1.2 Experimental design

The proteome analysis of *Dll1* wt and mutant embryos was performed by TopLab Company located in Martinsried, Germany. Ten wt and ten *Dll1$^{-/-}$* embryos of developmental stages E10.5 and E11.5 were used, respectively.

For each sample two pH gradients were analysed, pH4-7 and pH6-11. After focussing to the steady state, the second dimension was performed as a SDS-PAGE. Five gels of each sample were done under identical running conditions.

4.1.3 Image and statistical analysis

Gels were stained with Sypro Ruby and scanned using a fluorescence scanner. Spot detection, matching and quantification were carried out with the Definiens 2D image software ProteomeWeaver. Mastergels were created out of five replicas from one tissue in each gradient.

Statistical calculations were performed by the Definiens 2D image software ProteomeWeaver allowing the standard deviation within one group of five gels to be less than 30% and a confidence level of 0.05 in the Student T–test. A significant protein regulation was accepted by a difference in at least 1.5 fold of the proteins quantity. The Mastergel for the pH4-7 gradient of E10.5 embryos including the spots that were identified to be regulated is shown in Figure 15.
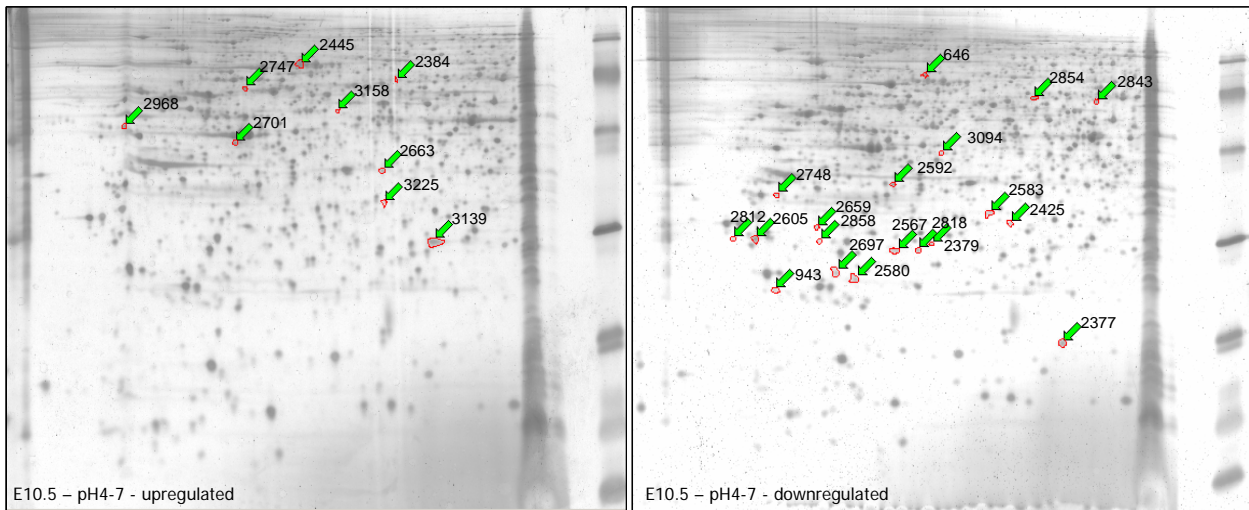
Figure 15: Mastergel of the pH4-7 gradient of E10.5 embryos. Up- (left picture) and downregulated (right picture) proteins as they were identified by the ProteomeWeaver software are marked.

The number of detected spots was around 1500 for pH4-7 and between 800-900 spots for pH6-11.

Two independent analyses have been performed for E10.5 embryos of the pH4-7 gradient. Applying these statistical criteria 50 proteins were identified to be differentially expressed in wt and mutant embryos at E10.5 and 23 proteins at E11.5.

4.1.3.1   Identification of regulated proteins

The identification of the selected protein spots was performed by a peptide mass fingerprint (PMF) - MALDI - TOF analysis.

For the peptide mass fingerprint, the spots were picked from the SDS gel and trypsin-digested over night. After subsequent sonication and concentration of the probe the peptides were put on a target and co-crystallised with dihydroxybenzoeic acid. The MALDI-TOF analysis was performed in a reflector mode in the peptide range from 700 to 4000 Daltons. The obtained spectra were matched with the NCBI database using the ProFound software to identify the corresponding protein.

The identified proteins for E10.5 and E11.5 are presented in Table 3.

Table 3: Differentially expressed proteins at E10.5 (a) and E11.5 (b). Proteins are sorted alphabetically. "Not identifiable" proteins were picked from the gel and analysed but the identification procedure failed due to low amounts of protein or the databank blast did not give a hit.

a

Spot	Upregulated proteins [E10.5 pH4-7, pH6-11]	Symbol	Acc. No.	Function
2701	Apolipoprotein A-IV precursor	Apoa4	P06728	cell metabolism
	Calreticulin	calr	6680836	ion binding
313	Elongation factor 2 (EF-2)	Eef2	P58252	cell metabolism
262	Hemoglobin alpha chain	Hba-a1	P01942	transport
131	Hemoglobin epsilon-Y2 chain	Hbb-y	P02104	transport
1732	Hemoglobin zeta chain	Hba-x	P06467	transport
18	Heterogeneous nuclear ribonucleoprotein A3 (hnRNP A3)	hnRNP A3	Q8BG05	no function
1798-2	Pyruvate kinase, M2 isozyme	Pkm2	P52480	ion binding
1798-1	stress-induced phosphoprotein 1	Stip1	gi|14389431	no function
2747	Ubiquitin carboxyl-terminal hydrolase 14	Usp14	Q9JMA1	cell cycle
2384	**not identifiable**			
2968	**not identifiable**			
3139	**not identifiable**			

Spot	Downregulated proteins [E10.5 pH4-7, pH6-11]	Symbol	Acc. No.	Function
2605	14-3-3 protein zeta/delta (Protein kinase C inhibitor protein-1)	Ywhaz	P35215	cell metabolism
1669	26S protease regulatory subunit S10B	Psmc6	Q92524	cell cycle
2425	26S proteasome non-ATPase regulatory subunit 8	Psmd8	Q9CX56	cell cycle
1580	Acetyl-Coenzyme A acetyltransferase 3	Actl	gi|23346599	cell metabolism
	Actin alpha, cardiac - mouse (fragment)	Actc1	627834	cell metabolism
646	Alpha-fetoprotein precursor (Alpha-fetoglobulin) (Alpha-1-fetoprotein)	Afp	P02772	ion binding
	ERp44 (Thioredoxin)	Txndc4	19072792	transport
	Eukaryotic translation elongation factor 1 beta 2	Eef1b2	9055210	cell signalling
	Eukaryotic translation initiation factor 3, subunit 5	Eif3s5	4503519	cell signalling
2812	Eukaryotic translation initiation factor 6 (eIF-6)	Itgb4bp	O55135	cell signalling
2583	**evtl.** C330027I04Rik protein		gi|15929772	no function
	Inorganic pyrophosphatase (pyrophosphate phospho-hydrolase) (PPase)	Pyp	585322	cell metabolism
	ISS -putative- syntaxin binding protein 3	Unc18-3, Stxbp3	12850132	transport
	Keratinocyte lipid binding protein (Fatty acid binding protein 5, epidermal)	Fabp5	6754450	transport
2697	Lactoylglutathione lyase (Methylglyoxalase)	Glo1	Q9CPU0	cell metabolism
	N-ethylmaleimide sensitive fusion protein attachment protein alpha	SKD2, Nsf, Napa	13385392	ion binding
	Nucleophosmin 1	Npm1	6679108	cell cycle
12	Proteasome subunit alpha type 2	Psma2	P49722	cell cycle
76	Proteasome subunit alpha type 4 (Proteasome component C9)	Psma4	Q9R1P0	cell cycle
195	Proteasome subunit beta type 2 (Proteasome component C7-I)	Psmb2	Q9R1P3	cell cycle
	Proteasome subunit, beta type, 4	Psmb4	20874725	cell cycle
304	Pyruvate kinase, M2 isozyme	Pkm2	P52480	ion binding
	ATP synthase, H+ transporting, mitochondrial F0 complex, subunit d	Atp5h	20913657	transport
2592	Serine/threonine protein phosphatase 2A, catalytic subunit, alpha isoform	Ppp2ca	P13353	cell cycle
	Similar to alpha internexin neronal intermediate filament protein	Ina	17390900	cell structure
158	S-methyl-5-thioadenosine phosphorylase (5'-methylthioadenosine phosphorylase)	Mtap	Q9CQ65	cell cycle
	Spermidine synthase	Srm, Spdsy	6678131	cell metabolism
2377	Superoxide dismutase [Cu-Zn]	Sod1	P08228	ion binding
	Transthyretin (Prealbumin)	Ttr	7305599	cell metabolism
	Tyrosine 3-monooxygenase/tryptophan 5-monooxygenase activationprotein	Ywhae	6678619	cell signalling
2567	**not identifiable**			
2659	**not identifiable**			
2843	**not identifiable**			
2854	**not identifiable**			
3094	**not identifiable**			
41	**not identifiable**			
1715	**not identifiable**			

b

Spot	Upregulated proteins [E11.5 pH4-7, pH6-11]	Symbol	Acc. No.	Function
237	40S ribosomal protein SA (P40) (34/67 kDa laminin receptor)	Lamr1	P14206	cell metabolism
120, 150	Aconitase 2, mitochondrial		gi|18079339	no function
5822	ARP3 actin-related protein 3 homolog; actin-related protein 3 homolog (yeast)	Actr3	gi|23956222	cell structure
1969	Eukaryotic translation initiation factor 3 subunit 7 (eIF-3 zeta)	Eif3s7	O70194	cell signalling
4290	Ferritin light chain 1 (Ferritin L subunit 1)	Ftl1	P29391	ion binding
1732	Hemoglobin zeta chain	Hba-x	P06467	transport
105	Heterogeneous nuclear ribonucleoprotein L	Hnrpl	gi|33667042	cell cycle
7207	Methionine aminopeptidase 2 (MetAP 2)	Metap2	O08663	cell metabolism
7945	OTU domain, ubiquitin aldehyde binding 1		gi|19527388	no function
440	Serotransferrin precursor (Transferrin)	Trf	Q921I1	ion binding
3173	**not identifiable**			
5945	**not identifiable**			
7548	**not identifiable**			
2244	**not identifiable**			

Spot	Downregulated proteins [E11.5 pH4-7, pH6-11]	Symbol	Acc. No.	Function
7451	60 kDa heat shock protein, mitochondrial precursor (Hsp60)	Hspd1, Hsp60	P19226	cell cycle
729, 7703	78 kDa glucose-regulated protein precursor (GRP 78)	Hspa5, Grp78	P20029	cell cycle
1891,	Heterogeneous nuclear ribonucleoprotein A1	Hnrpa1	P49312	cell signalling
7567	Heterogeneous nuclear ribonucleoprotein K (hnRNP K)	Hnrpk	Q07244	cell signalling
4586	mKIAA1541 protein		gi|37360436	no function
7169	Tubulin gamma-1 chain (Gamma-1 tubulin)	Tubg1	Q9Z310	cell structure
1246	**not identifiable**			
7593	**not identifiable**			
41	**not identifiable**			

4.2 Functional assessment of regulated proteins

Table 3 lists the proteins which are differentially expressed at E10.5 and E11.5 respectively. In order to assess the biological relevance of these proteins they were sorted according to their functional annotation in the gene ontology section of the MGI database (Harris et al. 2004).
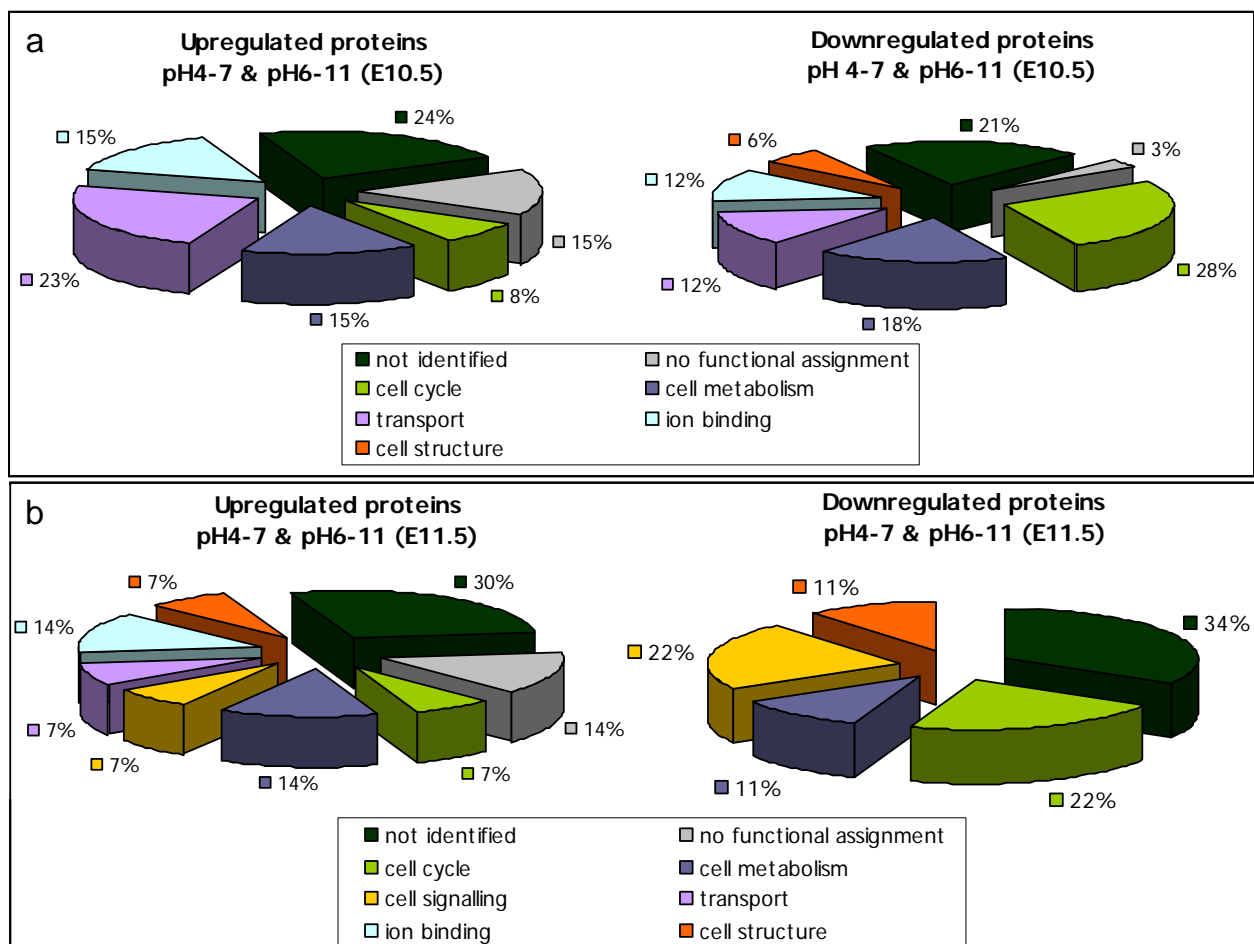
Figure 16: Functional assessment of regulated proteins at E10.5 (a) and E11.5 (b). Identified proteins were analysed using the Gene Ontology classification system. At E10.5 proteins involved in cell cycle, cell metabolism, transport, ion binding and cell structure were identified, while in E11.5 also proteins involved in cell signalling were found. Proteins without functional annotation and the number of non-identifiable proteins are also marked.

In Figure 16a, the distribution of functional annotations is presented for embryonic day 10.5. The upregulated proteins can be grouped into six classes. 24% make up proteins which could not be identified using PMF MALDI-TOF. Those spots were picked from the gel but either the amount of protein for the tryptic digest and the subsequent Maldi-TOF analysis was too low or the blast did not give a hit. Further 15% account for proteins without functional

annotation. The cell metabolism and ion binding classes make up 15% each while cell cycle proteins are represented by 8%. Involved in transport activities are 23% of the identified upregulated proteins.

Analysis of the downregulated proteins at E10.5 shows that the distribution of functional classes is different in some aspects. Quite similar as observed in the upregulated proteins 21% could not be identified. Only 3% are not functionally assigned so far. As compared to the upregulated proteins more than three times more (28%) proteins involved in cell cycle functions are downregulated indicating that in the *Dll1* mutant cell cycle processes are strongly influenced. Cell metabolism and ion binding proteins make up similar percentage as in the upregulated candidates (18% and 12% respectively). In the transport category almost half as many genes are down- (12%) than upregulated (23%). An obvious difference though is that within the set of downregulated proteins a class of proteins related to cell structure is present which is missing within the set of upregulated genes.

The functional classes of proteins differential at E11.5 is presented in Figure 16b. The 14 upregulated proteins fall into eight functional categories. 30% could not be identified and further 14% were not functionally assigned. 7% (corresponding to one protein) each have functions in cell cycle, cell signalling or signal transduction, transport and cell structure tasks. The sections cell metabolism and ion binding are represented by 14% each.

Nine proteins were found to be downregulated at E11.5 and fall into five functional classes. 34% could not be identified and for 11% (corresponding to one protein) a function is not known yet. 22% or two proteins make up for cell cycle proteins and cell signalling/signal transduction proteins each. One protein is involved in cell structure tasks.

4.3 Verification of 2D-analysis

The 2D-gelelectrophoresis analysis revealed proteins which have never been brought into context with Delta/Notch signalling. However it is necessary to verify the obtained results concerning regulation of the proteins. Therefore semi-quantitative immunoblotting was performed to check the previously obtained results. A set of regulated proteins from E10.5 and E11.5 was selected dependant on the fact if specific antibodies were commercially available.

4.3.1 Experimental setup

Protein was isolated from E10.5 embryos using the same protocol as was used for the preparation of 2D samples to ensure that solubility of proteins was the same. The protein was quantified using Bradford protocol.

In test experiments the expression level of the tested protein and quality and sensitivity of each antibody was tested. SDS-page was performed with different concentrations of embryonic protein extract and different control samples (HeLa and A431 cell protein extract, protein extracts from mouse brain, liver and kidney). Depending on the signal and background intensity observed after chemiluminescent detection the protein amount used for

the semi-quantitative analysis and the appropriate antibody dilution was determined for each antibody individually.

For the semi-quantification two different protein amounts of wt and *Dll1*$^{-/-}$ samples and two controls were run on a 10% acrylamide gel. After the signal detection, blots were stripped and incubated with anti-β-Actin antibody as control to ensure that equal amounts of protein have been loaded on the gel.

4.3.2 Verification using semi-quantitative Western Blotting

The results of the verification experiments using western blotting are presented in Figure 17.

For each analysed protein the two different protein concentrations are shown in the upper blot picture. The lower blot picture shows the β-Actin control. The analysis included proteins that were downregulated in the 2D-gel analysis at E10.5 (Figure 17a) and E11.5 (Figure 17b) and proteins that were upregulated at E10.5 (Figure 17c) and E11.5 (Figure 17d). For the verification experiments however only protein extract from E10.5 embryos has been used even for the candidates which were differentially expressed at E11.5.

Taking into account the limitations of this method such as the non-linear binding kinetics of secondary antibodies the results are the following. As shown in Figure 17a the downregulation was verified for 14-3-3 ε, 14-3-3 ζ, Afp, Cu/Zn Sod and Unc18-3. Expression of Nsf and PPP2Ca looks equally strong on the Western blots. The tendency of downregulation for the candidates identified for E11.5 embryos could be supported by western blot for γ-tubulin and hnRNP A1. GRP78 might show a tendency to downregulation in the mutant but this is not clearly identifiable. HSP60 seems to be equally expressed in E10.5 embryos.
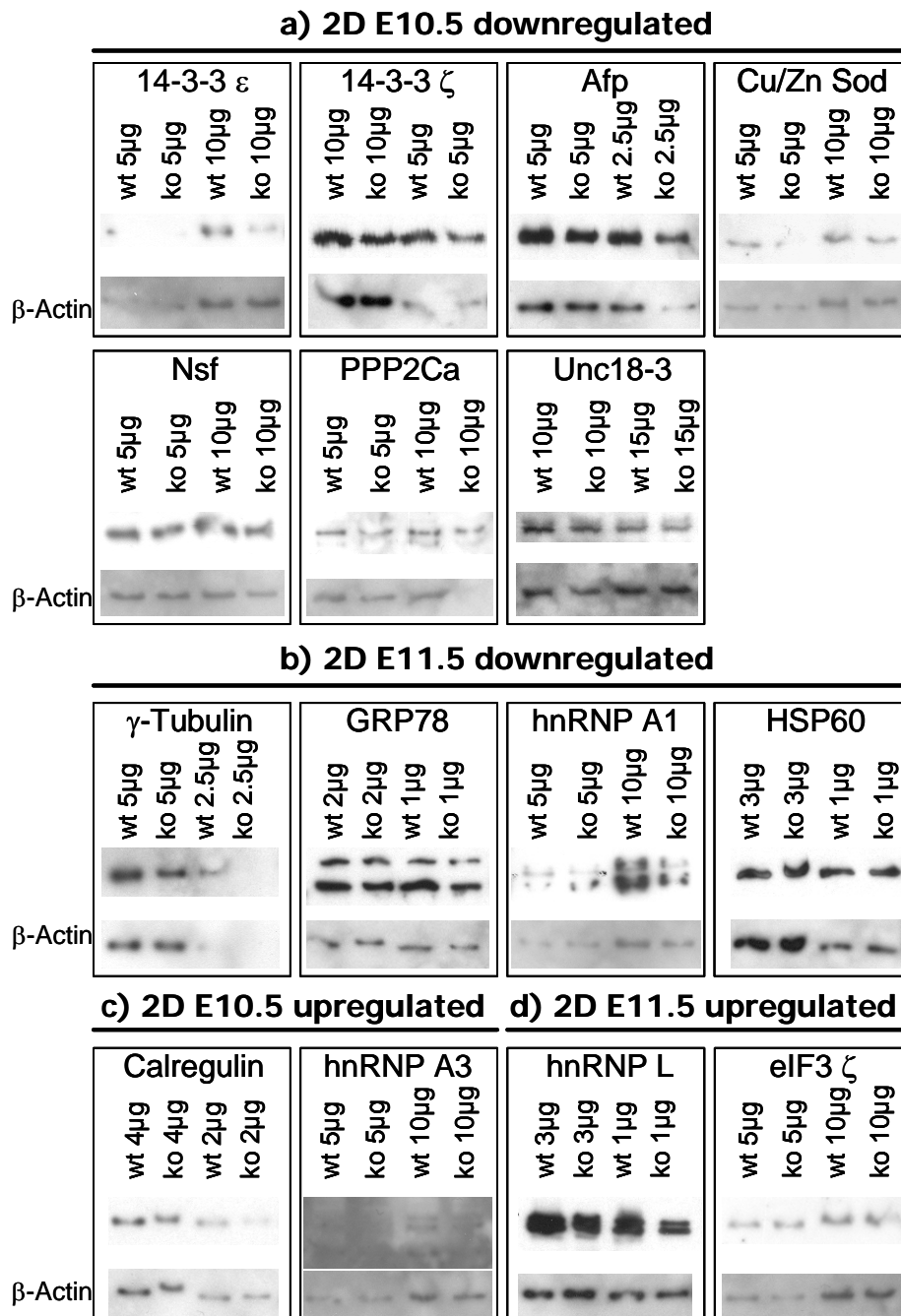
Figure 17: Results of semi-quantitative Western Blotting to verify 2D-analysis results. Two different concentrations of protein are presented in the upper blots while the β-actin control is shown in the lower blot. Proteins which were downregulated in E10.5 embryos in the 2D-analysis are shown in (a), proteins which were downregulated in E11.5 embryos in (b), upregulated proteins at E10.5 in (c) and upregulated proteins at E11.5 in (d).

The observed upregulation of Calregulin and hnRNP L in the 2D gel analysis could not be clearly confirmed by western blotting. In contrast to the 2D analysis calregulin and hnRNP L seem to be downregulated in the mutant. The expression of hnRNP A3, Apoa4, Eef2, haemoglobin α, Fabp5 (Mdgi), Lamr1, Mtap, Ttr, Txndc4 and Usp14 (data not shown) could not be clarified due to the quality of the antibody. Eif3s7 (eIF3ζ) might show a slight upregulation in the *Dll1*⁻/⁻ sample.

Protein	Symbol	Result 2D	Result qWB
Apolipoprotein A-IV precursor	Apoa4	E10.5 up	no clear signal
Calreticulin	Calr	E10.5 up	down
Heterogeneous nuclear ribonucleoprotein A3 (hnRNP A3)	hnRNP A3	E10.5 up	no clear signal
40S ribosomal protein SA (P40) (34/67 kDa laminin receptor)	Lamr1	E11.5 up	no clear signal
Eukaryotic translation initiation factor 3 subunit 7 (eIF-3 zeta)	Eif3s7	E11.5 up	equal
heterogeneous nuclear ribonucleoprotein L	Hnrpl	E11.5 up	down
14-3-3 protein zeta/delta (Protein kinase C inhibitor protein-1)	Ywhaz	E10.5 down	down
Alpha-fetoprotein precursor (Alpha-fetoglobulin) (Alpha-1-fetoprotein)	Afp	E10.5 down	down
N-ethylmaleimide sensitive fusion protein attachment protein alpha	SKD2, Nsf, Napa	E10.5 down	equal/down
Serine/threonine protein phosphatase 2A, catalytic subunit, alpha isoform	Ppp2ca	E10.5 down	down
Superoxide dismutase [Cu-Zn]	Sod1	E10.5 down	down/equal
tyrosine 3-monooxygenase/tryptophan 5-monooxygenase activationprotein	Ywhae	E10.5 down	down
60 kDa heat shock protein, mitochondrial precursor (Hsp60)	Hspd1, Hsp60	E11.5 down	equal
78 kDa glucose-regulated protein precursor (GRP 78)	Hspa5, Grp78	E11.5 down	down
Heterogeneous nuclear ribonucleoprotein A1	Hnrpa1	E11.5 down	down
Tubulin gamma-1 chain (Gamma-1 tubulin)	Tubg1	E11.5 down	down

Table 4: Comparison of 2D-gel analysis with semi-quantitative Western Blot results. Only analysed proteins are presented.

Table 4 shows a summary of 2D results and semi-quantitative Western blot results. It is obvious that none of the proteins which were upregulated on the 2D gels could be verified. However, except for Nsf and Hsp60, the downregulation of all analysed proteins could be confirmed by semi-quantitative Western blot.

4.3.3 Functions of regulated proteins

14-3-3ε (Ywhae; Tyrosine 3-monooxygenase/tryptophan 5-monooxygenase activatorprotein)

The 14-3-3 family of proteins plays critical roles in cell signalling events that control progress through the cell cycle, transcriptional alterations in response to environmental cues and programmed cell death (Yaffe 2002).

In the *Dll1* mutant the expression of 14-3-3ε at E10.5 is downregulated.

14-3-3ζ *(Ywhaz; 14-3-3 protein zeta/delta)*

14-3-3ζ is also a member of the 14-3-3 protein family. 14-3-3ε and 14-3-3ζ are known to form heterodimers *in vivo* (Jones et al. 1995). In Drosophila which normally expresses 14-3-3ε and 14-3-3ζ (also called Leonardo), complete loss of 14-3-3ζ, despite normal amounts of 14-3-3ε, causes embryonic lethality (Kockel et al. 1997).

14-3-3ζ was found to be downregulated in *Dll1*^{-/-} embryos.

AFP *(Alpha fetoprotein)*

AFP is the principal serum protein during embryogenesis. It is a glycoprotein and in mice is initially synthesized in the yolk sac endoderm (Dziadek 1978; Dziadek and Adamson 1978) and then in the liver with mRNA expression being detectable at E9.5 in the hepatic bud and endoderm of the midgut and hindgut (Jones et al. 2001).

At E10.5 AFP was downregulated in *Dll1* loss-of-function embryos.

Cu/Zn SOD *(Copper/Zinc superoxide dismutase)*

Cu/Zn SOD is a cytosolic, dimeric, copper/zinc containing enzyme. Together with catalases and glutathione peroxidase (Gpx1), SODs are a part of the antioxidant defence cascade. During embryonic development Cu/Zn SOD is expressed in many fetal organs such as brain, liver, heart, intestine, lung and kidney (de Haan et al. 1994).

In the *Dll1* mutant Cu/Zn SOD was downregulated.

Nsf *(N-ethylmaleimide sensitive fusion protein attachment protein alpha)*

Nsf is a key component of the membrane trafficking machinery in Drosophila. It contains two nucleotide binding domains and strong ATPase activity (Stewart et al. 2001).

The expression level of Nsf in the wt and the *Dll1* mutant seems to be similar or slightly downregulated although an exact conclusion is not possible since Western blotting cannot be used as a quantitative method.

PPP2Cα *(Serine/threonine protein phosphatase 2A, catalytic subunit, alpha isoform)*

Protein phosphatase 2A (PP2A) is a major Serine/Threonine phosphatase involved in several cellular signal transduction pathways. PP2A enzymes are ubiquitously expressed in eukaryotic cells and account for as much as 1% of total cellular proteins (Sontag 2001).

PPP2Cα was found to be downregulated in *Dll1*^{-/-} embryos.

Unc18-3 *(ISS-putative syntaxin binding protein 3)*

For SNARE-mediated membrane fusion to function properly (see Nsf) a number of additional factors, called SNARE regulators, are required. These include Munc18-3 (also called Unc18-3) which was also found to be downregulated in the *Dll1* mutant.

γ-tubulin (Tubulin gamma-1 chain)

Microtubules are dynamic cytoskeletal polymers that assemble from α/β-tubulin and are important for the establishment of cell polarity, vesicle trafficking and formation of the mitotic/meiotic spindle (Moritz and Agard 2001).

γ-tubulin was downregulated in the *Dll1* mutant embryos.

GRP78 (78 kDa glucose-related protein precursor)

GRP78 is a glucose-regulated protein. It responds to stress from the endoplasmatic reticulum such as hyperglycemia (Walsh et al. 1997). Expression of GRP78 has been found in several tissues such as the heart, neural tube, gut endoderm and somites (Barnes and Smoak 2000).

GRP78 was downregulated at E11.5 (2D-gels) and E10.5 (Western Blot) in *Dll1* mutants.

hnRNP A1, hnRNP A3, hnRNP L (heterogeneous nuclear ribonucleoprotein particles)

RNA intermediates in the nucleus do not exist as free RNA molecules. They are associated with an abundant set of nuclear proteins, hnRNPs.

Expression of hnRNP A3 could not be determined properly because the antibody did not produce clear bands. hnRNP A1 and hnRNP L are downregulated in the Western blots (Figure 17).

HSP60 (60 kDa heat shock protein, mitochondrial precursor)

HSP60 for example is expressed constitutively at normal growth temperatures and has basic functions in the life cycle of proteins as a molecular chaperone (Ohtsuka and Suzuki 2000). Molecular chaperones are able to inhibit the aggregation of partially denatured proteins and refold them. HSP60 encloses newly synthesized proteins to create a surrounding where the proteins can fold properly (Bukau and Horwich 1998; Fink 1999).

The expression of HSP60 in the wt and the *Dll1* mutant seemed to be equally strong.

Calr (Calregulin)

Calcium (Ca^{2+}) is a universal signalling molecule involved in many aspects of cellular function. The majority of intracellular Ca^{2+} is stored in the endoplasmatic reticulum (ER). When Ca^{2+} is released from the ER specific plasma membrane Ca^{2+} channels are activated resulting in increased intracellular Ca^{2+}. In the lumen of the ER Ca^{2+} is buffered by Ca^{2+} binding chaperones such as calreticulin (Groenendyk et al. 2004). Mice deficient for calreticulin die *in utero*, mostly in late gestation due to impaired cardiac development. Mutants sometimes also display encephaly secondary to a defect in neural tube closure (Rauch et al. 2000).

The upregulation of calreticulin on the 2D-gels could not be confirmed. Calreticulin seems to be downregulated in the *Dll1*^{-/-} embryos according to the Western blot results

eIF3ζ (Eif3s7; Eukaryotic translation initiation factor 3 subunit 7)

Eif3s7 is a subunit of the eukaryotic initiation factor-3 (eIF3) multi-subunit complexes. eIF3 is the largest of the mammalian translation initiation factors and consists of at least eight subunits.

Eif3s7 as well as Eif3s5, another subunit of the eIF3 complex, was downregulated in the *Dll1* mutants.

4.4 Summary – Proteome analysis

- Protein expression profiling has been performed using a combination of 2D-gelelectrophoresis and mass spectrometry.

- At E10.5 13 proteins were upregulated in *Dll1*$^{-/-}$ embryos and 37 proteins were downregulated in the mutant. At E11.5 14 proteins were up- and 9 proteins were downregulated in the *Dll1* mutant.

- For the verification of the proteomics results semi-quantitative Western Blotting was performed. Of 16 tested proteins 9 could be clearly verified using this method.

5 Results - Transcriptome/Proteome comparison

5.1 Experimental features

The experimental setup for the transcriptome analysis using DNA-chips and the proteome analysis using 2D-gelelectrophoresis combined with mass spectrometry techniques was rather similar. Wildtype and *Dll1* mutant embryos were collected, total RNA or protein, respectively, was isolated and the expression compared. However, both analyses are quite different with respect to certain features.

The number of detected signals differs greatly in DNA-chip experiments, where more than 13,000 genes were detected with sufficiently strong signal, and 2D-gel analysis, where roughly 1000-2000 proteins can be detected even with sensitive staining methods like silver or Sypro Ruby staining. The resolution influences the outcome of the analysis though. In 2D-ge mainly high abundant proteins can be identified while on DNA-chips even weakly expressed genes can be detected. An advantage of the proteomic analysis nevertheless is that post-translational modifications such as phosphorylation, glycosylation or sulphation can be seen on the 2D-gels while they cannot be predicted by the RNA expression level or sequence information.

It has been reported previously that protein and mRNA expression does not correlate well (Gygi, 1999, Pandey, 2000) but can be rather seen as being complementary.

5.2 Expression of differential proteins on DNA-chips

Comparison of the candidates obtained from the DNA-chip analysis and the 2D-gel analysis revealed that one candidate was found to be downregulated in both analyses: Atp5h. Since the data sets are completely different between transcriptome and proteome analyses and different statistical criteria were used to analyse the data this comparison was not sufficient. Additionally the expression of the identified protein candidates on the DNA-chips was checked. To identify the corresponding clone on the DNA-chip the sequence of the protein candidate was blasted against all gene sequences on the chip. If the blast revealed a hit the clone sequence was blasted against the mouse genome (Ensembl blast and NCBI blast) to ensure that the sequence on the DNA chip and the protein sequence encode for the same gene.

The regulated proteins could be grouped into different categories. Proteins that are upregulated on the chip, downregulated on the chip, not regulated, not found due to very low expression levels or that are not reproducibly regulated and finally proteins that are not represented on the chip. Figure 18 shows the tendency of regulation of candidate proteins on DNA-chips.

A total of 39 and 16 proteins at E10.5 and E11.5, respectively, were identified. Of the 39 proteins eight showed the same tendency of regulation on the DNA chips, 14 showed an opposite tendency, one was not differentially expressed, ten were not found and six were not represented on the chip. These classes can be split up as following. Three of nine upregulated proteins at E10.5 showed the same tendency on the DNA-chips. Further three proteins are downregulated on the chips, two of the upregulated proteins are either not found or not expressed reliably in all experiments and one protein was not represented on our chip. The 30 downregulated proteins split up as following. Five proteins are downregulated on RNA level and thus show the same tendency of regulation as in the 2D-ge analysis, eleven are upregulated (inverse tendency), one is not regulated, eight are not found or not reliably expressed and five proteins are not represented on the chip.

Of 16 regulated proteins at E11.5 six showed the same tendency of regulation on RNA level, two shoed the opposite tendency, six were not detected by the image analysis software and two were not on the DNA-chips. Regarding up- and downregulation the situation was the following. At E11.5 four of the ten upregulated proteins were also upregulated on RNA level, two were downregulated, two were not found or not reliably expressed and further two were not represented on the chip. Of the six downregulated proteins identified in the 2D-ge analysis two showed the same tendency on RNA level, and four were either not found or not reproducibly expressed.
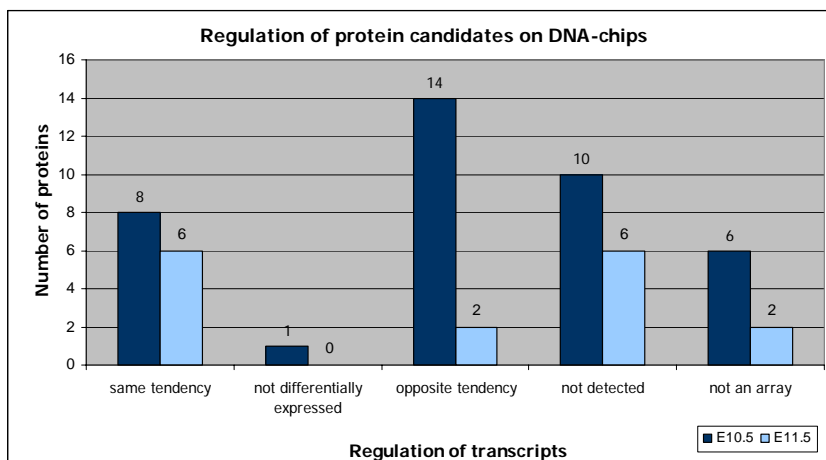
Figure 18: Tendency of regulation of identified proteins on DNA-chips. On the x-axis the regulation on DNA-chips is displayed. On the y-axis the number of proteins is shown. Results of E10.5 embryos are shown in dark blue, E11.5 embryos in light blue.
E10.5: Eight of the proteins found to be differentially expressed showed the same tendency of regulation on RNA level. 14 proteins showed the opposite tendency on RNA level, one was not differentially expressed, 10 were not detected due to low spot intensities and six were not on the array.
E11.5: At E11.5 six proteins showed the same tendency as the corresponding genes expressed at E10.5 on the DNA-chips, two showed the opposite tendency, six were not detected and two were not on the array.

5.3 Comparison of functional classes

Due to the basic differences in the two kinds of analyses one would expect that the identified candidates fall into different functional classes or show different distribution of frequencies. To assess this question the outcome of both analyses was checked with respect to functional annotation. The result is shown in Figure 19.

For each functional category four bars are displayed, dark red for upregulated genes, bright red for upregulated proteins, dark green for downregulated genes and light green for downregulated proteins.

For the functional classes cell cycle, cell metabolism, transport and ion binding candidates were identified in the transcriptome as well as the proteome analysis although in different amounts. In the cell signalling/signal transduction and the neurogenesis category only genes were identified while in the cell structure group only proteins were identified. Genes and proteins with unknown function were obtained in both analyses. "Not identified" were only proteins since the identification process which involves picking the spot in sufficient amounts from the 2D-gel is difficult for low expressed proteins.
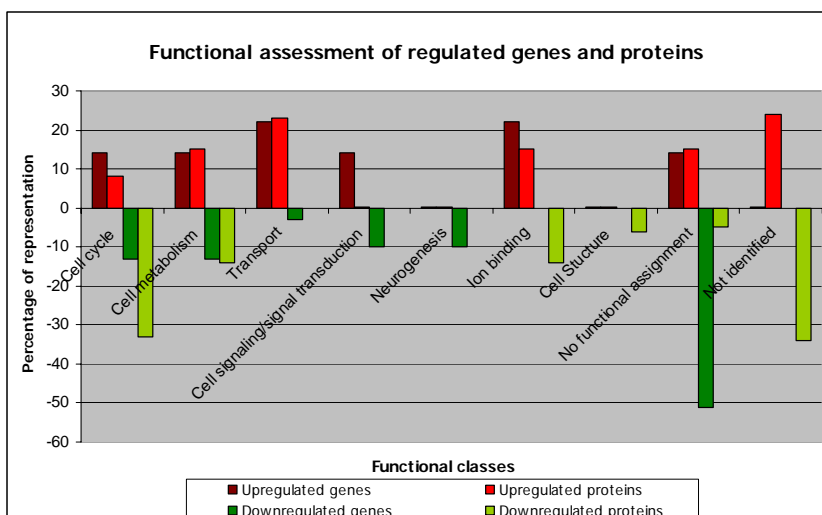
Figure 19: Assessment of candidate functions in the transcriptome and proteome analyses of E10.5 wt and Dll1$^{-/-}$ embryos. Dark coloured bars represent genes while light coloured bars represent proteins. Functional categories are shown on the x-axis. On the y-axis the percentage of genes or proteins that fall into a functional category is displayed. In the categories cell cycle, cell metabolism, transport and ion binding differentially expressed genes and proteins were identified. For cell signalling/signal transduction and neurogenesis only regulated genes were found while for cell structure only proteins were found.

Some interesting observations have been made. Many genes and proteins with transport functions were upregulated but almost no genes and no proteins were downregulated. In the cell signalling/signal transduction group only regulated genes were identified and no regulated proteins. The same was observed for neurogenesis genes but the only represented fraction is the downregulated genes. Further only downregulated proteins (no genes and no upregulated proteins) were found in the cell structure group. In the cell metabolism section the number of regulated proteins and genes is very similar, while in the cell cycle group the numbers differ. More genes are upregulated than proteins and more proteins are downregulated than genes.

5.4 Summary – Transcriptome/Proteome comparison

- Transcriptome and proteome analyses lead to different results concerning the number of detected signals/spots (13,000 genes versus 1000-2000 proteins), the resolution and the possibility to identify post-transcriptional modifications.

- Comparing the expression of differentially expressed proteins on DNA-chips revealed that 20% displayed the same tendency as on protein level, 36% displayed the opposite tendency, 26% were not detected on the DNA-chips, 3% were not differentially expressed on RNA level and 15% were not on the array.

- A comparison of the functional categories of differentially expressed genes and proteins showed that the same functional categories were hit and that the same tendencies of regulation could be observed in .cell cycle, cell metabolism, transport and ion binding.

6 Results - Functional analysis of *Ifitm1*

As shown in chapter 3.5 genes with differential expression patterns in several Delta/Notch pathway mutants were found. In order to understand the position of a gene in a network it is necessary to understand its function. One possibility to assess the function of a gene is to knock it out and analyse the resulting phenotype.

Gene Symbol	Synonyms	Synonyms
Ifitm1	Fragilis2	Mil2
Ifitm2	Fragilis3	Mil3
Ifitm3	Fragilis	Mil1
Ifitm5	Fragilis4	
Ifitm6	Fragilis5	
Ifitm7		Mil4

Table 5: Gene symbols and synonyms of the Ifitm gene family members in the mouse.

For several reasons *Ifitm1* (previous names *Mil-2*, *Fragilis2*; Table 5) is of special interest in context with the Delta/Notch pathway. At E10.5 the expression is restricted to the psm and the most recently built somites. The Delta/Notch signalling pathway plays an important role in the segmentation of the psm. Many genes which are known to be involved in this signal transduction cascade are expressed in the psm, the somites or somitic compartments (Johnston et al. 1997; Evrard et al. 1998; Kusumi et al. 1998; Barrantes et al. 1999; Dunwoodie et al. 2002). Furthermore the change in the expression pattern in Delta/Notch pathway mutants indicates close functional connection.

Ifitm1 was only recently discovered as a marker for primordial germ cells during germ cell differentiation (Tanaka and Matsui 2002; Lange et al. 2003) but until now no clear function could be assigned to it. A functional knock-out of *Ifitm1* would be a suitable tool to assess its exact function.

6.1 *Ifitm1* and family members

Ifitm1 belongs to a family of five genes which are clustered within a 68 kb region at the distal tip of chromosome 7 (Figure 20). The gene family seems to be evolutionary conserved since several homologous have been identified in human, cow and rat (Lange et al. 2003). The human *Ifitm* genes are also clustered and localise in the syntenic region on chromosome 11.

Except for *Ifitm1* most of the *Ifitm* family genes have been reported to be responsive to interferon signalling. Most of them have one or more interferon-stimuable response elements

(ISREs), which are necessary for the *Ifitm* expression in response to interferon stimulation (Tanaka and Matsui 2002).

The first identified gene of this family was *Ifitm3*. It has been shown to be expressed in proximal epiblast at E6.5, the region where primordial germ cell- (PGC) competent cells reside. It was shown that expression continues in cells which differentiate into germ cells (Saitou et al. 2002). *Ifitm1* and *Ifitm2* were subsequently shown to be also expressed in founder PGCs. Additional expression analysis by Lange et al. revealed expression of *Ifitm1* at E8.5 in the mesoderm in the caudal half of the embryo and the developing lung tissue (Lange et al. 2003). At E9.5 expression in the most caudal part of the embryo was observed in the psm, cells of the neural tube, single cells within the hindgut and in the body wall. At the 23rd somite level expression was detected in the forming somite, the body wall mesoderm, cells within the hindgut and in the floorplate of the neural tube. Sagittal sections of E10.5 embryos revealed expression in developing lung tissue and migrating cells along the hindgut anterior to the dorsal aorta.

Additional putative genes with high sequence homology exist in the mouse genome. They have few or mostly no reported ESTs and are coded by a single exon unlike the other *Ifitm* genes. Therefore those are considered to be pseudogenes (Lange et al. 2003).

For the pseudogene on chromosome 8 which contains the highest homology to *Ifitm1* a RT-PCR producing a 535 bp fragment followed by a MluNI restriction digest which would only cleave the pseudogene and produce a 221 bp and a 314 bp fragment was performed. This ensured that no transcript is produced which might substitute for the *Ifitm1* mRNA once it is knocked out.
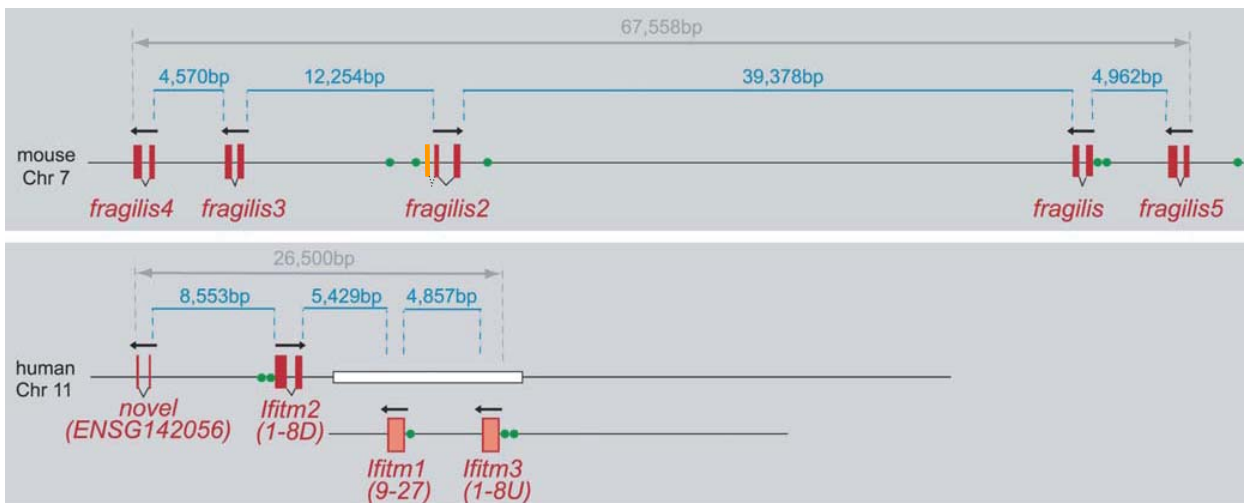
Figure 20: Genomic organization of the Ifitm gene cluster in mouse and human (Lange et al. 2003)(modified). The corresponding gene clusters localise on mouse chromosome 7 and human chromosome 11. The distances between homologous genes differ from mouse to human but the orientation of the genes is maintained. The orange bar in mouse fragilis2 (now Ifitm1) represents a third exon of the gene. This leads to two splice variants with different 5´ untranslated regions.

6.2 Genomic organisation of *Ifitm1*

Ifitm1 lies on the distal end of mouse chromosome 7 and spans a genomic region of 2870 bases. It contains three exons of 611 bp, 411 bp and 326 bp in length. Intron1 has a size of 462 bp and intron2 of 1049 bp. Using the Celera Discovery, Ensembl and NCBI databases two transcripts of different size were found indicating that at least two transcription start sites exist which would generate differentially spliced transcripts containing two exons. The transcripts are 870 bp (XM_133930) and 550 bp (AK004121) in length. Both transcripts have an identical open reading frame but different 5´-untranslated regions. The ATG of the open reading frame is at position 1301, the termination signal TGA at position 2856. The transcripts code for a peptide consisting of 106 amino acids. The peptide contains two transmembrane domains which are highly conserved intra- and inter-species (Lange et al. 2003).

6.3 Design and cloning of the *Ifitm1* targeting construct

In order to obtain a complete loss-of-function of *Ifitm1* a classical targeting construct was designed (Figure 21). As negative selection marker functions the diphtery toxin A (DT-A) gene which induces cell death upon expression. Thus only cells that replaced the *Ifitm1* gene through homologous recombination are able to survive. 5´ upstream of the ATG in exon2 lies the 4.9 kb sequence which was selected as mediator for homologous recombination. On the 3´ end of the transcription termination signal follows a 2.3 kb homologous region. To be able to analyse the endogenous expression lacZ was selected as reporter gene. It is cloned in frame with the ATG in exon2. The pGK/neo cassette which acts as selection marker for insertion of the construct into the genome is flanked by loxP sites in order to be able to remove the cassette after successful homologous recombination.
For the cloning of the construct a pBluescript KS (pBS) vector was used as backbone (Figure 21).

The homologous arms were amplified by PCR. To be able to clone the left arm into the pBS vector the recognition sites for SpeI (A'CTAGT) at the 5´ end and BfrBI (ATG'CAT) at the 3´ end were added to the primer sequence. Thus a fragment homologous to the genomic situation but containing two additional restriction sites was amplified. For the right arm a KpnI (GGTAC'C) recognition site was added to the 5´ end of the sense primer. The PCR fragments were gel purified and subcloned using the TopoTA cloning kit. Subsequently the fragments were sequenced to ensure homology to the genomic sequence.

As a first step the DT-A cassette was inserted using NotI/XbaI restriction sites. Secondly the lacZ gene was inserted at EcoRI/SmaI restriction sites. Subsequently the 4.9 kb fragment representing the left arm was inserted using SmaI/SpeI to open the pBluescript vector and BfrBI/SpeI to isolate the subcloned left arm. Then the right arm was cloned by a KpnI digest and subsequent control if the insertion had the correct direction. As a last step the pGK/neo cassette, flanked by loxP sites was cloned into the pBluescript using EcoRI/SalI restriction sites. The size of the complete vector containing the construct is 18 kb.
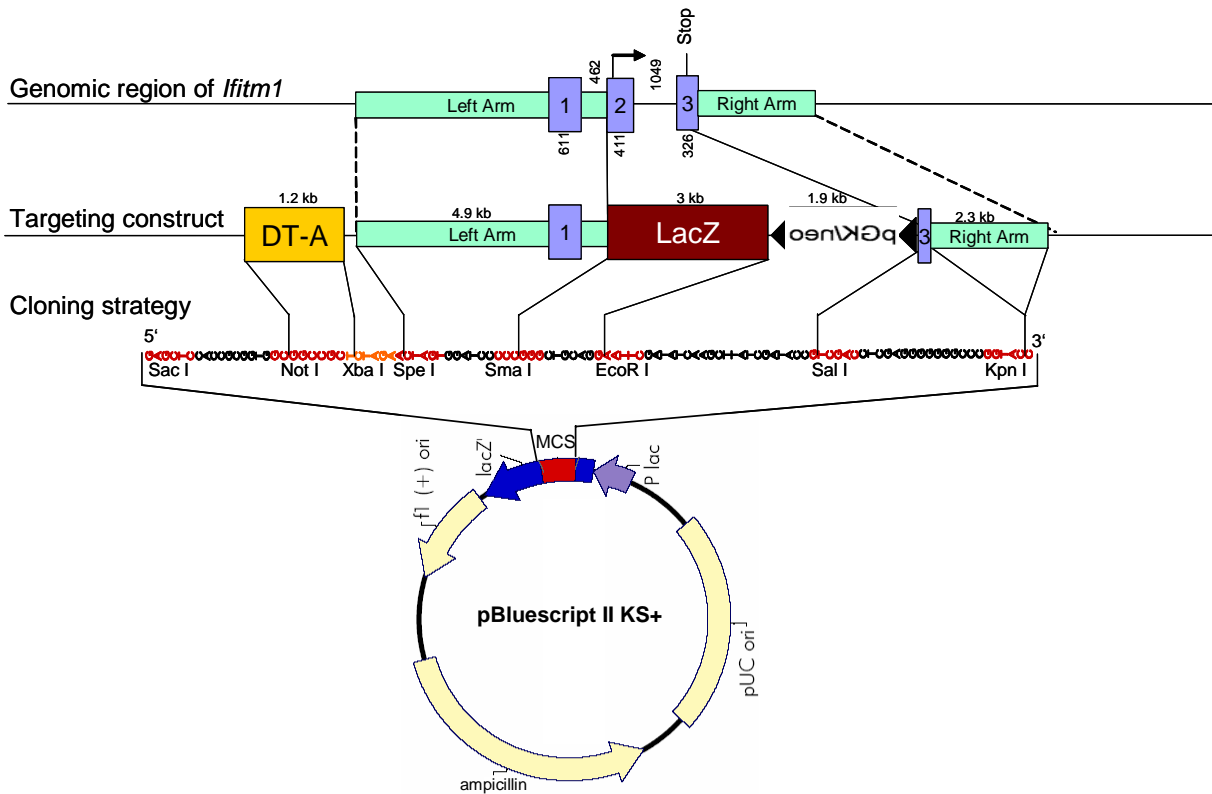
Figure 21: Design and cloning strategy of the Ifitm1 loss-of-function targeting construct. The first part shows the genomic region of Ifitm1 the second part shows a model of the targeting construct and the third part shows the chosen cloning strategy. Blue boxes indicate exons, light green boxes indicate regions selected for homologous arms. Black triangles represent loxP sites. Size of exons, introns and fragment sizes are indicated by numbers above or below the corresponding part. A pBluescript vector has been used as backbone. Restriction sites selected for the cloning procedure are marked.

6.4 Summary – Functional analysis of *Ifitm1*

- In the *in situ* screen *Ifitm1* was found to have a yet undescribed and very promising expression pattern concerning Delta/Notch signalling.

- *Ifitm1* is expressed in the tail tip, presomitic mesoderm, and latest built somites of E10.5 embryos.

- *Ifitm1* was identified as a marker for primordial germ cells but its exact function is not clear.

- In order to assess the function of Ifitm1 a classical knockout targeting construct was designed and prepared such that the complete coding sequence would be replaced by LacZ.

7 Discussion

7.1 Transcriptome and proteome approaches are complementary

Recent advances in development of large-scale analysis methods allow answering novel scientific questions. The whole status of RNA or protein expression came into focus while before single genes or proteins were the object of study.

The identification of novel target genes of *Dll1* was based on RNA expression analysis using DNA chips and protein expression analysis using 2D-gelelectrophoresis. The potential to discover new biological connections in before uncorrelated data is high. However, each method has to be understood in the right context.

DNA-chips have a great potential

DNA-chips offer the possibility to obtain large amounts of RNA expression data and thus to obtain new insights in the expression necessary for a certain condition. Not only the regulation of single genes can be of interest but also genes that are co-regulated under certain circumstances (Beckers et al. 2004; Mijalski et al. 2005). However, the reliability of this technique is highly dependent on many issues such as the various steps of chip production and hybridisation (Drobyshev et al. 2003a; Drobyshev et al. 2003b) as well as the biological material and the RNA isolation protocol used. Furthermore RNA quality, labelling quality which is sometimes RNA dependent, and dye quality are critical features (Figure 5, p. 18). For this analysis all these points have been kept as stable as possible by using chips of the same batch which proposes similar quality, a standardised RNA isolation protocol for all embryos used in the study, and a standardised labelling protocol (see Material & Methods).

The biological material is extremely important to ensure good results. The embryos were phenotyped. *Dll1*$^{+/+}$ and *Dll1*$^{+/-}$ embryos were pooled since no detectable differences have been reported. However, recently an analysis of adult *Dll1*$^{+/+}$ and *Dll1*$^{+/-}$ animals revealed that heterozygous animals do have a mild phenotype. Expression profiling of thymus, liver, spleen and brain of *Dll1*$^{+/-}$ and wt adult mice showed that genes involved in immune response, tumorigenesis and left-right determination were downregulated while genes involved in energy metabolism were upregulated (unpublished data from the German Mouse Clinic, GMC). This result might influence the chip results and should be remembered when analysing the data.

Using whole embryos for the analyses on the one hand offers the possibility to identify *Dll1* targets in all embryonic tissues. Even tissues and processes which previously have not been connected to Delta/Notch signalling can be identified. On the other hand though, it increases the chance of not detecting regulated genes because they are hidden within the biological noise produced by cells in the sample which are not important for the analysis.

Although the method is a great tool to analyse gene expression it has certain limitations. Despite the fact that the organ/tissue collection, RNA isolation and labelling procedure has to be standardised to a high extend also the amount of input RNA for a chip is critical. A rather large amount of 20-40 μg total RNA is necessary for one reaction. In the case of small organs or tissues with little RNA content (e.g. bone, thymus or embryos younger than 10.5 dpc) this means that RNA of several samples has to be pooled. Since the biological variability sometimes differs greatly between individuals this might falsify the data and thus lead to non reproducible results (Seltmann et al. 2005). During the statistical analysis several criteria are chosen to rate the data quality. This finally leads to the selection of a cut-off which separates putative candidates from the supposedly less interesting rest. This of course may lead to the exclusion of biologically interesting genes while others which, e.g., mark general conditions of the sample are included. In the *Dll1* data this might for example have been the case for genes such as *Bnip3*. The Bnip3 protein belongs to the family of Bcl-2 related proteins. The family consists of 19 members which share at least one distinctive Bcl-2 homology domain (BH). Based on their functional and structural features, members of the Bcl-2 family are currently classified into three subfamilies: "multidomain" anti-apoptotic, "multidomain" pro-apoptotic and "BH3 domain-only" members. Bnip3 belongs to the "BH3 domain-only" subfamily. Those members share sequence homology only in the BH3 domain. They are supposed to function as sensors to distinctive cellular stresses which lead the cell to apoptosis (Itoh et al. 2003). Dll1 mutant embryos die around E11.5. At E10.5 processes leading to death one day later might already have been induced, such as apoptosis. A further example might be *Atp5h*, an ion channel associated protein located at the mitochondrial membrane (Noh et al. 2004). Downregulation of *Atp5h* might be a secondary effect of beginning apoptosis such that ion channels are degraded and thus transport or exchange of ions across the mitochondrial membrane could be already reduced.

The quality of the data obtained from the DNA-chip experiments has been controlled at various stages during the complete process. Using stringent statistical criteria 22 upregulated and 30 downregulated genes have been selected.

General suggestions to obtain high quality data from microarray experiments include repetition of experiments (Lee et al. 2000) and existence of clone replicates on an array (Lee et al. 2000; Tseng et al. 2001). Using these internal controls still cannot avoid the production of false data since artefacts can be due to probe sequences and structures that cause unspecific hybridisation as well as biased labelling with fluorescent dyes or the label itself (Drobyshev et al. 2003b). To estimate the rate of cross-hybridisation on the in-lab produced 20k chip we used a technique called "Specificity Assessment from Fractionation Experiments" (SAFE) (Drobyshev et al. 2003b). This analysis revealed that at least 0.2-1.7% of the probes on the chip can produce non-specific hybridisation and that the exact value is dependent on the tissue used. This result leads to the conclusion that results obtained from DNA chip experiments need to be confirmed using independent methods. For the comparison of *Dll1* wt versus *Dll1*^{-/-} samples it is important to note that probes do exist that produce non-specific hybridisation and thus might produce false positive results. This leads to the conclusion that verification of microarray data using independent methods is necessary.

Verification of microarray data

A feasible method to confirm (or obtain) RNA expression data is real-time PCR. To confirm the candidate genes obtained from the DNA chip experiments of wildtype versus *Dll1*^{-/-} embryos at 10.5 dpc real-time PCR was used in this project.

In total expression of 32 genes was analysed in relation to the housekeeping gene *Hprt*. In 15% of the genes (*Csk, Eraf, Atp5h, Ifitm1, Nr1h2*) the two different primer pairs used for each gene produced opposite results (Table 2, p. 68). This might indicate that probably other fragments representing different genes were amplified. On the exact regulation of these genes cannot be stated. For 25% of the genes (*Gamt*, MG-4-3k8, MG-8-86g2, *Nup155, Rcvrn, S100a10, Wnt10b, Hmx2*) the real-time PCR produced inverse results compared to the DNA-chips. Since two independent primer pairs confirmed these results it is likely that these eight genes are false positives of the DNA chip analysis. This might be due to the fact that at least some of the genes only displayed very low levels of regulation of the DNA-chips (around 1.2-1.6) (Table 1, p. 56) which can occur, e.g., when the spot intensity is very low. In these cases even small differences produce presumably significant results. These genes may be excluded for in-depth analyses.

Nevertheless, real-time PCR data of further 19 genes (60%) supported the DNA-chip results. Within those *Mt1* and *Mt2* are worth to note since it is known that these genes are co-regulated (Michalska and Choo 1993; Masters et al. 1994). The DNA-chip results affirms this correlation with *Mt1* and *Mt2* being the two strongest upregulated genes.

Using DNA-chips and real-time PCR a list of genes showing regulation in the *Dll1* mutant is obtained. However, this did not give information about a potential biological relevance in the Delta/Notch signalling pathway. To address this question a systematic whole mount *in situ* hybridisation-screen was performed to gain insights into the expression pattern of the candidate genes *in situ*. All identified candidate genes were tested on E10.5 wt embryos. If a pattern indicative of Delta/Notch signalling was observed wish was also performed on *Dll1*^{-/-} embryos.

A subset of genes could be identified to have expression in the presomitic or somitic mesoderm or neural tissues where Delta/Notch signalling plays a vital role. These genes will be discussed later. However, also a number of DIG labelled probes resulted in no expression pattern, high background or ubiquitous expression pattern. Interestingly, this phenomenon has also been described by Buttitta et al. who also performed microarray analysis followed by wish of the candidate genes using DIG labelled riboprobes (Buttitta et al. 2003). The authors then used radioactively labelled gene specific probes which resulted in defined expression patterns (Buttitta et al. 2003). Radioactive *in situ* hybridisation (rish) was not performed in this Delta/Notch study because radioactive labelling is not applicable for the conduction of a large screen. Thus it remains to speculate if this had been the key to this problem. However it is not clear why genes which are expressed at a level clearly detectable on a DNA-chip are not visible in wish. Ubiquitous patterns may also have another reason. The clones from Lion Bioscience which were used for most *in situ* hybridisations contain an adapter sequence of roughly 150 bp at the 3´end of the gene specific sequence. This might lead to unspecific binding of the riboprobe to the mRNA species present in the embryo and result in rather high background levels. Furthermore, genes with ubiquitous expression

patterns do exist of course because of their function. The nucleoporin Nup155 for example is a major component of the nuclear pore complex and thus present in any cell of an organism (Figure 12, p. 66).

Proteome analysis is a versatile technique

Until recently 2D-gelelectrophoresis was mainly a method to display a status of protein composition of a sample. Only the development of mass spectrometric methods for biological molecules and the availability of complete genome sequences lead to the possibility to further analyse the proteome of a sample.

In case of the Delta/Notch signalling pathway no proteomic data has been published so far. In this study 2D-ge combined with MALDI-TOF was performed to discover regulated proteins and thus add a further level of biological understanding to the Delta/Notch puzzle. This presents a great improvement since protein identification was very difficult before the discovery of mass spectrometric techniques. This, however, is necessary to understand biological function because the majority of the active agents in a cell are proteins. Although it is becoming clear that there is no strict linear relationship between the transcriptome and the proteome, understanding the regulation of protein expression is a big issue in understanding gene function and regulation.

For proteomic analysis this technique is without doubt a basis. However, it has certain limitations. Standardization of all procedures from protein extraction to the gel electrophoresis, the image analysis and spot picking and the subsequent MALDI-TOF analysis is absolutely necessary to obtain reliable results. A further difficulty lies in the identification procedure. The mass spectra obtained as a peptide mass fingerprint need to be blasted against protein sequence databases. A clear identification is only possible if database entries already exist. Of course the databases will be more and more complete with better sequence annotation but this technique will always depend on that issue.

For the biological material for proteome analysis account the same stringent criteria as for the transcriptome analysis described above. The same is true for the use of whole embryos for the analysis.

The proteomic analysis of E10.5 wt and *Dll1* mutant embryos revealed 13 upregulated and 37 downregulated proteins. Ten of these were not identifiable in the MALDI-TOF analysis. Reasons for that might be that the amount of protein isolated from the gel is below the detection limit for the MALDI-TOF analysis or that the database blast did not reveal a hit due to missing entries in the databases. In one case from one excised spot (Table 3a, p. 76; spot number 1798) two proteins were identified: Pkm2 and Stip1. This is possible because two proteins of very similar pI and molecular weight come to lie at the same position or very close to each other on the gel. In these cases it is not clear which of the spots was initially regulated and which was not. Here it seems rather clear that the regulated of those two spots was Stip1 because Pkm2 was found in a single spot to be downregulated (Table 3a, p. 76; spot number 304).

One might be surprised to not find Dll1 in the protein list since in the mutant the protein should not be present. Dll1 is a membrane bound transmembrane protein and with the

protein isolation method used (see Material & Methods) membrane proteins can not be dissolved and will not be present on the 2D-gels. This leads to the question if this technique is useful for a large-scale analysis. Of course there are parts of the proteome of *Dll1* mutant embryos which were not analysed with this experimental setup. Since the number of proteins in a cell is estimated to be between some ten- to hundred-thousands reduction of complexity is essential. In future studies this could be implemented by the use of different protein fractions, such as the nuclear, cytosolic and membrane protein fractions.

Verification of proteomic data

As discussed for the microarray data conformation of results obtained by 2D-ge and subsequent mass spectrometry is necessary on the one hand to assess overall quality of the results and on the other hand to identify false positive candidates. However, assessing the quantities of proteins within a complex protein mixture is not trivial. In order to achieve this goal semi-quantitative Western blotting was selected. For each protein to test two different amounts of total protein isolated from wildtype and *Dll1* mutant embryos were run on a SDS-PAGE and immunoblotted. The intensities of the observed bands were compared between wt and *Dll1*$^{-/-}$ protein extracts.

With this method it is possible to state on the expression tendency of the analysed protein but certain facts should be taken into account. The determination of protein concentration is an indirect measurement technique. A standard solution containing a defined concentration of a protein (e.g. BSA) has to be produced and afterwards a dilution series with the standard solution and the protein mixture of interest is needed. In these steps pipetting errors can occur that might influence the outcome of the measurement. Additionally dye solution is added to subsequently measure the extinction of the sample. Comparison with the values produced by the standard protein allows determination of the protein concentration in the mixture. Thus this method might not be very exact. In order to address this problem each Western blot was stripped after the detection of the specific antibody against the protein of interest and incubated with the antibody for the house-keeping protein β-actin. Nevertheless one has to assume that β-actin is not regulated in the *Dll1* mutants (which seems to be the case). Further restrictions come from the fact that antibody binding is not in any case directly proportional to the amount of protein on the gel. This means that if bands show clear intensity differences it is very likely that unequal amounts of proteins are responsible. If the bands show similar intensities it is not sure that no quantitative differences exist.

Of course the availability and quality of commercially distributed antibodies is an important issue for the use of this technique. For many of the identified candidate proteins no antibody was commercially available. Of the 25 used antibodies six did not detect bands at all (Hemoglobin α, Lamr1, Eef2, Mdgi (Fabp5), Prealbumin, Usp14), two not at the correct band size (Mtap, Trx), and three detected numerous bands (Apoa4, hnRNP A3, TH). Those proteins had to be excluded from the analysis.

In two cases (Calr, Hnrpl) the upregulation found in the 2D-ge could clearly not be confirmed using semi-quantitative Western blots although the used antibodies were of good quality. The two proteins were downregulated in this analysis. Possible reasons might be that the spot which was identified to be regulated on the 2D-gels lied close to another spot in the gel. The

wrong spot might have been picked and analysed. However, if results in the Western blot are clear-cut (as for Calr) they overrule the results from the 2D-ge analysis. Three of the analysed proteins (Eif3s7, Nsf, Hsp60) seemed to have equally strong expression in the wt and the *Dll1⁻/⁻* protein extracts. As mentioned above those results are not definite due to the binding kinetics of antibodies and thus it is not possible to state on the exact regulation.

Perspectives for further analyses

The comparison of regulated proteins with the correspondent expression on DNA-chips basically revealed that the tendency of regulation between RNA and protein expression might be the same but might also be in the opposite direction. This shows clearly that it is in general not possible to state on either RNA or protein regulation if either one is known. Furthermore this finding emphasises the role of post-transcriptional and post-translational modification. On the one hand the transcribed mRNA might be masked or polyadenylated such that it cannot be translated at the ribosome (de Moor and Richter 1999; Minshall et al. 2001) or it is not transported out of the nucleus as a regulatory mechanism to prevent translation (Erkmann and Kutay 2004). On the other hand proteins might be kept in an inactive state instead of being degraded if they are not needed. This might be reached by phosphorylation, glycosylation or other reversible modifications or by regulation of subcellular compartmentalisation (Gill 2004; Greene and Chen 2004; Smal et al. 2004; Topisirovic et al. 2004). A protein might be present in the cell in a high amount but might not be active because it is not located at a place where it is needed.

As mentioned above samples with less complexity would improve the outcome of both types of analyses. Using laser micro-dissection it is possible to isolate specific regions from a tissue, e.g. single cells or groups of cells such as somitic cells. Subsequent analysis with DNA-chips or 2D-ge is difficult because of very limited amounts of total RNA or protein. The possibility for amplification exists for RNA. With T7-based RNA amplification it should be possible to linearly amplify the present RNA species. The focus of this method lies on the feature of linearly amplifying nucleic acids and not exponentially as in the case of PCR. This is extremely important since in expression analyses the ratio of expression in test and reference sample is of most interest. Thus the relative amounts of each RNA species must be maintained.

The feasibility and reproducibility of linear RNA amplification was assessed in different experiments. The comparison of three RNA isolation protocols (Figure 13, p. 70) revealed that this is an extremely critical step in the process. The detection limit as identified by RT-PCR using house-keeping genes ranges from roughly 100 cells (size of embryonic cells) (Phenol-chloroform extraction) to 4500 cells (Qiagen RNeasy Mini Kit). This leads to the conclusion that i) isolation of RNA from minute amounts is not trivial and ii) that far more than 100 cells are needed to be able to perform experiments and replications.

Furthermore, the reproducibility of T7 based linear RNA amplification was assessed using starting amounts of total RNA from 50 ng - 5 µg. It was found that with a starting amount of 800 ng the best results were obtained with 300-400 fold amplification. However, it was repeatedly observed that after the RNA amplification procedure no RNA was present. It is not clear during which step of the amplification protocol this loss usually occurs. This leads to the

speculation that the method is very sensitive to even minor changes and thus difficult to handle on a routine base. Additionally since the outcome of RNA after the amplification is not reproducible even for two probes containing the same starting material and amount of RNA this method needs to be further improved.

For proteins amplification is not possible. In order to be able to use very small amounts of protein for proteomic analysis hope lies on the recently developed protein or antibody arrays.

7.2 Functional assessment analyses

To assess the functions of the regulated genes and proteins in *Dll1*^{-/-} embryos they were grouped into functional classes according to the Gene Ontology classification (Harris et al. 2004) (Figure 9, p. 57; Figure 16, p. 78). Some interesting aspects will be discussed below.

Gene functions of candidate genes represent the status of the Dll1 mutant

Within the functional annotation of the genes it is interesting to note that some groups are up- and downregulated in the same proportions (cell cycle, cell metabolism and cell signalling), some functional categories show different proportions (transport) and some only appear in either the up- (ion binding) or the downregulated genes (neurogenesis). The functional classes of the regulated genes represent the direct output of the loss of the *Dll1* gene and thus seem to represent the status of the embryos at the time-point 10.5 dpc: the up- and downregulation of cell cycle and cell metabolism genes could indicate that normal regulation of these processes might be disturbed which could lead to activation or repression of further mechanisms in the cells that are not used in the wt condition. This situation is of course more obvious for functional groups that show drastic changes compared to the wt such as transport, neurogenesis and ion binding.

Transcriptional regulation is critical in Delta/Notch signalling

Among the three up- and four downregulated genes involved in cell signalling and signal transduction are five transcription factors (*Zinc finger protein Rlf, Hmx2, Lhx3, Tlx1, Nr1h2*). Although the exact regulation is not totally clear after the real-time PCR results this finding is of interest because in the Delta/Notch signalling pathway the binding of the receptor is known to lead to transcriptional activation of downstream targets such as *Hes* genes which as well are transcription factors. The identified transcription factors might also represent downstream targets of the signal transduction cascade. Since only the processes in the receiving cell are relatively well understood it might be possible that the identified transcription factors are involved in gene regulation in the signalling, Delta expressing cell. *Hmx2*, *Lhx3*, *Tlx1* and *Nr1h2* were downregulated on the DNA-chips which could indicate that they might be regulated by *Dll1*.

Functional connections to Delta/Notch signalling will be discussed in chapter 7.3.

Disruption of expression of genes with functions during neurogenesis

Two genes involved in neurogenesis were found to be downregulated in the $Dll1^{-/-}$ embryos: *Nes* and *Sema5b*. The whole mount *in situ* hybridisations clearly showed alterations in the expression of *Nes* and *Sema5b* (Figure 11s-v, p. 62). Neurogenesis is a complex process which is tightly connected with other developmental processes and is of high interest since Delta/Notch is known to play an important role in neurogenesis.

Is transport more important in the Dll1 mutant?

If one takes a closer look at the five upregulated genes with transport functions it turns out that three are chains of the hemoglobin molecule (Table 1, p. 56). This was also observed in the regulated transport proteins where also three hemoglobin chains were upregulated at E10.5 (Table 3, p. 76). Hematopoiesis starts in mouse embryos at E9.5 and Delta/Notch signalling is known to be involved in this process (Milner and Bigas 1999; Kojika and Griffin 2001; von Boehmer 2001; Ohishi et al. 2003). At E10.5 the $Dll1^{-/-}$ embryos are severely hemorrhagic with blood in the head and neural tube where it is absent in wt embryos of the same developmental stage. Pecam staining has shown that the vessels lead into the lumen of the neural tube while in the wt they do not (Przemeck, unpublished results). This could indicate that formation of the vascular system is disrupted in the *Dll1* mutant. Furthermore since the blood in the neural tube is not circulating in the embryo as it normally would hematopoiesis might be upregulated to compensate for the reduced amount of circulating blood. Suggesting this hypothesis it would indicate that expression of transport genes is not due to the enhanced need of, for example, removal of toxic by-products produced due to disturbed metabolism but is a secondary effect due to malformations during blood vessel development.

Regulated proteins give insights into altered biological processes

Analysing the functional annotation of the regulated proteins at E10.5 revealed that twice as many proteins involved in transport functions are upregulated, three times as much cell cycle proteins are downregulated and proteins involved in cell structure are only found in the downregulated proteins (Figure 16, p. 78). At E11.5 the differences between up- and downregulated proteins seem to be bigger but it has to be taken into account that only few proteins were regulated at E11.5. This means that 7% for the upregulated and 11% for the downregulated proteins correspond to one candidate. Keeping this in mind it shows that the differences are rather little.

Regulated degradation of proteins seems to be disrupted in Dll1 mutants

Regulated degradation of proteins via the ubiquitin-proteasome pathway is a major regulatory mechanism in all cells (Ciechanover 1998). It has been shown that this process also is important for the regulation of Delta/Notch signalling (Baron et al. 2002; Schweisguth 2004). In the *Dll1* mutant six subunits of the proteasome complex are downregulated at E10.5 (Table 3a, p. 76). This could indicate that the function of the proteasome might be affected such that processing of proteins is not possible in the normal manner.

Possible biological effects will be discussed in chapter 7.3.

Comparing the functions of regulated genes and proteins

By analysing the functions of regulated genes and proteins (Figure 9, p. 57 and Figure 16, p. 78) it becomes obvious that most of the candidates fall into the same classes. Cell cycle, cell metabolism, transport and ion binding genes/proteins are found in the regulated proteins as well as the regulated genes. The cell signalling and neurogenesis sections however are unique to the regulated genes. This distribution is graphically shown in Figure 19 (p. 89). This might be explained by the resolution of the different techniques used. With DNA-chips it is possible to detect even low expressed genes. In contrast, with 2D-ge it is difficult to detect or rather identify very low expressed proteins because the detection limit of the gels lie at 50-100 ng (for Coomassie staining) and 1-2 ng (for fluorescent staining). After spot picking and tryptic digest the protein amount might be too low for proper Maldi-TOF analysis.

However, the overall similar distribution of regulated proteins and genes on functional levels shows that the analysis on the one hand supports each others results. On the other hand it emphasises the relevance of the regulations occurring in the *Dll1* mutant.

7.3 Biological relevance of the identified candidates

Dll1$^{-/-}$ embryos die around day 11.5 of embryonic development. At this stage they display a variety of abnormal symptoms. These include besides an overall altered morphology, an undulated neural tube, irregular somites, a hydrocephalic head and bleeding in the head and neural tube (Hrabe de Angelis et al. 1997). Delta/Notch signalling is known to be involved in many developmental processes such as neurogenesis, somitogenesis, pancreatic development, inner ear development and hematopoiesis (Conlon et al. 1995; Oka et al. 1995; Hrabe de Angelis et al. 1997; Lewis et al. 1998; Apelqvist et al. 1999; Baker 2000; Dale and Pourquie 2000; Jiang et al. 2000; Lammert et al. 2000; Schnell and Maini 2000; Kiernan et al. 2001; Kojika and Griffin 2001; Lutolf et al. 2002; Krebs et al. 2003; Ohishi et al. 2003; Przemeck et al. 2003). However it is not known so far how regulation of these diverse processes can be obtained with the known mechanisms of Delta/Notch signalling. To address this question the screening of the transcriptome and the proteome was performed in order to identify further target genes that might give insights into the regulatory mechanisms lying below.

7.3.1 Regulation of Delta/Notch pathway members

Analysing the candidate genes identified by DNA-chip experiments (Table 1, p. 56) it is striking that none of the known Delta/Notch related genes, such as *Cbf1, Hes1, Lfng, Notch1, Rbp-Jk* and others, is present in the list although most of them are present on the DNA-chip. Checking the expression of these genes on the arrays revealed that most were "not found". This means that the expression intensity was very weak and the signal was at the background level. Therefore it is not possible to analyse their regulation. Possible reasons might be that whole embryos were used for the gene expression profiling. Most of the Delta/Notch pathway genes are expressed in defined regions of the embryo such as the presomitic mesoderm, somitic compartments or single cells in the neural tube, indicating that the expression level or RNA copy number might be rather low. Within the huge amount of

different transcript species present in the E10.5 embryo genes with very low expression levels might fall into the region of biological noise.

Although the known Delta/Notch relevant genes could not be analysed on the DNA-chips and thus be used as an internal control it was still possible to identify a number of yet unknown genes possibly involved in Delta/Notch signalling. On the one hand known genes have been found that have not been brought into context with Delta/Notch. On the other hand many genes or ESTs without any functional annotation so far were detected, such as several Riken clones and hypothetical proteins.

Using 2D-ge also a number of proteins not known to be involved in the Delta/Notch signalling pathway have been identified. As for the DNA-chip analysis it was not possible to identify known pathway genes such as *Dll1, Notch1, Hes1* and others. This might be due to the experimental protocol used. Since the proteome of mouse embryos has not been the subject of intense studies we did not know what outcome to expect from the analysis. The focus was put on the isolation and resolution of as many proteins as possible. Therefore the experimental conditions, namely the protein isolation buffer, protein amount loaded on the gels and pH-gradients were selected accordingly. Thus it was not possible to resolve, e.g., membrane bound proteins. Also very acidic or basic proteins might not be resolved properly on the used gels. Nevertheless, a large number of new proteins could be identified and also verified. This suggests that the method was the right tool for the proteomic analysis of wt and *Dll1* mutant embryos and furthermore might be a promising tool for analyses of similar kinds.

7.3.2 Cellular processes altered by *Dll1* deficiency

The identified candidates from both, the transcriptome and the proteome analyses were analysed together to obtain a complete picture of the cellular processes running or failing in the *Dll1* mutant.

Indications for alterations of regulation on the genomic and RNA level

The coordinated processes leading to mRNA transcripts of a gene follow strict regulations. The modification of the nucleosome structure is an important regulatory process during development. Numerous chromatin-remodelling complexes involved in transcription regulation have been identified and characterized (Armstrong and Emerson 1998; Kingston and Narlikar 1999; Klochendler-Yeivin et al. 2000). They function by modification of histones or altering chromatin structure. It has been shown that NICD is able to associate with histone acetyltransferases (HATs) (Kurooka and Honjo 2000). HATs are attracted to specific chromosomal sites via physical interactions with DNA-bound transcription factors such as CSL (Brownell et al. 1996; Bresnick et al. 2000). Furthermore it was found in *in vitro* studies and mammalian two-hybrid assays that the NICD can bind to the HATs Gcn5 and PCAF via its ankyrin repeats (Kurooka and Honjo 2000). Taking all these data into account Bresnik et al. suggests a model for Notch-mediated transcriptional activation (Bresnick et al. 2000). In this model the transcriptionally inactive and the active state are distinguished. In the inactive state (absence of NICD) DNA-bound CSL associates with SKIP (Ski interacting protein) and a SMRT-containing HDAC complex which leads to histone deacetylation and thus decreases

the DNA accessibility and represses the target gene. In the active state which is characterized by the presence of NICD, a complex is formed consisting of DNA-bound CSL, NICD, Mam1 (Mastermind) and SKIP. This leads to the attraction and binding of the HATs Gcn5 and PCAF to the NICD ankyrin repeats. These HATs subsequently acetylate the histones locally which, in turn leads to increased accessibility of the DNA and to transcriptional activation (Bresnick et al. 2000).

The mammalian SWI/SNF complexes are ATP-dependent chromatin remodelling complexes which can locally disrupt or alter the association of histones with DNA (Kim et al. 2001). The SWI/SNF complex consists of nine to 12 subunits, with those from different tissues showing significant heterogeneity. The subunit diversity of SWI/SNF complexes suggest that different complexes might have tissue-specific roles during development (Wang et al. 1996a; Wang et al. 1996b).

Smarcc1 is a core component of the mouse SWI/SNF complex which is required for the regulation of transcriptional processes associated with development, cellular differentiation and proliferation (Choi et al. 2001; Kim et al. 2001). Furthermore it is known to be involved in glucocorticoid (GC)-induced apoptosis during T-cell development, where the expression level of *Smarcc1* determines the GC sensitivity of thymocytes (Choi et al. 2001). GC-induced apoptosis of thymocytes has been reported to be affected by *Notch1*. Expression of the intracellular domain of Notch (NICD) reduced GC sensitivity and thus inhibited GC-induced apoptosis in a thymic lymphoma line and a T-cell hybridoma without affecting the GC receptor and known GC-regulated genes (Deftos et al. 1998). Studies with transgenic mice expressing NICD showed that activated Notch1 downregulates Smarcc1 protein expression in the thymus (Choi et al. 2001). Promotor analysis of *Smarcc1* revealed that the promoter sequence contains five E-box like sequences and that mutations in one E-box like sequence abolished the downregulation effect of Notch1 (Choi et al. 2001). These findings indicate that NICD suppresses the promoter activity of *Smarcc1* through an E-box sequence (Choi et al. 2001).

In the *Dll1* mutant *Smarrc1* is downregulated indicating that alterations of the SWI/SNF chromatin-remodelling complexes might occur. Furthermore it has been shown that NICD can downregulate *Smarcc1* which suggests that it is a downstream target of *Notch1* (Choi et al. 2001). As shown in wish (Figure 11, p. 62) *Smarcc1* is expressed in the somites, the presomitic mesoderm and the neuroepithelium of the neural tube of E10.5 wt embryos. The downregulation in the tail region of *Dll1*^{-/-} embryos could suggest that the chromatin-remodelling machinery is inactive or reduced in the number of molecules at this site and thus regulation of transcription of Delta/Notch pathway genes might be disrupted. If the principle of regulation between *Notch1* and *Smarcc1* could be transferred to other developmental processes than T-cell development as the expression of *Smarcc1* in the mesoderm and neural tissue would suggest, a novel mechanism of regulation of Delta/Notch signalling would have been hit.

Further evidence for the involvement of processes controlling transcription and RNA processing in the Delta/Notch signalling pathway might come from the identification of regulated heterogeneous nuclear ribonucleoproteins (hnRNPs) in *Dll1* mutants (Table 3, p. 76) which associate with RNA intermediates in the cytoplasm to prevent the formation of

secondary structures (Singh 2001; Dreyfuss et al. 2002). RNA intermediates in the nucleus do not exist as free RNA molecules. They are associated with an abundant set of nuclear proteins, hnRNPs. In humans many different hnRNP species exist which are named from A1 to U and have molecular weights between 34-120 kDa. The most common RNA binding motif in hnRNP proteins, called the RNP motif, is also found in many other RNA-binding proteins. This motif contains about 90 amino acids and includes one highly conserved 8 amino acid sequence (RNP1) towards the C-terminal end and a region of hydrophobic amino acids (RNP2) towards the N-terminal end (Naranda et al. 1994). A further protein involved in RNA processing tasks is Ddx6 (Table 1, p. 56). It is a RNA helicase from the evolutionary conserved DEAD-box family with important roles in transcription, pre-mRNA processing, nuclear mRNA export and RNA turnover (Minshall et al. 2001; Rocak and Linder 2004). DEAD-box family proteins have nine characteristic motifs, which are organised in a core domain. They are required for different cellular processes such as transcription, pre-mRNA processing, ribosome biogenesis, nuclear mRNA export, translation initiation, RNA turnover and organelle function (Rocak and Linder 2004). *Ddx6* is involved in ATP binding and ATP dependant helicase activity.

Regulation on post-transcriptional levels is disturbed in Dll1 mutants

Regulation on post-transcriptional level is absolutely essential for cellular processes. Different ways exist for this regulation: regulation of translation, regulation via post-translational modifications such as phosphorylations and glycosylations and regulation via controlled protein degradation. Components of all three post-transcriptional regulation mechanisms were identified in the transcriptome and the proteome screen.

Four proteins involved in translation initiation or elongation have been identified to be regulated. Two of those (Itgb4bp, Eef1b2) represent subunits of eukaryotic translation initiation factor 6 and elongation factor 1 complexes. The other two (Eif3s5, Eif3s7) are subunits of the eukaryotic initiation factor-3 (eIF3). eIF3 is the largest of the mammalian translation initiation factors and consists of at least eight subunits ranging in mass from 35 to 170 kDa. eIF3 binds to the 40S ribosome in an early step of translation initiation and promotes the binding of methionyl-tRNA$_i$ and mRNA (Asano et al. 1997). The explicit functions of the subunit are still mostly unclear except that Eif3s7 is a strong RNA-binding protein (Nygard and Westermann 1982). All four identified subunits were downregulated in the *Dll1*^{-/-} embryo. This finding would indicate that either the number of eIF complexes per cell might be reduced or that physiological functions might be altered due to the downregulation of specific subunits of the molecule. Furthermore it is known that the rate of protein synthesis is rapidly downregulated in mammalian cells following the induction of apoptosis (Clemens et al. 2000) which would suggest that in the *Dll1* mutant apoptosis is increased. Since the mutant embryos die around day 11.5dpc it might be possible that apoptosis could be already induced in subsets of cells. This would in consequence lead to a downregulation of the translation initiation factor complexes and thus might result in overall downregulation of protein synthesis.

The 26S proteasome-, ubiquitin- and ATP-dependent pathway is important in the non-lysosomal degradation of proteins involved in cell cycle regulation, metabolic adaptation, removal of abnormal proteins, processing of inactive transcription factor precursors and in

the degradation of some membrane proteins (Coux et al. 1996). Proteins to be degraded are tagged with a chain of ubiquitin molecules which represents the signal for degradation by the proteasome (see Introduction). In the *Dll1* mutant six subunits of the proteasome were downregulated and the ubiquitin-specific protease Usp14 was upregulated (Table 3, p. 76). These findings suggest that the ubiquitin-dependent protein degradation machinery via the proteasome is severely disrupted.

It has been shown that proteins involved in regulated degradation of proteins play roles in the Delta/Notch signalling pathway in different species. These include *Sel10, Nrarp, Neur, Mib, dx, Su(dx)* (Baron et al. 2002; Schweisguth 2004). Most of these proteins are either E3 ligases (*Neur*, *Mib*, *Su(dx)* and maybe *dx*) or are able to stimulate ubiquitination or degradation but the importance of the proteasome as the essential organelle for degradation has not been analysed so far. The downregulation of several proteasome subunits indicates that not only the determination which proteins need to be degraded is essential but also the degradation process performed by the proteasome itself. The exact consequences of the downregulation of single subunits of the proteasome are not clear but it might be possible that this leads to reduced functionality of the proteasome and thus to reduced, slower or ineffective protein degradation. In these cases the amount of certain proteins in the cell would not be reduced as much as they normally would. In consequence this could lead to disturbed feedback loops which often regulate the amount of a transcript and the corresponding protein present in a cell (e.g. Hirata et al. 2002). Regulation via feedback loops is a common mechanism used in the Delta/Notch signalling pathway (Hirata et al. 2002).

Usp14 belongs to a large family of cysteine proteases that specifically cleave ubiquitin conjugates. Disruption of Usp14 in the mouse leads to defects in synaptic transmission in the central and peripheral nervous system which suggests that ubiquitin proteases are important in regulating synaptic activity in mammals (Wilson et al. 2002). Substrates of Usp14 are only mono-ubiquitinated proteins (Wilson et al. 2002). Proteins tagged for degradation usually are poly-ubiquitinated. Removal of the ubiquitin from a mono-ubiquitinated protein could therefore be a regulatory element, influencing protein activity (Hicke 2001) and protein localization in the cell (Katzmann et al. 2001). The importance of intracellular localization and involved control mechanisms will be discussed in the next section as well as protein phosphatases and kinases.

Regulation on the cellular level via intracellular trafficking?

Until now all findings and hypotheses have been brought into context of direct interaction between molecules. However, a major pre-requisite is of course that the molecules are physically able to directly interact with their partner. Therefore the transcripts, proteins, organelles etc have to be in the same region of the cell where the process takes place.

It is known that dynamic phosphorylation and de-phosphorylation as well as ubiquitination of proteins are fundamental mechanisms utilized by cells to transduce signals (Sontag 2001; Wilson et al. 2002). As mentioned above Usp14 might influence protein activity and localization via ubiquitination and de-ubiquitination in cells and might be altered in the *Dll1*

mutant. The involvement of phosphorylation and de-phosphorylation has not been analysed in the context of Delta/Notch signalling so far.

The protein phosphatase 2A (PP2A) family has been implicated in many different facets of cellular function (Cohen 1989). PP2A, the major serine/threonine phosphatase in eukaryotic cells, is very abundant and ubiquitously expressed. It dephosphorylates many substrates *in vitro* and is involved in the regulation of nearly all cellular activities (Sontag 2001). The multimeric enzyme consists of a catalytic subunit of 65 kDA complexed with two regulatory subunits of various sizes to form different heterotrimers (Gotz and Kues 1999). The catalytic subunit PP2A C is encoded by the two genes $C\alpha$ and $C\beta$. In the *Dll1* mutant the $C\alpha$ (PPP2Cα) subunit was downregulated indicating that PP2A action in the cells might be reduced.

It has been shown that the knockout of the $C\alpha$ subunit is embryonic lethal around E6.5 of embryonic development. In the $C\alpha$ mutants no mesoderm is formed. It is suggested that PP2A has functions during neurogenesis because of several observations. i) The highest expression of PP2A during embryogenesis is found in cells forming the nervous system and in adult animals in the brain. ii) PP2A is thought to be involved in the regulation of microtubule assembly and disassembly during neurulation and has been shown to be able to associate with microtubules (Sontag et al. 1995). iii) Responsible for the folding of the neural tube are cell shape changes which are microtubule dependent. Taken all these data together it can be suggested that PPP2Cα is necessary for the onset of gastrulation and mesoderm formation and might play an important role in the maintenance of neural tissues, probably by regulating the microtubule turnover during axonal transport of proteins (Gotz and Kues 1999).

14-3-3 proteins were the first signalling molecules to be identified as discrete phosphoserine/threonine binding modules. The family of proteins plays critical roles in cell signalling events that control progress through the cell cycle, transcriptional alterations in response to environmental cues and programmed cell death (Yaffe 2002). 14-3-3 proteins are known to interact with a number of proteins involved in the regulation of cell signalling. Deletion of 14-3-3ε in humans leads to Miller-Dieker Syndrome. Mice deficient for 14-3-3ε have defects in brain development and neuronal migration (Toyo-oka et al. 2003). 14-3-3s are mostly ubiquitously expressed but all seven mammalian isoforms are expressed in the brain (Yaffe 2002). They represent adaptor and scaffolding proteins that interact with proteins containing distinct phosphoserine/threonine motifs (Oksvold et al. 2004). Two optimal motifs have been identified: RSXpS/pTXP and RXXXpS/pTXP with X representing arbitrary amino acids and pS/pT representing the phosphoserine or phosphothreonine in the motif (Yaffe 2002; Oksvold et al. 2004). However they can also form complexes with proteins containing different phosphorylated motifs (Oksvold et al. 2004). 14-3-3 proteins can regulate their binding partners by altering their intracellular localization, catalytic activity or complex formation with other proteins (Tzivion and Avruch 2002; Yaffe 2002).

In the *Dll1* mutant 14-3-3ε and 14-3-3ζ were downregulated. It has been shown that these two proteins can form heterodimers (Jones et al. 1995) and that loss of 14-3-3ζ in Drosophila leads to embryonic lethality (Yaffe 2002). It might be possible that 14-3-3ε or 14-3-3ζ or the heterodimeric version of the two proteins could bind to Delta/Notch pathway members and thus influence, e.g., their intracellular localization. Binding of substrates to 14-3-3 proteins

induce conformational changes that might facilitate subcellular relocalisation by deforming and/or masking of nuclear localization signals (NLS) or nuclear export signals (NES) (Yaffe 2002). To check for possible interactions the serine/threonine motif was searched *in silico* in the ligand proteins (Dll1, Dll3, Dll4, Jag1, Jag2) and the receptors (Notch1-4) and the likelihood for phosphorylation assessed using the NetPhos 2.0 Server (http://www.cbs.dtu.dk/services/NetPhos/) (Blom et al. 1999). The ligands and receptors were chosen because after activation of the ligands and receptors the intracellular domains need to be transferred to the nucleus and maybe other cellular compartments. The mechanisms of translocation involved in the Delta/Notch pathway are not known. In the Dll1, Dll4, Jag1, Jag2 and Notch2 sequences no motif was found. In the Dll3, Notch1 and Notch3 polypeptide sequences the motifs could be found but only the one in the Notch3 sequence is likely to be phosphorylated according to the NetPhos analysis. This suggests that binding to Delta/Notch members would either be promoted by binding to other phosphorylated motifs, non-phosphorylated sites or might involve other components of the pathway than the ligands and receptors.

14-3-3 proteins bind to phosphoserine/threonine motifs while PP2A dephosphorylates phosphoserines and phosphothreonines. This could lead to a hypothesis of interaction. PP2A can be switched "on" and "off" through regulation of the subunit composition (Sontag 2001). In an "on" state PP2A dephosphorylates phosphoserine or –threonine containing proteins leading to non-phosphorylated proteins which would inhibit the binding of 14-3-3 proteins. Thus regulation of intracellular localization would be diminished. In an "off" state of PP2A substrates would not be dephosphorylated what would enable 14-3-3 proteins to bind and translocate the substrates or regulate their catalytic activity.

A similar mechanism has been proposed for the NUDEL protein which can bind to 14-3-3ε in a phosphorylated state and thus is protected from dephosphorylation by PP2A (Toyo-oka et al. 2003). In the *Dll1* mutant the core catalytic subunit of PP2A is downregulated which suggests that PP2A function might be altered similar as if it was in an "off" state. This deregulation could lead to increased amounts of phosphorylated substrates for 14-3-3 proteins. However it seems likely that the amount of phosphorylated target needed in the cell is limited. This in turn could lead to a downregulation of 14-3-3 proteins to avoid interaction and regulation of too many target proteins. This hypothesis would be in agreement with the observation of the downregulation of PPP2ACα, 14-3-3ε and 14-3-3ζ. However, it has been shown that 14-3-3ζ can also bind to non-phosphorylated targets such as the EGF receptor (Oksvold et al. 2004). It is not known so far if the other six 14-3-3 isoforms also can bind non-phosphorylated substrates.

As in this section much emphasis has been laid on phosphatases it should not be forgotten that kinases also play important roles in directed trafficking of proteins between various locations within cells. *Csk*, a member of the Src family kinases (SFKs) was upregulated in the *Dll1* mutant. *Csk* is a gene coding for a non-receptor protein tyrosine kinase involved in intracellular trafficking processes (Avrov and Kazlauskas 2003). SFKs have been brought into context with ligand-stimulated internalization of growth factors such as platelet derived growth factor receptor alpha and beta (Pdgfrα, Pdgfrβ) and epidermal growth factor receptor (EGFR) (Avrov and Kazlauskas 2003). Furthermore it has been shown that overexpression of *Csk* promotes the internalization of the EGFR (Ware et al. 1997). This might also be the

case in the *Dll1* mutant since Csk is upregulated. Additionally the alteration in *Csk* expression might influence the internalization of Pdgfrα which was found to be downregulated.

The upregulation of *Csk* is suggested to disturb intracellular trafficking as higher expression of a kinase might result in more phosphorylated protein than in the wt. Thus two misregulations were observed, the upregulation of the kinase *Csk* and the downregulation of the phosphatase PP2A, that both would increase the amount of phosphorylated proteins in the cell. However, it is not clear if these enzymes have the same targets or are located in the same cells but disrupted expression of opposing enzymes both involved in intracellular trafficking suggest that this cellular process is altered.

The cytoskeleton is essential for asymmetry in cells

Further aspects of intracellular trafficking include the establishment and maintenance of cell asymmetry. These mechanisms often involve the cytoskeleton. Specificity of PP2A signalling is dependent on specific protein-protein interactions. The interaction with paxillin, vimentin and tubulin which are all filament proteins direct selective holoenzymes to discrete cellular domains (i.e. focal adhesions, intermediate filaments, microtubules or the Golgi apparatus) (Sontag et al. 1995; Hiraga and Tamura 2000; Lechward et al. 2001). In the *Dll1*^{-/-} embryos γ-tubulin as a member of the tubulin family and *nestin* as an intermediate filament protein are downregulated. γ-tubulin which is a protein related to α/β-tubulin is the key protein responsible for microtubule nucleation in vivo (Moritz and Agard 2001). Cytosolic γ-tubulin is found in two major complexes: the large γ-tubulin ring complex (γTuRC) and the γ-tubulin small complex (γTuSC) (Moritz and Agard 2001). γTuRC consists of an even number of γ-tubulin molecules and caps the minus end of microtubules. Thus it nucleates microtubules but also has a separate capping activity that may be very important for modulating microtubule minus-end dynamics (Moritz and Agard 2001). *Nestin* expression was lost in the neuroepithelium (Figure 11, p. 62) which is in good agreement with the known facts that 14-3-3 proteins as well as PP2A play important roles in the development of the nervous system (Gotz and Kues 1999; Yaffe 2002). The downregulation of tubulin and intermediate filaments might influence the possibility to establish and/or maintain cell asymmetry since it is known that deregulation of PP2A leads to defects in the actin and microtubule cytoskeleton (Sontag 2001).

Additionally 14-3-3ε has been shown to be involved in very early left-right determination during amphibian embryogenesis. In the unfertilized egg 14-3-3ε is expressed in a tight spot in the centre of the egg while at the two-cell stage it is strongly expressed in one blastomere only (Bunney et al. 2003). Injection of a large amount of 14-3-3ε mRNA into one-cell embryos resulted in heterotaxia (Bunney et al. 2003) indicating that the distribution of 14-3-3ε mRNA is essential for proper left-right development. Different hypotheses for asymmetric localization mechanisms of 14-3-3ε have been proposed. These include differential degradation, anchoring or directed transport by motor proteins. In the *Dll1* mutant determination of left-right development is randomized (Krebs et al. 2003; Przemeck et al. 2003). The mechanisms leading to this phenotype are not exactly clear although it has been reported that the structure of the node, which is believed to play a role in establishing asymmetry in the embryo, is disrupted (Krebs et al. 2003; Przemeck et al. 2003). It might be

possible that left-right development in mammals starts much earlier than has been thought and that asymmetric expression in very early embryos determines the body axis as it is observed in amphibians.

Intracellular membrane trafficking is altered in Dll1 mutants

Intracellular trafficking can also be obtained through vesicular transport. Transport vesicles and tubovesicular structures are utilized to deliver cargo proteins and lipids from one internal compartment to another (Gerst 2003). To assure specific transport from, e.g., ER to Golgi, from Golgi to lysosome or from Golgi to the plasma membrane distinct combinations of mutually recognizable factors are necessary (Gerst 2003). SNAREs (soluble N-ethylmaleimide-sensitive fusion protein attachment protein receptors) comprise three conserved families of membrane-associated proteins (e.g. the Synaptobrevin/VAMP, Syntaxin and SNAP-25/light chain families) that act late in the events involving tight docking and subsequent fusion of membrane bilayers (Bennett and Scheller 1993; Rothman and Warren 1994). Members of the three families assemble into a complex *in trans* that bridges membranes (Rothman and Warren 1994). The SNARE complex is a parallel four-helix bundle with one helix contributed by Syntaxin, one by VAMP and two contributed by SNAP-25 (Sutton et al. 1998). This *trans*-membrane complex with VAMP on the transport vesicle and Syntaxin and SNAP-25 on the target membrane is supposed to lead to the fusion of the two membranes which results in a *cis*-membrane complex (Stewart et al. 2001). In a next step the *cis*-residing protein complexes need to be broken apart to make those proteins available for further *trans*-complex formation (Stewart et al. 2001). The breakdown of the complex occurs by the action of the ATPase Nsf (Malhotra et al. 1988). Nsf is a key component of the membrane trafficking machinery in Drosophila (Stewart et al. 2001). It contains two nucleotide binding domains and strong ATPase activity (Stewart et al. 2001). The role of Nsf in vesicular transport appears to be primarily one of priming vesicles for fusion and dissociation of SNARE complexes to permit their recycling (Stewart et al. 2001). Nsf-dependent ATP hydrolysis is required to disassemble SNARE complexes. In Drosophila two homologues of Nsf exist: dNSF1 and dNSF2. While dNSF1 is primarily expressed in neurons, dNSF2 is additionally expressed in non-neural tissues such as the imaginal disc, salivary gland and the ring gland (Ordway et al. 1994; Boulianne and Trimble 1995). Expression of a dominant negative form of dNSF2 in the marginal zone of the wing disc results in a notched-wing phenotype which is enhanced when combined with mutations of VAMP/Synaptobrevin or Syntaxin as well as mutations in the *wingless* gene or components of the Delta/Notch signalling pathway (Stewart et al. 2001). These findings suggest that the Wnt-pathway as well as the Notch pathway is disrupted by the loss of dNSF2 (Stewart et al. 2001).

The mammalian homologue of Drosophila NSF was downregulated in *Dll1* loss-of-function mutants. This could implicate that SNARE-mediated membrane trafficking processes are altered especially concerning the dissociation of SNARE complexes. Further evidence for disruption of SNARE-dependent signalling comes from the finding that Munc18-3 (also called Stxbp3, munc-18c), a homologue of the Yeast Sec1 and SNARE regulator, involved in all trafficking steps and necessary for maintenance of SNAREs in their active conformation after disassembly (GERST, 2003) is also downregulated in the *Dll1* mutant.

7.3.3 Developmental processes altered by *Dll1* deficiency

Novel transcription factors involved in Delta/Notch signalling?

Regulation of transcription is an important feature in most developmental processes. In the Delta/Notch signalling pathway some downstream targets of *Notch1* are transcription factors. The transcriptome analysis identified four transcription factors which have not been shown to be involved in the Delta/Notch signalling cascade before.

Hmx2 is a member of the evolutionary conserved homeobox containing *Hmx* gene family. The family which contains three members (*Hmx1-3*) might play a role in regional specification and cell fate determination in the inner ear and is expressed in the nervous system in mice and Drosophila (Wang et al. 2000). Common expression domains shared by the *Hmx* genes are the first and second branchial arches, central and peripheral nervous system, and the uterus. At E10.5 *Hmx2* shows its first expression in the central nervous system of the mouse. It can be found in several regions of the developing brain such as the future hypothalamus, pons, ganglionic eminence, medulla oblongata, chord invagination and the choroid plexus in the myelencephalon (Wang et al. 2000). *Hmx2* is also expressed in the developing inner ear (Wang et al. 2004). Mice deficient for *Hmx2* display severe defects in the gross morphology of the inner ear while no overt defect in the nervous system can be observed (Wang et al. 2004). This might be due to a functional redundancy of *Hmx2* and *Hmx3* which are expressed in the same tissues at the same time (Wang et al. 2004).

Delta/Notch signalling plays an important role during development of the nervous system (Lewis 1998; Baker 2000; Lutolf et al. 2002) and also during formation of the sensory hair in the inner ear (Kiernan et al. 2001). At E10.5 *Dll1* is expressed in the tail tip, psm, caudal half of the 12-14 posteriormost somites, brain vesicles, neural tube, neural crest, dorsal root ganglia, optic and otic vesicles, in scattered cells of the nasal placode and in ectodermal placodes overlaying the developing craniofacial ganglia VIII-X (Bettenhausen et al. 1995). Expression of Delta/Notch pathway genes and *Hmx2* in overlapping regions of the developing embryo such as the brain, the neural tube and the otic vesicles might indicate a potential role of the transcription factor in the pathway. Furthermore until now only the processes in the receiving cell have been analysed in detail. Only recently it is becoming clear that signal transduction into the nucleus of the Delta expressing cell might also occur (Pfister et al. 2003b; Six et al. 2004; Wright et al. 2004).

Lhx3 is a transcription factor of the family of LIM homeobox genes. In cells undergoing neurogenesis *Lhx3* is important for specification of motor neurons and V2 interneurons in the ventral neural tube (Sander et al. 2000; Thaler et al. 2002). Combinatorial expression of homeodomain and bHLH transcription factors is necessary for the specification of distinct cell types (Thor et al. 1999; Thaler et al. 2002; Lee and Pfaff 2003). Sole expression of *Lhx3* leads to differentiation into V2 interneurons while expression of *Lhx3* together with *Isl1*, another LIM homeodomain DNA binding protein, leads to differentiation into motorneurons (Thaler et al. 2002; Lee and Pfaff 2003).

Lhx3 was downregulated in the *Dll1* mutants. This is in good agreement with the results that in *Dll1* mutant embryos the amount of V2 interneurons is reduced at the expense of motor neurons (Przemeck, unpublished results). It could also been shown that *Isl1* expression is upregulated which also directs the differentiation into the direction of motor neurons.

Tlx1 (also known as *Hox11*) is a member of the homeobox containing transcription factors. It is expressed at E10.5 in the peripheral margins of the trigeminal and the facioacustic ganglia and the glossopharyngeal ganglion, as well as in the 1st-4th branchial arches, the surface ectoderm and central mesenchyme of mandibular and hyroid arches and in the developing spinal chord (Raju et al. 1993). Further expression analysis showed that *Tlx1* marks subpopulations of cells destined to give rise to specific components of the tongue and mandibular primordial (Raju et al. 1993). At E10.5 *Tlx1* was downregulated in the mutant indicating that the development of branchial arches and subsequent structures might be altered.

Migration of neural crest cells is disrupted

Although the role of *Delta* in Drosophila neurogenesis has been established a long time ago (Rebay et al. 1991; Muskavitch 1994; Artavanis-Tsakonas et al. 1995) the exact function of *Dll1* during neurogenesis in the mouse is still not defined. Studies of the ventral neural tube of *Dll1* mutant embryos showed that markers for ventral interneurons are downregulated while markers for ventral motorneurons are upregulated. The motorneuron markers can be detected earlier and with a higher level than in wt control embryos (unpublished results; Przemeck, Hrabe de Angelis, personal communication). Further studies on *Dll1* loss-of-function mouse embryos revealed that the number of neural crest cells is reduced and neural crest migration is severely disrupted. The reduction of neural crest cells could be confirmed with wish for *nestin*, an intermediate filament protein expressed in the neuroepithelium of the neural tube, migrating neural crest cells and dorsal root ganglia (Dahlstrand et al. 1995; Lutolf et al. 2002). Furthermore a diminution of neurons and glia in peripheral ganglia was observed (De Bellard et al. 2002). Normally neural crest cells migrate from the dorsal neural tube through the rostral part of the somites due to restrictions by ephrinB2 expression in the caudal part of the somites. This mechanism is disrupted in *Dll1* mutants with the consequence that neural crest cells migrate through the complete somite rather than selectively through the rostral part (De Bellard et al. 2002). These findings suggest that *Dll1* is essential for proper migration and differentiation of neural crest cells (De Bellard et al. 2002) and that it has different functions in different neuronal cell populations.

Except for ephrins a number of molecules have been shown to be involved in neural crest and/or axonal guidance. All members contain a conserved domain of 500 amino acids and 16 conserved cysteins, the so called semaphorin domain. Among those is *Semaphorin3A* (Eickholt et al. 1999). With the DNA-chip experiments another member of the semaphorin family, *Semaphorin5B,* was identified to be downregulated in the *Dll1$^{-/-}$* embryos. *Sema5b* is likely to encode an integral membrane protein containing seven thrombospondin repeats but no Ig motif. As described by Adams et al. 1996 semaphorins have been shown to be involved in axonal guidance the exact role of *Sema5B* remains to be determined.

Wish of wt, *Dll1$^{-/-}$*, *Dll3$^{pu/+}$* and *Dll3$^{pu/pu}$* embryos (Figure 13, p. 70) was performed to analysed the expression pattern of *Sema5B* in Delta/Notch pathway mutants. In the wt strong expression was observed in the neuroepithelium of the neural tube which could indicate a function of *Sema5B* in initiating or directing the emigration of postmitotic neuroblasts from the ventricular zone of the neural tube (Adams et al. 1996). In the *Dll1* mutant the expression was severely downregulated and in the *Dll3* mutants it was downregulated but not to the

same extend. As shown by de Bellard et al. reduced neurogenesis in the *Dll1* mutants is represented by a reduced number of neural crest cells (De Bellard et al. 2002). The analysis of ventral neural tube revealed that some neuron classes differentiate earlier than normal. If this might be also the case for neural crest cells they might already have migrated out of the neural tube by E10.5. *Sema5B* expression is downregulated after cells leave the ventricular zone (Adams et al. 1996). To check if the migration process is finished earlier than in the wt wish at earlier developmental stages, e.g. E9.5 would need to be done.

It is not known if *Sema5B* or *Sema3A* lie downstream of *Dll1* or how they are regulated. However, if *Dll1* was upstream of *Sema5B* the loss of *Dll1* could lead to a downregulation of *Sema5B* which might subsequently lead to misguided neural crest cells or axons from commissural neurons in the neural tube, which could extend into the neuroepithelium (Adams et al. 1996). Staining for neurofilaments could help to answer this question.

Is Ifitm1 a novel gene relevant for somitogenesis?

The involvement of Delta/Notch signalling during somitogenesis has been intensely studied (Conlon et al. 1995; Hrabe de Angelis et al. 1997; Evrard et al. 1998; Forsberg et al. 1998a; Gossler and Hrabe de Angelis 1998; Zhang and Gridley 1998; Dale and Pourquie 2000; Rawls et al. 2000; Saga and Takeda 2001; Baron et al. 2002; Schweisguth 2004). Many genes have been identified which are expressed in the somites, somitic compartments or the presomitic mesoderm and which are altered when either the Delta/Notch pathway or the Wnt pathway is disrupted (Barrantes et al. 1999; Beckers et al. 2000; Jiang et al. 2000; Jouve et al. 2000; Aulehla et al. 2003; Galceran et al. 2004; Hofmann et al. 2004). Besides it has been shown that for the proper functioning of the segmentation clock Delta/Notch and Wnt signalling is essential (Aulehla et al. 2003; Galceran et al. 2004; Hofmann et al. 2004). However it is still not clear which factors are responsible for the coordinated budding of somites and how this process is regulated. *Ifitm1* which was only recently identified as a marker for primordial germ cells (Tanaka and Matsui 2002; Lange et al. 2003), showed strong expression in the tail tip, psm and the latest somites in the wt. This expression was strongly reduced in *Dll1* mutants as the expression level was reproducibly lower, expression in the tail tip and somites was lost and the expression domain in the psm was smaller than in control embryos (Figure 11w, x, p. 62). This result suggests that *Ifitm1* is regulated by components of the Delta/Notch pathway. It seems unlikely that *Ifitm1* is a direct downstream target of *Dll1* because in this case the expression should be completely lost in the *Dll1* mutant. *In situ* hybridisation with mice carrying mutations in the *Dll3* and the *Jag1* gene also revealed reduced expression (Figure 13, p. 70). Thus it could be clearly shown that *Ifitm1* expression is dependant on Delta/Notch signalling.

To test whether *Ifitm1* shows cyclic expression in the wt numerous embryos were analysed. Although the expression slightly differs in the number of somites showing expression no clear evidence for cyclic expression could be observed which could indicate that *Ifitm1* represents rather a coordinator of the segmentation clock than an executing gene.

To assess the exact function of *Ifitm1* a targeting construct to knockout the gene was cloned. It is not clear which phenotype could be expected since very little is known about *Ifitm1*. However, it remains the possibility that the knockout might be embryonic lethal since *Ifitm1* has been shown to be expressed in primordial germ cells (PGCs). *Ifitm1* seems to be

involved in the acquisition of germ cell competence in epiblast cells which happens around E6.5 (Tanaka and Matsui 2002; Lange et al. 2003). Thus a conditional knockout might help to overcome this problem. The design of a cloning strategy is in progress.

Is differential protein expression due to developmental retardation of Dll1 mutants?

An obvious phenotypically difference between wt and *Dll1* mutant embryos is that mutants are in general smaller compared to wt littermates. In some aspects mutant embryos even seem to be retarded in their development. Although littermates have been selected for the analyses slight differences in their developmental stage might be possible. Greene *et al.* performed a study in which the proteomes of E8.5, E9.5 and E10.5 embryos were compared to analyse changes in the protein composition of an embryo during neural tube closure (Greene et al. 2002). Between E8.5 and E10.5 major developmental events occur such as the formation of the neural tube, embryonic turning, formation of differentiated somites and extensive remodelling of the heart. Proteins differentially expressed between the developmental stages and proteins not regulated between the stages were isolated and characterised (Greene et al. 2002). Interestingly a number of proteins found by Greene *et al.* were also identified in the analysis of *Dll1* mutant and wt embryos. Proteins differentially expressed in the analysis of Greene *et al.* and *Dll1* mutants are Hemoglobin zeta chain, Afp and GRP78. This might indicate that these proteins are regulated due to differences in the stage of development. Additionally further proteins were identified in both analyses that belong to the same gene families such as Atp5b/Atp5h, Vimentin/Nestin and α-tubulin/γ-tubulin. This finding suggests that these proteins are regulated in a tight temporal manner, and that slight changes in the developmental stage influence the expression. Greene *et al.* also isolated proteins that showed constant expression between E8.5-E10.5. Interestingly in the analysis of *Dll1*$^{-/-}$ embryos also proteins from this category were identified. These were Calr, eIF3 and Pkm2. This, however, might indicate that the regulation of those proteins in the *Dll1* mutant is due to the loss-of-function phenotype.

These results demonstrate the importance of exact staging of embryos which should be used for either transcriptomics or proteomics analyses as even slight differences in the developmental stage might influence the results.

8 Outlook

Taken the results from the transcriptome and proteome analyses together it can be suggested that in future studies of Delta/Notch signalling more emphasis should be put on investigations of cellular processes such as chromatin remodelling, intracellular transport and trafficking, regulated degradation processes and post-transcriptional, reversible regulation through protein kinases and phosphatases and transcription factor activity as well as the combination of these processes.

Thus in-depth analysis of targets and interaction partners of the identified genes and proteins should be performed. Furthermore, detailed biochemical studies of the regulation of phosphorylation and dephosphorylation might help to understand the regulatory processes not only in the context of Delta/Notch signalling but also in the context of numerous other developmental biology related questions. As for the understanding of Delta/Notch signal transduction the analysis of the identified transcription factors might give insights on the events happening in the Delta expressing (signalling) cell.

Furthermore it could be shown that RNA- and protein expression profiling are different approaches complementing each other. Thus it was possible to gain new insights which would not have been possible with one approach alone.

The functional analysis of *Ifitm1* using gene targeting technology will help in the understanding of the *Ifitm1* gene function during embryonic development. Phenotypic studies including skeletal preparations, histological sections and stainings as well as *in situ* hybridisations might clarify *Ifitm1*'s position in the Delta/Notch signalling pathway.

For future transcriptome studies it could be important to analyse subsets of cells or specific compartments of a tissue or even single cells independently from a whole biological system. Thus laser microdissection will become an important method. Improvements of RNA amplification techniques or the production of microarrays (DNA or protein) where only minute amount of starting materials would be necessary as starting material will further support the laser microdissection approach.

9 Literature

Adams, R.H., H. Betz, and A.W. Puschel. 1996. A novel class of murine semaphorins with homology to thrombospondin is differentially expressed during early embryogenesis. *Mech Dev* **57**: 33-45.

Anderson, P. 1995. Mutagenesis. *Methods Cell Biol* **48**: 31-58.

Apelqvist, A., H. Li, L. Sommer, P. Beatus, D.J. Anderson, T. Honjo, M. Hrabe de Angelis, U. Lendahl, and H. Edlund. 1999. Notch signalling controls pancreatic cell differentiation. *Nature* **400**: 877-81.

Appel, B. and J.S. Eisen. 1998. Regulation of neuronal specification in the zebrafish spinal cord by Delta function. *Development* **125**: 371-80.

Armstrong, J.A. and B.M. Emerson. 1998. Transcription of chromatin: these are complex times. *Curr Opin Genet Dev* **8**: 165-72.

Artavanis-Tsakonas, S., K. Matsuno, and M.E. Fortini. 1995. Notch signaling. *Science* **268**: 225-32.

Artavanis-Tsakonas, S., M.D. Rand, and R.J. Lake. 1999. Notch signaling: cell fate control and signal integration in development. *Science* **284**: 770-6.

Asano, K., T.G. Kinzy, W.C. Merrick, and J.W. Hershey. 1997. Conservation and diversity of eukaryotic translation initiation factor eIF3. *J Biol Chem* **272**: 1101-9.

Ashburner, M. 1982. The genetics of a small autosomal region of Drosophila melanogaster containing the structural gene for alcohol dehydrogenase. III. Hypomorphic and hypermorphic mutations affecting the expression of hairless. *Genetics* **101**: 447-59.

Aulehla, A. and R.L. Johnson. 1999. Dynamic expression of lunatic fringe suggests a link between notch signaling and an autonomous cellular oscillator driving somite segmentation. *Dev Biol* **207**: 49-61.

Aulehla, A., C. Wehrle, B. Brand-Saberi, R. Kemler, A. Gossler, B. Kanzler, and B.G. Herrmann. 2003. Wnt3a plays a major role in the segmentation clock controlling somitogenesis. *Dev Cell* **4**: 395-406.

Avrov, K. and A. Kazlauskas. 2003. The role of c-Src in platelet-derived growth factor alpha receptor internalization. *Exp Cell Res* **291**: 426-34.

Baker, N.E. 2000. Notch signaling in the nervous system. Pieces still missing from the puzzle. *Bioessays* **22**: 264-73.

Balling, R. 2001. ENU mutagenesis: analyzing gene function in mice. *Annu Rev Genomics Hum Genet* **2**: 463-92.

Barnes, J.A. and I.W. Smoak. 2000. Glucose-regulated protein 78 (GRP78) is elevated in embryonic mouse heart and induced following hypoglycemic stress. *Anat Embryol (Berl)* **202**: 67-74.

Baron, M. 2003. An overview of the Notch signalling pathway. *Semin Cell Dev Biol* **14**: 113-9.

Baron, M., H. Aslam, M. Flasza, M. Fostier, J.E. Higgs, S.L. Mazaleyrat, and M.B. Wilkin. 2002. Multiple levels of Notch signal regulation (review). *Mol Membr Biol* **19**: 27-38.

Barrantes, I.B., A.J. Elia, K. Wunsch, M.H. Hrabe de Angelis, T.W. Mak, J. Rossant, R.A. Conlon, A. Gossler, and J.L. de la Pompa. 1999. Interaction between Notch signalling

and Lunatic fringe during somite boundary formation in the mouse. *Curr Biol* **9**: 470-80.

Beckers, J., F. Herrmann, S. Rieger, A.L. Drobyshev, M. Horsch, M. Hrabe de Angelis, and B. Seliger. 2004. Identification and validation of novel ERBB2 (HER2, NEU) targets including genes involved in angiogenesis. *Int J Cancer*.

Beckers, J., N. Schlautmann, and A. Gossler. 2000. The mouse rib-vertebrae mutation disrupts anterior-posterior somite patterning and genetically interacts with a Delta1 null allele. *Mech Dev* **95**: 35-46.

Beddington, R.S. and E.J. Robertson. 1999. Axis development and early asymmetry in mammals. *Cell* **96**: 195-209.

Beier, D.R. and B.J. Herron. 2004. Genetic mapping and ENU mutagenesis. *Genetica* **122**: 65-9.

Beissbarth, T., K. Fellenberg, B. Brors, R. Arribas-Prat, J. Boer, N.C. Hauser, M. Scheideler, J.D. Hoheisel, G. Schutz, A. Poustka, and M. Vingron. 2000. Processing and quality control of DNA array hybridization data. *Bioinformatics* **16**: 1014-22.

Bennett, M.K. and R.H. Scheller. 1993. The molecular machinery for secretion is conserved from yeast to neurons. *Proc Natl Acad Sci U S A* **90**: 2559-63.

Bessho, Y., H. Hirata, Y. Masamizu, and R. Kageyama. 2003. Periodic repression by the bHLH factor Hes7 is an essential mechanism for the somite segmentation clock. *Genes Dev* **17**: 1451-6.

Bessho, Y. and R. Kageyama. 2003. Oscillations, clocks and segmentation. *Curr Opin Genet Dev* **13**: 379-84.

Bessho, Y., G. Miyoshi, R. Sakata, and R. Kageyama. 2001a. Hes7: a bHLH-type repressor gene regulated by Notch and expressed in the presomitic mesoderm. *Genes Cells* **6**: 175-85.

Bessho, Y., R. Sakata, S. Komatsu, K. Shiota, S. Yamada, and R. Kageyama. 2001b. Dynamic expression and essential functions of Hes7 in somite segmentation. *Genes Dev* **15**: 2642-7.

Bettenhausen, B., M. Hrabe de Angelis, D. Simon, J.L. Guenet, and A. Gossler. 1995. Transient and restricted expression during mouse embryogenesis of Dll1, a murine gene closely related to Drosophila Delta. *Development* **121**: 2407-18.

Blaumueller, C.M., H. Qi, P. Zagouras, and S. Artavanis-Tsakonas. 1997. Intracellular cleavage of Notch leads to a heterodimeric receptor on the plasma membrane. *Cell* **90**: 281-91.

Blom, N., S. Gammeltoft, and S. Brunak. 1999. Sequence and structure-based prediction of eukaryotic protein phosphorylation sites. *J Mol Biol* **294**: 1351-62.

Boulianne, G.L. and W.S. Trimble. 1995. Identification of a second homolog of N-ethylmaleimide-sensitive fusion protein that is expressed in the nervous system and secretory tissues of Drosophila. *Proc Natl Acad Sci U S A* **92**: 7095-9.

Bresnick, E.H., J. Chu, H.M. Christensen, B. Lin, and J. Norton. 2000. Linking Notch signaling, chromatin remodeling, and T-cell leukemogenesis. *J Cell Biochem Suppl* **Suppl 35**: 46-53.

Brou, C., F. Logeat, N. Gupta, C. Bessia, O. LeBail, J.R. Doedens, A. Cumano, P. Roux, R.A. Black, and A. Israel. 2000. A novel proteolytic cleavage involved in Notch signaling: the role of the disintegrin-metalloprotease TACE. *Mol Cell* **5**: 207-16.

Brown, S.D. and P.M. Nolan. 1998. Mouse mutagenesis-systematic studies of mammalian gene function. *Hum Mol Genet* **7**: 1627-33.

Brownell, J.E., J. Zhou, T. Ranalli, R. Kobayashi, D.G. Edmondson, S.Y. Roth, and C.D. Allis. 1996. Tetrahymena histone acetyltransferase A: a homolog to yeast Gcn5p linking histone acetylation to gene activation. *Cell* **84**: 843-51.

Bukau, B. and A.L. Horwich. 1998. The Hsp70 and Hsp60 chaperone machines. *Cell* **92**: 351-66.

Bulman, M.P., K. Kusumi, T.M. Frayling, C. McKeown, C. Garrett, E.S. Lander, R. Krumlauf, A.T. Hattersley, S. Ellard, and P.D. Turnpenny. 2000. Mutations in the human delta homologue, DLL3, cause axial skeletal defects in spondylocostal dysostosis. *Nat Genet* **24**: 438-41.

Bunney, T.D., A.H. De Boer, and M. Levin. 2003. Fusicoccin signaling reveals 14-3-3 protein function as a novel step in left-right patterning during amphibian embryogenesis. *Development* **130**: 4847-4858.

Buttitta, L., T.S. Tanaka, A.E. Chen, M.S. Ko, and C.M. Fan. 2003. Microarray analysis of somitogenesis reveals novel targets of different WNT signaling pathways in the somitic mesoderm. *Dev Biol* **258**: 91-104.

Cabrera, C.V. 1990. Lateral inhibition and cell fate during neurogenesis in Drosophila: the interactions between scute, Notch and Delta. *Development* **110**: 733-42.

Campos-Ortega, J.A. and E. Knust. 1990. Molecular analysis of a cellular decision during embryonic development of Drosophila melanogaster: epidermogenesis or neurogenesis. *Eur J Biochem* **190**: 1-10.

Capobianco, A.J., P. Zagouras, C.M. Blaumueller, S. Artavanis-Tsakonas, and J.M. Bishop. 1997. Neoplastic transformation by truncated alleles of human NOTCH1/TAN1 and NOTCH2. *Mol Cell Biol* **17**: 6265-73.

Cecconi, F. and B.I. Meyer. 2000. Gene trap: a way to identify novel genes and unravel their biological function. *FEBS Lett* **480**: 63-71.

Chitnis, A., D. Henrique, J. Lewis, D. Ish-Horowicz, and C. Kintner. 1995. Primary neurogenesis in Xenopus embryos regulated by a homologue of the Drosophila neurogenic gene Delta [see comments]. *Nature* **375**: 761-6.

Choi, Y.I., S.H. Jeon, J. Jang, S. Han, J.K. Kim, H. Chung, H.W. Lee, H.Y. Chung, S.D. Park, and R.H. Seong. 2001. Notch1 confers a resistance to glucocorticoid-induced apoptosis on developing thymocytes by down-regulating SRG3 expression. *Proc Natl Acad Sci U S A* **98**: 10267-72.

Christoffolete, M.A., C.C.G. Linardi, L. de Jesus, K.N. Ebina, S.D. Carvalho, M.O. Ribeiro, R. Rabelo, C. Curcio, L. Martins, E.T. Kimura, and A.C. Bianco. 2004. Mice with Targeted Disruption of the Dio2 Gene Have Cold-Induced Overexpression of the Uncoupling Protein 1 Gene but Fail to Increase Brown Adipose Tissue Lipogenesis and Adaptive Thermogenesis. *Diabetes* **53**: 577-584.

Ciechanover, A. 1998. The ubiquitin-proteasome pathway: on protein death and cell life. *Embo J* **17**: 7151-60.

Clemens, M.J., M. Bushell, I.W. Jeffrey, V.M. Pain, and S.J. Morley. 2000. Translation initiation factor modifications and the regulation of protein synthesis in apoptotic cells. *Cell Death Differ* **7**: 603-15.

Coffman, C., W. Harris, and C. Kintner. 1990. Xotch, the Xenopus homolog of Drosophila notch. *Science* **249**: 1438-41.

Cohen, P. 1989. The structure and regulation of protein phosphatases. *Annu Rev Biochem* **58**: 453-508.

Conlon, R.A., A.G. Reaume, and J. Rossant. 1995. Notch1 is required for the coordinate segmentation of somites. *Development* **121**: 1533-45.

Consortium, I.H.G.S. 2004. Finishing the euchromatic sequence of the human genome. *Nature* **431**: 931-45.

Cooke, J. and E.C. Zeeman. 1976. A clock and wavefront model for control of the number of repeated structures during animal morphogenesis. *J Theor Biol* **58**: 455-76.

Corbin, V., A.M. Michelson, S.M. Abmayr, V. Neel, E. Alcamo, T. Maniatis, and M.W. Young. 1991. A role for the Drosophila neurogenic genes in mesoderm differentiation. *Cell* **67**: 311-23.

Coux, O., K. Tanaka, and A.L. Goldberg. 1996. Structure and functions of the 20S and 26S proteasomes. *Annu Rev Biochem* **65**: 801-47.

Dahlstrand, J., M. Lardelli, and U. Lendahl. 1995. Nestin mRNA expression correlates with the central nervous system progenitor cell state in many, but not all, regions of developing central nervous system. *Brain Res Dev Brain Res* **84**: 109-29.

Dale, K.J. and O. Pourquie. 2000. A clock-work somite. *Bioessays* **22**: 72-83.

Danos, M.C. and H.J. Yost. 1995. Linkage of cardiac left-right asymmetry and dorsal-anterior development in Xenopus. *Development* **121**: 1467-74.

Davidson, B.P., S.J. Kinder, K. Steiner, G.C. Schoenwolf, and P.P. Tam. 1999. Impact of node ablation on the morphogenesis of the body axis and the lateral asymmetry of the mouse embryo during early organogenesis. *Dev Biol* **211**: 11-26.

De Bellard, M., W. Ching, A. Gossler, and M. Bronner-Fraser. 2002. Disruption of segmental neural crest migration and ephrin expression in delta-1 null mice. *Dev Biol* **249**: 121-130.

de Haan, J.B., M.J. Tymms, F. Cristiano, and I. Kola. 1994. Expression of copper/zinc superoxide dismutase and glutathione peroxidase in organs of developing mouse embryos, fetuses, and neonates. *Pediatr Res* **35**: 188-96.

de Moor, C.H. and J.D. Richter. 1999. Cytoplasmic polyadenylation elements mediate masking and unmasking of cyclin B1 mRNA. *Embo J* **18**: 2294-303.

De Strooper, B., W. Annaert, P. Cupers, P. Saftig, K. Craessaerts, J.S. Mumm, E.H. Schroeter, V. Schrijvers, M.S. Wolfe, W.J. Ray, A. Goate, and R. Kopan. 1999. A presenilin-1-dependent gamma-secretase-like protease mediates release of Notch intracellular domain. *Nature* **398**: 518-22.

Deftos, M.L., Y.W. He, E.W. Ojala, and M.J. Bevan. 1998. Correlating notch signaling with thymocyte maturation. *Immunity* **9**: 777-86.

Del Amo, F.F., D.E. Smith, P.J. Swiatek, M. Gendron-Maguire, R.J. Greenspan, A.P. McMahon, and T. Gridley. 1992. Expression pattern of Motch, a mouse homolog of Drosophila Notch, suggests an important role in early postimplantation mouse development. *Development* **115**: 737-44.

deLapeyriere, O., V. Ollendorff, J. Planche, M.O. Ott, S. Pizette, F. Coulier, and D. Birnbaum. 1993. Expression of the Fgf6 gene is restricted to developing skeletal muscle in the mouse embryo. *Development* **118**: 601-11.

Donato, R. 1999. Functional roles of S100 proteins, calcium-binding proteins of the EF-hand type. *Biochim Biophys Acta* **1450**: 191-231.

Dreyfuss, G., V.N. Kim, and N. Kataoka. 2002. Messenger-RNA-binding proteins and the messages they carry. *Nat Rev Mol Cell Biol* **3**: 195-205.

Drobyshev, A.L., Angelis M.H.d., and B. J. 2003a. Artefacts and Reliability of DNA Microarray Expression Profiling. *Current Genomics* **4**: 615-621.

Drobyshev, A.L., C. Machka, M. Horsch, M. Seltmann, V. Liebscher, M. Hrabe de Angelis, and J. Beckers. 2003b. Specificity assessment from fractionation experiments

(SAFE): a novel method to evaluate microarray probe specificity based on hybridisation stringencies. *Nucleic Acids Res* **31**: E1-1.

Duboule, D. 1994. Temporal colinearity and the phylotypic progression: a basis for the stability of a vertebrate Bauplan and the evolution of morphologies through heterochrony. *Dev Suppl*: 135-42.

Dubrulle, J., M.J. McGrew, and O. Pourquie. 2001. FGF signaling controls somite boundary position and regulates segmentation clock control of spatiotemporal Hox gene activation. *Cell* **106**: 219-32.

Dunwoodie, S.L., M. Clements, D.B. Sparrow, X. Sa, R.A. Conlon, and R.S. Beddington. 2002. Axial skeletal defects caused by mutation in the spondylocostal dysplasia/pudgy gene Dll3 are associated with disruption of the segmentation clock within the presomitic mesoderm. *Development* **129**: 1795-806.

Dunwoodie, S.L., D. Henrique, S.M. Harrison, and R.S. Beddington. 1997. Mouse Dll3: a novel divergent Delta gene which may complement the function of other Delta homologues during early pattern formation in the mouse embryo. *Development* **124**: 3065-76.

Dziadek, M. 1978. Modulation of alphafetoprotein synthesis in the early postimplantation mouse embryo. *J Embryol Exp Morphol* **46**: 135-46.

Dziadek, M. and E. Adamson. 1978. Localization and synthesis of alphafoetoprotein in post-implantation mouse embryos. *J Embryol Exp Morphol* **43**: 289-313.

Ehling, U.H., D.J. Charles, J. Favor, J. Graw, J. Kratochvilova, A. Neuhauser-Klaus, and W. Pretsch. 1985. Induction of gene mutations in mice: the multiple endpoint approach. *Mutat Res* **150**: 393-401.

Eickholt, B.J., S.L. Mackenzie, A. Graham, F.S. Walsh, and P. Doherty. 1999. Evidence for collapsin-1 functioning in the control of neural crest migration in both trunk and hindbrain regions. *Development* **126**: 2181-9.

Erkmann, J.A. and U. Kutay. 2004. Nuclear export of mRNA: from the site of transcription to the cytoplasm. *Exp Cell Res* **296**: 12-20.

Evrard, Y.A., Y. Lun, A. Aulehla, L. Gan, and R.L. Johnson. 1998. lunatic fringe is an essential mediator of somite segmentation and patterning. *Nature* **394**: 377-81.

Faisst, A.M., G. Alvarez-Bolado, D. Treichel, and P. Gruss. 2002. Rotatin is a novel gene required for axial rotation and left-right specification in mouse embryos. *Mech Dev* **113**: 15-28.

Fink, A.L. 1999. Chaperone-mediated protein folding. *Physiol Rev* **79**: 425-49.

Floss, T., H.H. Arnold, and T. Braun. 1997. A role for FGF-6 in skeletal muscle regeneration. *Genes Dev* **11**: 2040-51.

Forsberg, H., F. Crozet, and N.A. Brown. 1998a. Waves of mouse Lunatic fringe expression, in four-hour cycles at two- hour intervals, precede somite boundary formation. *Curr Biol* **8**: 1027-30.

-. 1998b. Waves of mouse Lunatic fringe expression, in four-hour cycles at two-hour intervals, precede somite boundary formation. *Curr Biol* **8**: 1027-30.

Fujinaga, M. 1997. Development of sidedness of asymmetric body structures in vertebrates. *Int J Dev Biol* **41**: 153-86.

Galceran, J., C. Sustmann, S.C. Hsu, S. Folberth, and R. Grosschedl. 2004. LEF1-mediated regulation of Delta-like1 links Wnt and Notch signaling in somitogenesis. *Genes Dev* **18**: 2718-23.

Gerst, J.E. 2003. SNARE regulators: matchmakers and matchbreakers. *Biochim Biophys Acta* **1641**: 99-110.

Gill, G. 2004. SUMO and ubiquitin in the nucleus: different functions, similar mechanisms? *Genes Dev* **18**: 2046-59.

Gossler, A. and M. Hrabe de Angelis. 1998. Somitogenesis. *Curr Top Dev Biol* **38**: 225-87.

Gotz, J. and W. Kues. 1999. The role of protein phosphatase 2A catalytic subunit Calpha in embryogenesis: evidence from sequence analysis and localization studies. *Biol Chem* **380**: 1117-20.

Grandbarbe, L., J. Bouissac, M. Rand, M. Hrabe de Angelis, S. Artavanis-Tsakonas, and E. Mohier. 2003. Delta-Notch signaling controls the generation of neurons/glia from neural stem cells in a stepwise process. *Development* **130**: 1391-402.

Greene, N.D., K.Y. Leung, R. Wait, S. Begum, M.J. Dunn, and A.J. Copp. 2002. Differential protein expression at the stage of neural tube closure in the mouse embryo. *J Biol Chem* **277**: 41645-51.

Greene, W.C. and L.F. Chen. 2004. Regulation of NF-kappaB action by reversible acetylation. *Novartis Found Symp* **259**: 208-17; discussion 218-25.

Greenwald, I. 1985. lin-12, a nematode homeotic gene, is homologous to a set of mammalian proteins that includes epidermal growth factor. *Cell* **43**: 583-90.

Gridley, T. 2003. Notch signaling and inherited disease syndromes. *Hum Mol Genet* **12**: R9-R13.

-. 2004. Kick it up a Notch: NOTCH1 activation in T-ALL. *Cancer Cell* **6**: 431-2.

Groenendyk, J., J. Lynch, and M. Michalak. 2004. Calreticulin, Ca2+, and calcineurin - signaling from the endoplasmic reticulum. *Mol Cells* **17**: 383-9.

Gullans, S.R. 2000. Of microarrays and meandering data points. *Nat Genet* **26**: 4-5.

Guo, K., G. Searfoss, D. Krolikowski, M. Pagnoni, C. Franks, K. Clark, K.T. Yu, M. Jaye, and Y. Ivashchenko. 2001. Hypoxia induces the expression of the pro-apoptotic gene BNIP3. *Cell Death Differ* **8**: 367-76.

Gygi, S.P., Y. Rochon, B.R. Franza, and R. Aebersold. 1999. Correlation between protein and mRNA abundance in yeast. *Mol Cell Biol* **19**: 1720-30.

Haddon, C., Y.J. Jiang, L. Smithers, and J. Lewis. 1998a. Delta-Notch signalling and the patterning of sensory cell differentiation in the zebrafish ear: evidence from the mind bomb mutant. *Development* **125**: 4637-44.

Haddon, C., L. Smithers, S. Schneider-Maunoury, T. Coche, D. Henrique, and J. Lewis. 1998b. Multiple delta genes and lateral inhibition in zebrafish primary neurogenesis. *Development* **125**: 359-70.

Halgren, R.G., M.R. Fielden, C.J. Fong, and T.R. Zacharewski. 2001. Assessment of clone identity and sequence fidelity for 1189 IMAGE cDNA clones. *Nucleic Acids Res* **29**: 582-8.

Hansen, J., T. Floss, P. Van Sloun, E.M. Fuchtbauer, F. Vauti, H.H. Arnold, F. Schnutgen, W. Wurst, H. von Melchner, and P. Ruiz. 2003. A large-scale, gene-driven mutagenesis approach for the functional analysis of the mouse genome. *Proc Natl Acad Sci U S A* **100**: 9918-22.

Harford, J.B. and D.R. Morris. 1997. Post-transcriptional gene regulation. *Wiley-Liss Inc., New York, N.Y.*

Harris, M.A., J. Clark, A. Ireland, J. Lomax, M. Ashburner, R. Foulger, K. Eilbeck, S. Lewis, B. Marshall, C. Mungall, J. Richter, G.M. Rubin, J.A. Blake, C. Bult, M. Dolan, H.

Drabkin, J.T. Eppig, D.P. Hill, L. Ni, M. Ringwald, R. Balakrishnan, J.M. Cherry, K.R. Christie, M.C. Costanzo, S.S. Dwight, S. Engel, D.G. Fisk, J.E. Hirschman, E.L. Hong, R.S. Nash, A. Sethuraman, C.L. Theesfeld, D. Botstein, K. Dolinski, B. Feierbach, T. Berardini, S. Mundodi, S.Y. Rhee, R. Apweiler, D. Barrell, E. Camon, E. Dimmer, V. Lee, R. Chisholm, P. Gaudet, W. Kibbe, R. Kishore, E.M. Schwarz, P. Sternberg, M. Gwinn, L. Hannick, J. Wortman, M. Berriman, V. Wood, N. de la Cruz, P. Tonellato, P. Jaiswal, T. Seigfried, and R. White. 2004. The Gene Ontology (GO) database and informatics resource. *Nucleic Acids Res* **32 Database issue**: D258-61.

Heitzler, P. and P. Simpson. 1991. The choice of cell fate in the epidermis of Drosophila. *Cell* **64**: 1083-92.

Heller, R.A., M. Schena, A. Chai, D. Shalon, T. Bedilion, J. Gilmore, D.E. Woolley, and R.W. Davis. 1997. Discovery and analysis of inflammatory disease-related genes using cDNA microarrays. *Proc Natl Acad Sci U S A* **94**: 2150-5.

Henderson, S.T., D. Gao, E.J. Lambie, and J. Kimble. 1994. lag-2 may encode a signaling ligand for the GLP-1 and LIN-12 receptors of C. elegans. *Development* **120**: 2913-24.

Henkel, T., P.D. Ling, S.D. Hayward, and M.G. Peterson. 1994. Mediation of Epstein-Barr virus EBNA2 transactivation by recombination signal-binding protein J kappa. *Science* **265**: 92-5.

Henrique, D., J. Adam, A. Myat, A. Chitnis, J. Lewis, and D. Ish-Horowicz. 1995. Expression of a Delta homologue in prospective neurons in the chick [see comments]. *Nature* **375**: 787-90.

Henrique, D., E. Hirsinger, J. Adam, I. Le Roux, O. Pourquie, D. Ish-Horowicz, and J. Lewis. 1997. Maintenance of neuroepithelial progenitor cells by Delta-Notch signalling in the embryonic chick retina. *Curr Biol* **7**: 661-70.

Henzel, W.J., T.M. Billeci, J.T. Stults, S.C. Wong, C. Grimley, and C. Watanabe. 1993. Identifying proteins from two-dimensional gels by molecular mass searching of peptide fragments in protein sequence databases. *Proc Natl Acad Sci U S A* **90**: 5011-5.

Hicke, L. 2001. Protein regulation by monoubiquitin. *Nat Rev Mol Cell Biol* **2**: 195-201.

Hiraga, A. and S. Tamura. 2000. Protein phosphatase 2A is associated in an inactive state with microtubules through 2A1-specific interaction with tubulin. *Biochem J* **346 Pt 2**: 433-9.

Hirata, H., Y. Bessho, H. Kokubu, Y. Masamizu, S. Yamada, J. Lewis, and R. Kageyama. 2004. Instability of Hes7 protein is crucial for the somite segmentation clock. *Nat Genet*.

Hirata, H., S. Yoshiura, T. Ohtsuka, Y. Bessho, T. Harada, K. Yoshikawa, and R. Kageyama. 2002. Oscillatory expression of the bHLH factor Hes1 regulated by a negative feedback loop. *Science* **298**: 840-3.

Hofmann, M., K. Schuster-Gossler, M. Watabe-Rudolph, A. Aulehla, B.G. Herrmann, and A. Gossler. 2004. WNT signaling, in synergy with T/TBX6, controls Notch signaling by regulating Dll1 expression in the presomitic mesoderm of mouse embryos. *Genes Dev* **18**: 2712-7.

Hrabe de Angelis, M. and R. Balling. 1998. Large scale ENU screens in the mouse: genetics meets genomics. *Mutat Res* **400**: 25-32.

Hrabe de Angelis, M., J. McIntyre, 2nd, and A. Gossler. 1997. Maintenance of somite borders in mice requires the Delta homologue DII1. *Nature* **386**: 717-21.

Hughes, T.R., M.J. Marton, A.R. Jones, C.J. Roberts, R. Stoughton, C.D. Armour, H.A. Bennett, E. Coffey, H. Dai, Y.D. He, M.J. Kidd, A.M. King, M.R. Meyer, D. Slade, P.Y.

Lum, S.B. Stepaniants, D.D. Shoemaker, D. Gachotte, K. Chakraburtty, J. Simon, M. Bard, and S.H. Friend. 2000. Functional discovery via a compendium of expression profiles. *Cell* **102**: 109-26.

Itoh, T., A. Itoh, and D. Pleasure. 2003. Bcl-2-related protein family gene expression during oligodendroglial differentiation. *J Neurochem* **85**: 1500-12.

Jarriault, S., C. Brou, F. Logeat, E.H. Schroeter, R. Kopan, and A. Israel. 1995. Signalling downstream of activated mammalian Notch. *Nature* **377**: 355-8.

Jen, W.C., D. Wettstein, D. Turner, A. Chitnis, and C. Kintner. 1997. The Notch ligand, X-Delta-2, mediates segmentation of the paraxial mesoderm in Xenopus embryos. *Development* **124**: 1169-78.

Jiang, Y.J., B.L. Aerne, L. Smithers, C. Haddon, D. Ish-Horowicz, and J. Lewis. 2000. Notch signalling and the synchronization of the somite segmentation clock. *Nature* **408**: 475-9.

Jiang, Y.J., M. Brand, C.P. Heisenberg, D. Beuchle, M. Furutani-Seiki, R.N. Kelsh, R.M. Warga, M. Granato, P. Haffter, M. Hammerschmidt, D.A. Kane, M.C. Mullins, J. Odenthal, F.J. van Eeden, and C. Nusslein-Volhard. 1996. Mutations affecting neurogenesis and brain morphology in the zebrafish, Danio rerio. *Development* **123**: 205-16.

Johnston, S.H., C. Rauskolb, R. Wilson, B. Prabhakaran, K.D. Irvine, and T.F. Vogt. 1997. A family of mammalian Fringe genes implicated in boundary determination and the Notch pathway. *Development* **124**: 2245-54.

Jones, D.H., S. Ley, and A. Aitken. 1995. Isoforms of 14-3-3 protein can form homo- and heterodimers in vivo and in vitro: implications for function as adapter proteins. *FEBS Lett* **368**: 55-8.

Jones, E.A., M. Clement-Jones, O.F. James, and D.I. Wilson. 2001. Differences between human and mouse alpha-fetoprotein expression during early development. *J Anat* **198**: 555-9.

Joutel, A. and E. Tournier-Lasserve. 1998. Notch signalling pathway and human diseases. *Semin Cell Dev Biol* **9**: 619-25.

Jouve, C., I. Palmeirim, D. Henrique, J. Beckers, A. Gossler, D. Ish-Horowicz, and O. Pourquie. 2000. Notch signalling is required for cyclic expression of the hairy-like gene HES1 in the presomitic mesoderm. *Development* **127**: 1421-9.

Joyner, A.L., A. Auerbach, and W.C. Skarnes. 1992. The gene trap approach in embryonic stem cells: the potential for genetic screens in mice. *Ciba Found Symp* **165**: 277-88; discussion 288-97.

Justice, M.J., J.K. Noveroske, J.S. Weber, B. Zheng, and A. Bradley. 1999. Mouse ENU mutagenesis. *Hum Mol Genet* **8**: 1955-63.

Katzmann, D.J., M. Babst, and S.D. Emr. 2001. Ubiquitin-dependent sorting into the multivesicular body pathway requires the function of a conserved endosomal protein sorting complex, ESCRT-I. *Cell* **106**: 145-55.

Kerszberg, M. and L. Wolpert. 2000. A clock and trail model for somite formation, specialization and polarization. *J Theor Biol* **205**: 505-10.

Kiernan, A.E., N. Ahituv, H. Fuchs, R. Balling, K.B. Avraham, K.P. Steel, and M. Hrabe de Angelis. 2001. The Notch ligand Jagged1 is required for inner ear sensory development. *Proc Natl Acad Sci U S A* **98**: 3873-8.

Kim, J.K., S.-O. Huh, H. Choi, K.-S. Lee, D. Shin, C. Lee, J.-S. Nam, H. Kim, H. Chung, H.W. Lee, S.D. Park, and R.H. Seong. 2001. Srg3, a Mouse Homolog of Yeast SWI3, Is

Essential for Early Embryogenesis and Involved in Brain Development. *Mol. Cell. Biol.* **21**: 7787-7795.

Kimble, J. and P. Simpson. 1997. The LIN-12/Notch signaling pathway and its regulation. *Annu Rev Cell Dev Biol* **13**: 333-61.

Kimura, T., I. Oguro, J. Kohroki, M. Takehara, N. Itoh, T. Nakanishi, and K. Tanaka. 2000a. Metallothionein-Null Mice Express Altered Genes during Development. *Biochemical and Biophysical Research Communications* **270**: 458-461.

-. 2000b. Metallothionein-null mice express altered genes during development. *Biochem Biophys Res Commun* **270**: 458-61.

Kingston, R.E. and G.J. Narlikar. 1999. ATP-dependent remodeling and acetylation as regulators of chromatin fluidity. *Genes Dev* **13**: 2339-52.

Klochendler-Yeivin, A., L. Fiette, J. Barra, C. Muchardt, C. Babinet, and M. Yaniv. 2000. The murine SNF5/INI1 chromatin remodeling factor is essential for embryonic development and tumor suppression. *EMBO Rep* **1**: 500-6.

Kockel, L., G. Vorbruggen, H. Jackle, M. Mlodzik, and D. Bohmann. 1997. Requirement for Drosophila 14-3-3 zeta in Raf-dependent photoreceptor development. *Genes Dev* **11**: 1140-7.

Koizumi, K., M. Nakajima, S. Yuasa, Y. Saga, T. Sakai, T. Kuriyama, T. Shirasawa, and H. Koseki. 2001. The role of presenilin 1 during somite segmentation. *Development* **128**: 1391-402.

Kojika, S. and J.D. Griffin. 2001. Notch receptors and hematopoiesis. *Exp Hematol* **29**: 1041-52.

Kopan, R., E.H. Schroeter, H. Weintraub, and J.S. Nye. 1996. Signal transduction by activated mNotch: importance of proteolytic processing and its regulation by the extracellular domain. *Proc Natl Acad Sci U S A* **93**: 1683-8.

Krantz, I.D. 2002. Alagille syndrome: chipping away at the tip of the iceberg. *Am J Med Genet* **112**: 160-2.

Krantz, I.D., D.A. Piccoli, and N.B. Spinner. 1997. Alagille syndrome. *J Med Genet* **34**: 152-7.

Krebs, L.T., N. Iwai, S. Nonaka, I.C. Welsh, Y. Lan, R. Jiang, Y. Saijoh, T.P. O'Brien, H. Hamada, and T. Gridley. 2003. Notch signaling regulates left-right asymmetry determination by inducing Nodal expression. *Genes Dev* **17**: 1207-12.

Kurooka, H. and T. Honjo. 2000. Functional interaction between the mouse notch1 intracellular region and histone acetyltransferases PCAF and GCN5. *J Biol Chem* **275**: 17211-20.

Kusumi, K., S.L. Dunwoodie, and R. Krumlauf. 2001. Dynamic expression patterns of the pudgy/spondylocostal dysostosis gene Dll3 in the developing nervous system. *Mech Dev* **100**: 141-4.

Kusumi, K., M.S. Mimoto, K.L. Covello, R.S. Beddington, R. Krumlauf, and S.L. Dunwoodie. 2004. Dll3 pudgy mutation differentially disrupts dynamic expression of somite genes. *Genesis* **39**: 115-21.

Kusumi, K., E.S. Sun, A.W. Kerrebrock, R.T. Bronson, D.C. Chi, M.S. Bulotsky, J.B. Spencer, B.W. Birren, W.N. Frankel, and E.S. Lander. 1998. The mouse pudgy mutation disrupts Delta homologue Dll3 and initiation of early somite boundaries. *Nat Genet* **19**: 274-8.

Lambie, E.J. and J. Kimble. 1991. Two homologous regulatory genes, lin-12 and glp-1, have overlapping functions. *Development* **112**: 231-40.

Lammert, E., J. Brown, and D.A. Melton. 2000. Notch gene expression during pancreatic organogenesis. *Mech Dev* **94**: 199-203.

Lander, E.S. et al. 2001. Initial sequencing and analysis of the human genome. *Nature* **409**: 860-921.

Lange, U.C., M. Saitou, P.S. Western, S.C. Barton, and M.A. Surani. 2003. The fragilis interferon-inducible gene family of transmembrane proteins is associated with germ cell specification in mice. *BMC Dev Biol* **3**: 1.

Lardelli, M. and U. Lendahl. 1993. Motch A and motch B--two mouse Notch homologues coexpressed in a wide variety of tissues. *Exp Cell Res* **204**: 364-72.

Larsson, C., M. Lardelli, I. White, and U. Lendahl. 1994. The human NOTCH1, 2, and 3 genes are located at chromosome positions 9q34, 1p13-p11, and 19p13.2-p13.1 in regions of neoplasia-associated translocation. *Genomics* **24**: 253-8.

Lechward, K., O.S. Awotunde, W. Swiatek, and G. Muszynska. 2001. Protein phosphatase 2A: variety of forms and diversity of functions. *Acta Biochim Pol* **48**: 921-33.

Lee, M.L., F.C. Kuo, G.A. Whitmore, and J. Sklar. 2000. Importance of replication in microarray gene expression studies: statistical methods and evidence from repetitive cDNA hybridizations. *Proc Natl Acad Sci U S A* **97**: 9834-9.

Lee, S.-K. and S.L. Pfaff. 2003. Synchronization of Neurogenesis and Motor Neuron Specification by Direct Coupling of bHLH and Homeodomain Transcription Factors. *Neuron* **38**: 731-745.

Leimeister, C., K. Dale, A. Fischer, B. Klamt, M. Hrabe de Angelis, F. Radtke, M.J. McGrew, O. Pourquie, and M. Gessler. 2000. Oscillating expression of c-Hey2 in the presomitic mesoderm suggests that the segmentation clock may use combinatorial signaling through multiple interacting bHLH factors. *Dev Biol* **227**: 91-103.

Lewis, A.K., G.D. Frantz, D.A. Carpenter, F.J. de Sauvage, and W.Q. Gao. 1998. Distinct expression patterns of notch family receptors and ligands during development of the mammalian inner ear. *Mech Dev* **78**: 159-63.

Lewis, J. 1998. Notch signalling and the control of cell fate choices in vertebrates. *Semin Cell Dev Biol* **9**: 583-9.

Lindsell, C.E., C.J. Shawber, J. Boulter, and G. Weinmaster. 1995. Jagged: a mammalian ligand that activates Notch1. *Cell* **80**: 909-17.

Logeat, F., C. Bessia, C. Brou, O. LeBail, S. Jarriault, N.G. Seidah, and A. Israel. 1998. The Notch1 receptor is cleaved constitutively by a furin-like convertase. *Proc Natl Acad Sci U S A* **95**: 8108-12.

Lutolf, S., F. Radtke, M. Aguet, U. Suter, and V. Taylor. 2002. Notch1 is required for neuronal and glial differentiation in the cerebellum. *Development* **129**: 373-85.

Malhotra, V., L. Orci, B.S. Glick, M.R. Block, and J.E. Rothman. 1988. Role of an N-ethylmaleimide-sensitive transport component in promoting fusion of transport vesicles with cisternae of the Golgi stack. *Cell* **54**: 221-7.

Martinez Arias, A., V. Zecchini, and K. Brennan. 2002. CSL-independent Notch signalling: a checkpoint in cell fate decisions during development? *Curr Opin Genet Dev* **12**: 524-33.

Masters, B.A., E.J. Kelly, C.J. Quaife, R.L. Brinster, and R.D. Palmiter. 1994. Targeted disruption of metallothionein I and II genes increases sensitivity to cadmium. *Proc Natl Acad Sci U S A* **91**: 584-8.

Matsunami, N., Y. Hamaguchi, Y. Yamamoto, K. Kuze, K. Kangawa, H. Matsuo, M. Kawaichi, and T. Honjo. 1989. A protein binding to the J kappa recombination

sequence of immunoglobulin genes contains a sequence related to the integrase motif. *Nature* **342**: 934-7.

Meinhardt. 1986. Models for segmentation. In "Somites in developing embryos" (Bellairs R, Ede DA, Lash JW, editors). *New York: Plenum Press*: 179-191.

Michalska, A.E. and K.H. Choo. 1993. Targeting and germ-line transmission of a null mutation at the metallothionein I and II loci in mouse. *Proc Natl Acad Sci U S A* **90**: 8088-92.

Mijalski, T., A. Harder, T. Halder, M. Kersten, M. Horsch, T. Strom, V. Liebscher, F. Lottspeich, M. Hrabe de Angelis, and J. Beckers. 2005. Identification of co-expressed gene clusters in a comparative analysis of transcriptome and proteome in mouse tissues. *Proc Natl Acad Sci U S A* **102**: 8621-26.

Miki, R., K. Kadota, H. Bono, Y. Mizuno, Y. Tomaru, P. Carninci, M. Itoh, K. Shibata, J. Kawai, H. Konno, S. Watanabe, K. Sato, Y. Tokusumi, N. Kikuchi, Y. Ishii, Y. Hamaguchi, I. Nishizuka, H. Goto, H. Nitanda, S. Satomi, A. Yoshiki, M. Kusakabe, J.L. DeRisi, M.B. Eisen, V.R. Iyer, P.O. Brown, M. Muramatsu, H. Shimada, Y. Okazaki, and Y. Hayashizaki. 2001. Delineating developmental and metabolic pathways in vivo by expression profiling using the RIKEN set of 18,816 full-length enriched mouse cDNA arrays. *Proc Natl Acad Sci U S A* **98**: 2199-204.

Milner, L.A. and A. Bigas. 1999. Notch as a mediator of cell fate determination in hematopoiesis: evidence and speculation. *Blood* **93**: 2431-48.

Minshall, N., G. Thom, and N. Standart. 2001. A conserved role of a DEAD box helicase in mRNA masking. *Rna* **7**: 1728-42.

Mishra-Gorur, K., M.D. Rand, B. Perez-Villamil, and S. Artavanis-Tsakonas. 2002. Down-regulation of Delta by proteolytic processing. *J Cell Biol* **159**: 313-24.

Moritz, M. and D.A. Agard. 2001. Gamma-tubulin complexes and microtubule nucleation. *Curr Opin Struct Biol* **11**: 174-81.

Mumm, J.S., E.H. Schroeter, M.T. Saxena, A. Griesemer, X. Tian, D.J. Pan, W.J. Ray, and R. Kopan. 2000. A ligand-induced extracellular cleavage regulates gamma-secretase-like proteolytic activation of Notch1. *Mol Cell* **5**: 197-206.

Muskavitch, M.A. 1994. Delta-notch signaling and Drosophila cell fate choice. *Dev Biol* **166**: 415-30.

Myat, A., D. Henrique, D. Ish-Horowicz, and J. Lewis. 1996. A chick homologue of Serrate and its relationship with Notch and Delta homologues during central neurogenesis. *Dev Biol* **174**: 233-47.

Nadeau, J.H., R. Balling, G. Barsh, D. Beier, S.D. Brown, M. Bucan, S. Camper, G. Carlson, N. Copeland, J. Eppig, C. Fletcher, W.N. Frankel, D. Ganten, D. Goldowitz, C. Goodnow, J.L. Guenet, G. Hicks, M. Hrabe de Angelis, I. Jackson, H.J. Jacob, N. Jenkins, D. Johnson, M. Justice, S. Kay, D. Kingsley, H. Lehrach, T. Magnuson, M. Meisler, A. Poustka, E.M. Rinchik, J. Rossant, L.B. Russell, J. Schimenti, T. Shiroishi, W.C. Skarnes, P. Soriano, W. Stanford, J.S. Takahashi, W. Wurst, and A. Zimmer. 2001. Sequence interpretation. Functional annotation of mouse genome sequences. *Science* **291**: 1251-5.

Naranda, T., W.B. Strong, J. Menaya, B.J. Fabbri, and J.W. Hershey. 1994. Two structural domains of initiation factor eIF-4B are involved in binding to RNA. *J Biol Chem* **269**: 14465-72.

Noh, H.S., H.P. Lee, D.W. Kim, S.S. Kang, G.J. Cho, J.M. Rho, and W.S. Choi. 2004. A cDNA microarray analysis of gene expression profiles in rat hippocampus following a ketogenic diet. *Brain Res Mol Brain Res* **129**: 80-7.

Nonaka, S., H. Shiratori, Y. Saijoh, and H. Hamada. 2002. Determination of left-right patterning of the mouse embryo by artificial nodal flow. *Nature* **418**: 96-9.

Nonaka, S., Y. Tanaka, Y. Okada, S. Takeda, A. Harada, Y. Kanai, M. Kido, and N. Hirokawa. 1998. Randomization of left-right asymmetry due to loss of nodal cilia generating leftward flow of extraembryonic fluid in mice lacking KIF3B motor protein. *Cell* **95**: 829-37.

Nygard, O. and P. Westermann. 1982. Specific interaction of one subunit of eukaryotic initiation factor eIF-3 with 18S ribosomal RNA within the binary complex, eIF-3 small ribosomal subunit, as shown by cross-linking experiments. *Nucleic Acids Res* **10**: 1327-34.

Oda, T., A.G. Elkahloun, P.S. Meltzer, and S.C. Chandrasekharappa. 1997. Identification and cloning of the human homolog (JAG1) of the rat Jagged1 gene from the Alagille syndrome critical region at 20p12. *Genomics* **43**: 376-9.

Ohishi, K., N. Katayama, H. Shiku, B. Varnum-Finney, and I.D. Bernstein. 2003. Notch signalling in hematopoiesis. *Semin Cell Dev Biol* **14**: 143-50.

Ohtsuka, K. and T. Suzuki. 2000. Roles of molecular chaperones in the nervous system. *Brain Res Bull* **53**: 141-6.

Ohtsuka, T., M. Ishibashi, G. Gradwohl, S. Nakanishi, F. Guillemot, and R. Kageyama. 1999. Hes1 and Hes5 as notch effectors in mammalian neuronal differentiation. *Embo J* **18**: 2196-207.

Oka, C., T. Nakano, A. Wakeham, J.L. de la Pompa, C. Mori, T. Sakai, S. Okazaki, M. Kawaichi, K. Shiota, T.W. Mak, and T. Honjo. 1995. Disruption of the mouse RBP-J kappa gene results in early embryonic death. *Development* **121**: 3291-301.

Okada, Y., S. Nonaka, Y. Tanaka, Y. Saijoh, H. Hamada, and N. Hirokawa. 1999. Abnormal nodal flow precedes situs inversus in iv and inv mice. *Mol Cell* **4**: 459-68.

Okajima, T. and K.D. Irvine. 2002. Regulation of notch signaling by o-linked fucose. *Cell* **111**: 893-904.

Oksvold, M.P., H.S. Huitfeldt, and W.Y. Langdon. 2004. Identification of 14-3-3[zeta] as an EGF receptor interacting protein. *FEBS Letters* **569**: 207-210.

Ordway, R.W., L. Pallanck, and B. Ganetzky. 1994. Neurally expressed Drosophila genes encoding homologs of the NSF and SNAP secretory proteins. *Proc Natl Acad Sci U S A* **91**: 5715-9.

Orr-Urtreger, A. and P. Lonai. 1992. Platelet-derived growth factor-A and its receptor are expressed in separate, but adjacent cell layers of the mouse embryo. *Development* **115**: 1045-58.

Pandey, A. and M. Mann. 2000. Proteomics to study genes and genomes. *Nature* **405**: 837-46.

Pennington, Wilkins M.R., Hochstrasser D.F., and M.J. Dunn. 1997. Proteome analysis: from protein characterization to biological function. *Trends Cell Biol* **7**: 168-173.

Petcherski, A.G. and J. Kimble. 2000. LAG-3 is a putative transcriptional activator in the C. elegans Notch pathway. *Nature* **405**: 364-8.

Pfister, S., G.K. Przemeck, J.K. Gerber, J. Beckers, J. Adamski, and M.H. de Angelis. 2003a. Interaction of the MAGUK family member Acvrinp1 and the cytoplasmic domain of the Notch ligand Delta1. *J Mol Biol* **333**: 229-35.

Pfister, S., G.K. Przemeck, J.K. Gerber, J. Beckers, J. Adamski, and M. Hrabe de Angelis. 2003b. Interaction of the MAGUK family member Acvrinp1 and the cytoplasmic domain of the Notch ligand Delta1. *J Mol Biol* **333**: 229-35.

Pourquie, O. 2003. The segmentation clock: converting embryonic time into spatial pattern. *Science* **301**: 328-30.

Przemeck, G.K., U. Heinzmann, J. Beckers, and M. Hrabe de Angelis. 2003. Node and midline defects are associated with left-right development in Delta1 mutant embryos. *Development* **130**: 3-13.

Raju, K., S. Tang, I.D. Dube, S. Kamel-Reid, D.M. Bryce, and M.L. Breitman. 1993. Characterization and developmental expression of Tlx-1, the murine homolog of HOX11. *Mech Dev* **44**: 51-64.

Ramsdell, A.F. and H.J. Yost. 1998. Molecular mechanisms of vertebrate left-right development. *Trends Genet* **14**: 459-65.

Rand, M.D., L.M. Grimm, S. Artavanis-Tsakonas, V. Patriub, S.C. Blacklow, J. Sklar, and J.C. Aster. 2000. Calcium depletion dissociates and activates heterodimeric notch receptors. *Mol Cell Biol* **20**: 1825-35.

Rauch, F., J. Prud'homme, A. Arabian, S. Dedhar, and R. St-Arnaud. 2000. Heart, brain, and body wall defects in mice lacking calreticulin. *Exp Cell Res* **256**: 105-11.

Rawls, A., J. Wilson-Rawls, and E.N. Olson. 2000. Genetic regulation of somite formation. *Curr Top Dev Biol* **47**: 131-54.

Rebay, I., R.J. Fleming, R.G. Fehon, L. Cherbas, P. Cherbas, and S. Artavanis-Tsakonas. 1991. Specific EGF repeats of Notch mediate interactions with Delta and Serrate: implications for Notch as a multifunctional receptor. *Cell* **67**: 687-99.

Rocak, S. and P. Linder. 2004. DEAD-box proteins: the driving forces behind RNA metabolism. *Nat Rev Mol Cell Biol* **5**: 232-41.

Rothman, J.E. and G. Warren. 1994. Implications of the SNARE hypothesis for intracellular membrane topology and dynamics. *Curr Biol* **4**: 220-33.

Saga, Y. and H. Takeda. 2001. The making of the somite: molecular events in vertebrate segmentation. *Nat Rev Genet* **2**: 835-45.

Saitou, M., S.C. Barton, and M.A. Surani. 2002. A molecular programme for the specification of germ cell fate in mice. *Nature* **418**: 293-300.

Sander, M., S. Paydar, J. Ericson, J. Briscoe, E. Berber, M. German, T.M. Jessell, and J.L. Rubenstein. 2000. Ventral neural patterning by Nkx homeobox genes: Nkx6.1 controls somatic motor neuron and ventral interneuron fates. *Genes Dev* **14**: 2134-9.

Sawada, A., M. Shinya, Y.J. Jiang, A. Kawakami, A. Kuroiwa, and H. Takeda. 2001. Fgf/MAPK signalling is a crucial positional cue in somite boundary formation. *Development* **128**: 4873-80.

Schena, M., D. Shalon, R.W. Davis, and P.O. Brown. 1995. Quantitative monitoring of gene expression patterns with a complementary DNA microarray. *Science* **270**: 467-70.

Schnell, S. and P.K. Maini. 2000. Clock and induction model for somitogenesis. *Dev Dyn* **217**: 415-20.

Schuchhardt, J., D. Beule, A. Malik, E. Wolski, H. Eickhoff, H. Lehrach, and H. Herzel. 2000. Normalization strategies for cDNA microarrays. *Nucleic Acids Res* **28**: E47.

Schweisguth, F. 2004. Notch signaling activity. *Curr Biol* **14**: R129-38.

Seltmann, M., M. Horsch, A.L. Drobyshev, Y. Chen, M. Hrabe de Angelis, and J. Beckers. 2005. Assessment of a systematic expression profiling approach in ENU induced mouse mutant lines. *Mamm. Gen.* **accepted**.

Shawber, C., J. Boulter, C.E. Lindsell, and G. Weinmaster. 1996a. Jagged2: a serrate-like gene expressed during rat embryogenesis. *Dev Biol* **180**: 370-6.

Shawber, C., D. Nofziger, J.J. Hsieh, C. Lindsell, O. Bogler, D. Hayward, and G. Weinmaster. 1996b. Notch signaling inhibits muscle cell differentiation through a CBF1-independent pathway. *Development* **122**: 3765-73.

Shutter, J.R., S. Scully, W. Fan, W.G. Richards, J. Kitajewski, G.A. Deblandre, C.R. Kintner, and K.L. Stark. 2000. Dll4, a novel Notch ligand expressed in arterial endothelium. *Genes Dev* **14**: 1313-8.

Singh, O.P. 2001. Functional diversity of hnRNP proteins. *Indian J Biochem Biophys* **38**: 129-34.

Six, E., D. Ndiaye, Y. Laabi, C. Brou, N. Gupta-Rossi, A. Israel, and F. Logeat. 2003. The Notch ligand Delta1 is sequentially cleaved by an ADAM protease and gamma-secretase. *Proc Natl Acad Sci U S A* **100**: 7638-43.

Six, E.M., D. Ndiaye, S. Sauer, Y. Laâbi, R. Athman, A. Cumano, C. Brou, A. Israël, and F. Logeat. 2004. The Notch ligand Delta1 recruits Dlg1 at cell-cell contacts and regulates cell migration. *J Biol Chem* **Epub ahead of print**.

Smal, C., L. Bertrand, E. Van den Neste, S. Cardoen, M. Veiga-da-Cunha, S. Marie, V. Race, A. Ferrant, G. Van den Berghe, and F. Bontemps. 2004. New evidences for a regulation of deoxycytidine kinase activity by reversible phosphorylation. *Nucleosides Nucleotides Nucleic Acids* **23**: 1363-5.

Sontag, E. 2001. Protein phosphatase 2A: the Trojan Horse of cellular signaling. *Cell Signal* **13**: 7-16.

Sontag, E., V. Nunbhakdi-Craig, G.S. Bloom, and M.C. Mumby. 1995. A novel pool of protein phosphatase 2A is associated with microtubules and is regulated during the cell cycle. *J Cell Biol* **128**: 1131-44.

Soriano, P. 1997. The PDGF alpha receptor is required for neural crest cell development and for normal patterning of the somites. *Development* **124**: 2691-700.

Stewart, B.A., M. Mohtashami, L. Zhou, W.S. Trimble, and G.L. Boulianne. 2001. SNARE-dependent signaling at the Drosophila wing margin. *Dev Biol* **234**: 13-23.

Stollewerk, A., M. Schoppmeier, and W.G. Damen. 2003. Involvement of Notch and Delta genes in spider segmentation. *Nature* **423**: 863-5.

Struhl, G. and I. Greenwald. 1999. Presenilin is required for activity and nuclear access of Notch in Drosophila. *Nature* **398**: 522-5.

-. 2001. Presenilin-mediated transmembrane cleavage is required for Notch signal transduction in Drosophila. *Proc Natl Acad Sci U S A* **98**: 229-34.

Sutton, R.B., D. Fasshauer, R. Jahn, and A.T. Brunger. 1998. Crystal structure of a SNARE complex involved in synaptic exocytosis at 2.4 A resolution. *Nature* **395**: 347-53.

Tanaka, S.S. and Y. Matsui. 2002. Developmentally regulated expression of mil-1 and mil-2, mouse interferon-induced transmembrane protein like genes, during formation and differentiation of primordial germ cells. *Gene Expr Patterns* **2**: 297-303.

Thaler, J.P., S.-K. Lee, L.W. Jurata, G.N. Gill, and S.L. Pfaff. 2002. LIM Factor Lhx3 Contributes to the Specification of Motor Neuron and Interneuron Identity through Cell-Type-Specific Protein-Protein Interactions. *Cell* **110**: 237-249.

Thor, S., S.G.E. Andersson, A. Tomlinson, and J.B. Thomas. 1999. A LIM-homeodomain combinatorial code for motor-neuron pathway selection. *Nature* **397**: 76-80.

Topisirovic, I., M. Ruiz-Gutierrez, and K.L. Borden. 2004. Phosphorylation of the eukaryotic translation initiation factor eIF4E contributes to its transformation and mRNA transport activities. *Cancer Res* **64**: 8639-42.

Toyo-oka, K., A. Shionoya, M.J. Gambello, C. Cardoso, R. Leventer, H.L. Ward, R. Ayala, L.H. Tsai, W. Dobyns, D. Ledbetter, S. Hirotsune, and A. Wynshaw-Boris. 2003. 14-3-3epsilon is important for neuronal migration by binding to NUDEL: a molecular explanation for Miller-Dieker syndrome. *Nat Genet* **34**: 274-85.

Tsacopoulos, M. 2002. Metabolic signaling between neurons and glial cells: a short review. *J Physiol Paris* **96**: 283-8.

Tseng, G.C., M.K. Oh, L. Rohlin, J.C. Liao, and W.H. Wong. 2001. Issues in cDNA microarray analysis: quality filtering, channel normalization, models of variations and assessment of gene effects. *Nucleic Acids Res* **29**: 2549-57.

Turnpenny, P.D., N. Whittock, J. Duncan, S. Dunwoodie, K. Kusumi, and S. Ellard. 2003. Novel mutations in DLL3, a somitogenesis gene encoding a ligand for the Notch signalling pathway, cause a consistent pattern of abnormal vertebral segmentation in spondylocostal dysostosis. *J Med Genet* **40**: 333-9.

Tzivion, G. and J. Avruch. 2002. 14-3-3 proteins: active cofactors in cellular regulation by serine/threonine phosphorylation. *J Biol Chem* **277**: 3061-4.

Urlinger, S., K. Kuchler, T.H. Meyer, S. Uebel, and R. Tampe. 1997. Intracellular location, complex formation, and function of the transporter associated with antigen processing in yeast. *Eur J Biochem* **245**: 266-72.

van den Heuvel, R.H., B. Curti, M.A. Vanoni, and A. Mattevi. 2004. Glutamate synthase: a fascinating pathway from L-glutamine to L-glutamate. *Cell Mol Life Sci* **61**: 669-81.

Varshavsky, A. 1996. The N-end rule: functions, mysteries, uses. *Proc Natl Acad Sci U S A* **93**: 12142-9.

Venter, J.C. et al. 2001. The sequence of the human genome. *Science* **291**: 1304-51.

von Boehmer, H. 2001. Coming to grips with Notch. *J Exp Med* **194**: F43-6.

Walsh, D., Z. Li, Y. Wu, and K. Nagata. 1997. Heat shock and the role of the HSPs during neural plate induction in early mammalian CNS and brain development. *Cell Mol Life Sci* **53**: 198-211.

Wang, W., J. Cote, Y. Xue, S. Zhou, P.A. Khavari, S.R. Biggar, C. Muchardt, G.V. Kalpana, S.P. Goff, M. Yaniv, J.L. Workman, and G.R. Crabtree. 1996a. Purification and biochemical heterogeneity of the mammalian SWI-SNF complex. *Embo J* **15**: 5370-82.

Wang, W., J.F. Grimmer, T.R. Van De Water, and T. Lufkin. 2004. Hmx2 and Hmx3 Homeobox Genes Direct Development of the Murine Inner Ear and Hypothalamus and Can Be Functionally Replaced by Drosophila Hmx. *Developmental Cell* **7**: 439-453.

Wang, W., P. Lo, M. Frasch, and T. Lufkin. 2000. Hmx: an evolutionary conserved homeobox gene family expressed in the developing nervous system in mice and Drosophila. *Mech Dev* **99**: 123-37.

Wang, W., Y. Xue, S. Zhou, A. Kuo, B.R. Cairns, and G.R. Crabtree. 1996b. Diversity and specialization of mammalian SWI/SNF complexes. *Genes Dev* **10**: 2117-30.

Ware, M.F., D.A. Tice, S.J. Parsons, and D.A. Lauffenburger. 1997. Overexpression of cellular Src in fibroblasts enhances endocytic internalization of epidermal growth factor receptor. *J Biol Chem* **272**: 30185-90.

Weinmaster, G., V.J. Roberts, and G. Lemke. 1992. Notch2: a second mammalian Notch gene. *Development* **116**: 931-41.

Weng, A.P. and J.C. Aster. 2004. Multiple niches for Notch in cancer: context is everything Multiple niches for Notch in cancer: context is everything. *Curr Opin Genet Dev* **14**: 48–54.

Wharton, K.A., K.M. Johansen, T. Xu, and S. Artavanis-Tsakonas. 1985. Nucleotide sequence from the neurogenic locus notch implies a gene product that shares homology with proteins containing EGF-like repeats. *Cell* **43**: 567-81.

White, K.P., S.A. Rifkin, P. Hurban, and D.S. Hogness. 1999. Microarray analysis of Drosophila development during metamorphosis. *Science* **286**: 2179-84.

Wilkins, W. K.L., A.R.D. and, and H. D.F. 1997. Proteome research: new frontiers in functional genomics. *Springer, Berlin*: 1-243.

Wilson, S.M., B. Bhattacharyya, R.A. Rachel, V. Coppola, L. Tessarollo, D.B. Householder, C.F. Fletcher, R.J. Miller, N.G. Copeland, and N.A. Jenkins. 2002. Synaptic defects in ataxia mice result from a mutation in Usp14, encoding a ubiquitin-specific protease. *Nat Genet* **32**: 420-5.

Wright, G.J., J.D. Leslie, L. Ariza-McNaughton, and J. Lewis. 2004. Delta proteins and MAGI proteins: an interaction of Notch ligands with intracellular scaffolding molecules and its significance for zebrafish development. *Development* **131**: 5659-5669.

Wurst, W., J. Rossant, V. Prideaux, M. Kownacka, A. Joyner, D.P. Hill, F. Guillemot, S. Gasca, D. Cado, A. Auerbach, and et al. 1995. A large-scale gene-trap screen for insertional mutations in developmentally regulated genes in mice. *Genetics* **139**: 889-99.

Yaffe, M.B. 2002. How do 14-3-3 proteins work?-- Gatekeeper phosphorylation and the molecular anvil hypothesis. *FEBS Lett* **513**: 53-7.

Ye, Y., N. Lukinova, and M.E. Fortini. 1999. Neurogenic phenotypes and altered Notch processing in Drosophila Presenilin mutants. *Nature* **398**: 525-9.

Zammatteo, N., L. Jeanmart, S. Hamels, S. Courtois, P. Louette, L. Hevesi, and J. Remacle. 2000. Comparison between different strategies of covalent attachment of DNA to glass surfaces to build DNA microarrays. *Anal Biochem* **280**: 143-50.

Zhang, N. and T. Gridley. 1998. Defects in somite formation in lunatic fringe-deficient mice. *Nature* **394**: 374-7.

Zhang, X., H. Yang, J. Yu, C. Chen, G. Zhang, J. Bao, Y. Du, M. Kibukawa, Z. Li, and J. Wang. 2002. Genomic organization, transcript variants and comparative analysis of the human nucleoporin 155 (NUP155) gene. *Gene* **288**: 9-18.

Zhang, X.Q., G.B. Afink, K. Svensson, J.J. Jacobs, T. Gunther, K. Forsberg-Nilsson, E.J. van Zoelen, B. Westermark, and M. Nister. 1998. Specific expression in mouse mesoderm- and neural crest-derived tissues of a human PDGFRA promoter/lacZ transgene. *Mech Dev* **70**: 167-80.

10 Appendix

10.1 Abbreviations

A	Adenine
APS	Ammoniumpersulfate
ATP	Adenosintriphosphate
aRNA	Antisense RNA
bp	Basepair
BSA	Bovine Serum Albumin
c	Centi-(10^{-2})
C	Cytosine
°C	Grad Celsius
cDNA	copy DNA
Cy3	Cyanin 3 fluorescent dye
Cy5	Cyanin 5 fluorescent dye
cm	Centimeter
D	Day
2D-ge	2D-gelelectrophoresis
dATP	Desoxyadenosintriphosphate
dCTP	Desoxycytosintriphosphate
dGTP	Desoxyguanintriphosphate
ddH$_2$O	Double deionised H$_2$O
DIG	Digoxygenin
DMSO	Dimethylsulfoxide
DNA	Desoxyribonucleicacid
Dnase	Desoxiribonuclease
dNTP	Desoxynucleotidtriphosphate mixture
dTTP	Desoxythymidintriphosphate
DTT	Dithiothreitol
E	Day of embryonic development
E.coli	*Escherichia coli*
EDTA	Ethylendiamintetraacetate
ENU	N-Ethyl-N-Nitroso-Urea
FA	Formamide

x g	Earth gravity; g = 9,81 m/s
g	Gram
G	Guanine
h	Hour
HCl	Hydrochloric acid
H_2O_2	Hydrogenperoxide
Hprt	Hypoxanthin-Guanin-Phosphoribosyltransferase
HRP	Horse Raddish-Peroxidase
IPTG	Isopropyl-ß-D-thiogalaktopyranoside
K	Kilo- (10^3)
kb	Kilobase
KCl	Potassium chloride
kDA	Kilo Dalton
l	Liter
LB	Luria Bertani
LiCl	Lithiumchloride
LR	Left-right
µ	mikro- (10^{-6})
m	milli- (10^{-3})
m	Meter
M	Molar (mol/L)
ß-Me	ß-Mercaptoethanol
$MgCl_2$	Magnesium chloride
min.	Minute
Mol	Mol (6,023 x 10 23 Teilchen)
mRNA	Messenger RNA
n	Total number
n	nano- (10^{-9})
NaCl	Sodium chloride
NaOH	Sodium hydroxide
nm	Nanometer
OD	Optic density
p	pico (10^{-12})
p	posterior
PBS	Phosphate Buffered Saline
PCR	Polymerase chain reaction
PFA	Paraformaldehyde

psm	Presomitic mesoderm
RNA	Ribonucleicacid
RNase	Ribonuclease
rpm	Round per minute
RT	Room temperature
RT	Reverse Transkription
SDS	Sodiumdodecylsulfate
sec.	Second
SSC	Saline-Sodium Citrate
T	Thymidin
Taq	Thermus aquaticus
TE	Tris-EDTA
TEMED	N,N,N',N'-Tetramethylethylenediamine
Tris	Tris-Hydroxymethyl-Aminoethan
tRNA	Transfer-Ribonucleicacid
U	Unit (Enzymeactivity)
UV	Ultraviolet
V	Volt
Vol.	Volume
v/v	Volume per Volume
wish	Whole mount *in situ* hybridisation
wt	wildtype
w/v	Weight per Volume
X-Gal	5-Bromo-4-chloro-3-indolyl-ß-D-galaktopyranosid